The Dynamic Interactome: A Proteomic Investigation of Ligand-dependent HSP90 Complexes

Jacob J. Gano

A dissertation submitted in partial fulfillment of the
requirements for the degree of

Doctor of Philosophy

University of Washington

2007

Program authorized to Offer Degree:
Molecular and Cellular Biology Program

University of Washington
Graduate School

This is to certify that I have examined this copy of a doctoral dissertation by

Jacob J. Gano

and have found that it is complete and satisfactory in all respects, and that any and all revisions required by the final examining committee have been made.

Chair of the Supervisory Committee:

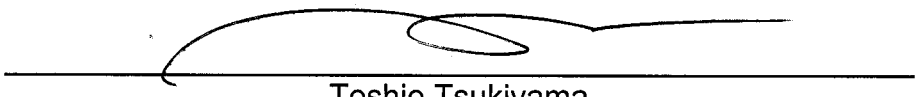

Toshio Tsukiyama

Reading Committee:

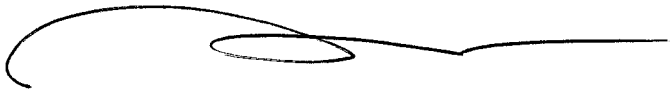

Toshio Tsukiyama

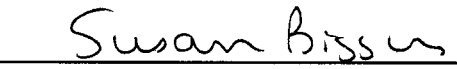

Susan Biggins

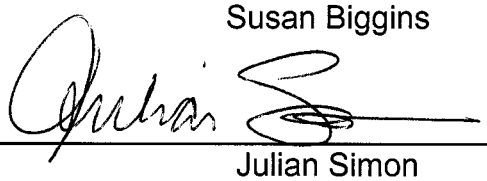

Julian Simon

Date: 12 09 07

In presenting this dissertation in partial fulfillment of the requirements for the doctoral degree at the University of Washington, I agree that the Library shall make its copies freely available for inspection. I further agree that extensive copying of the dissertation is allowable only for scholarly purposes, consistent with "fair use" as prescribed in the U.S. Copyright Law. Requests for copying or reproduction of this dissertation may be referred to ProQuest Information and Learning, 300 North Zeeb Road, Ann Arbor, MI 48106-1346, 1-800-521-0600, to whom the author has granted "the right to reproduce and sell (a) copies of the manuscript in microform and/or (b) printed copies of the manuscript made from microform."

Signature 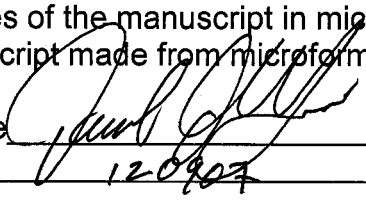

Date 12-09-07

University of Washington

Abstract

The Dynamic Interactome: A Proteomic Investigation of Ligand-dependent HSP90 Complexes

Jacob J. Gano

Chair of the Supervisory Committee:
Associate Professor Biochemistry
Toshio Tsukiyama

The molecular chaperone HSP90 and its many co-chaperones function to fold and fully activate a plethora of proteins involved in virtually every cellular process including oncogenesis. The ATPase activity of HSP90 is essential for its cellular functions and it is believed that conformational changes elicited by ATP binding and hydrolysis are required for client protein loading and refolding in a process referred to as the ATPase cycle. The discovery that HSP90 binds ADP at a 10-fold higher affinity than ATP led to the possibility that ADP binding may also have some biological significance and the particular nucleotide bound to HSP90 may control its interactions with client proteins and co-chaperones and therefore altering functions within the cell. To better understand the biological functions of HSP90, several groups have attempted to systematically identify HSP90 interacting proteins using proteomic and genetic approaches; however, these studies were conducted under single experimental conditions-producing a static picture of the HSP90 interactome without regard to the nucleotide-bound state of HSP90. With the development of quantitative proteomic tools, it is now possible to observe changes in the HSP90 interaction

network on a proteome-wide scale under various experimental conditions. In this work, we show the human HSP90 interactome to be dynamic with respect to nucleotide and drug ligands. We purified TAP-tagged HSP90 complexes in the presence of the HSP90 ligands ATP, ADP and the pharmacological inhibitor geldanamycin and observed changes in the relative abundance of constituents of these complexes using label-free quantitative mass spectrometry. In addition to identifying new HSP90 interacting proteins, we identified several putative ligand-dependent interactions including a geldanamycin-dependent HSP90 complex enriched for core subunits of the transcriptional apparatus, suggesting possible mechanisms of action for the activity of this drug. We go further to characterize a novel ADP-dependent interaction with the co-chaperone CHORDC1 (Chp1) and link the CHORD domain to ADP-stimulated interactions.

Table of Contents

List of Figures

List of Tables

Acknowledgments

The author wishes to acknowledge the CMB training grant and the Clinical Department of the Fred Hutchinson Cancer Research Center for financial support. He also thanks the FHCRC Proteomics Facility staff including Phil Gafken and Jason Hogan. He especially thanks Michele Karantsavelos and the other MCB administrators including MaryEllin Robinson, Diane Darling and Jayne Muir for their assistance. He would also like to acknowledge his wife Joan Haab for all the support, love and encouragement.

Introduction

HSP90 Function and Co-chaperones

The cell has evolved specialized coping mechanisms to deal with sudden environmental changes. Stressors such as non-physiological variations in temperature, pH, and nutrient availability can perturb protein stability and derail essential cellular processes. To survive these insults, the cell must either degrade these misfolded, inactive proteins or salvage them through the use of molecular chaperones. Chaperones are a broad class of proteins functioning to guide *de novo* folding of newly synthesized proteins, re-fold denatured proteins trapped in non-productive intermediates, and stabilize inherently unstable mature proteins in active conformations. Arguably one of the most studied groups of chaperones is the family of heat shock proteins. These proteins, aptly named, were originally discovered by virtue of their increased expression after sudden increases in temperature. Almost four decades after their first discovery, the functions of these proteins are finally starting to be understood on the molecular level. One of the best characterized members of this group is the 90 kDa heat shock protein, HSP90, which assists stress-denatured protein refolding as well as maintaining proteins in folded, active conformations under normal physiological conditions.

The dimeric HSP90 is a highly abundant molecular chaperone, comprising about 1-2% of the total protein content in cells. In mammals, yeast and plants there are at least two major isoforms of HSP90 which are nearly identical and are commonly considered to be functionally equivalent: HSP90β is constitutively expressed, while HSP90α is expressed at a basal level and is induced by stressors such as heat shock. Both isoforms can readily form heterodimers. There is little evidence that these proteins function differently, so both isofroms will be referred to simply as HSP90 and distinctions will be made as necessary. This essential protein assists stress-denatured and inherently unstable proteins to regain and maintain their native conformations. In contrast to other chaperones, HSP90 functions almost exclusively in later stages of protein folding by correcting relatively subtle, yet destabilizing conformational anomalies. Another unique characteristic of HSP90 is that it any denatured or unstable protein may not serve as a substrate. Rather, it functions to refold and stabilize *specific* proteins. These substrate proteins, called "client proteins" are dependent upon HSP90 for their stability or full activity. Interestingly, HSP90 client proteins are members of virtually every class of protein: transcription factors, kinases, metabolic enzymes, structural proteins and receptors- all with functions in diverse cellular processes. The fact that these client proteins do not share common structural features or functional roles in related biological pathways precludes a direct and simple

understanding of HSP90 function on a cellular level. The mechanisms that restrict HSP90 activity to a specific set of structurally and functionally unrelated client proteins are poorly understood and remain to be the focus of intense research.

HSP90 Structural Domains

The structure of HSP90 is generally described by three domains: the C-terminus responsible for dimerization (1) and binding of cofactor proteins called co-chaperones, the middle domain known to interact with client proteins (2,3), and the N-terminal ATPase domain known to bind p23 and other co-chaperones (Figure 1). HSP90 is a member of the GHKL ATPase family, sharing significant homolougey in the ATPase domain with DNA gyrase B and MutL DNA mismatch repair proteins and histidine kinases (4,5). These proteins are functionally diverse but contain significant homolougey in the ATPase domain and bind ATP through a mechanism distinct from other ATPases (6).

HSP90 ATPase Domain- Early attempts to detect HSP90 ATPase activity were unsuccessful, casting into doubt HSP90 as an ATPase (7). However,

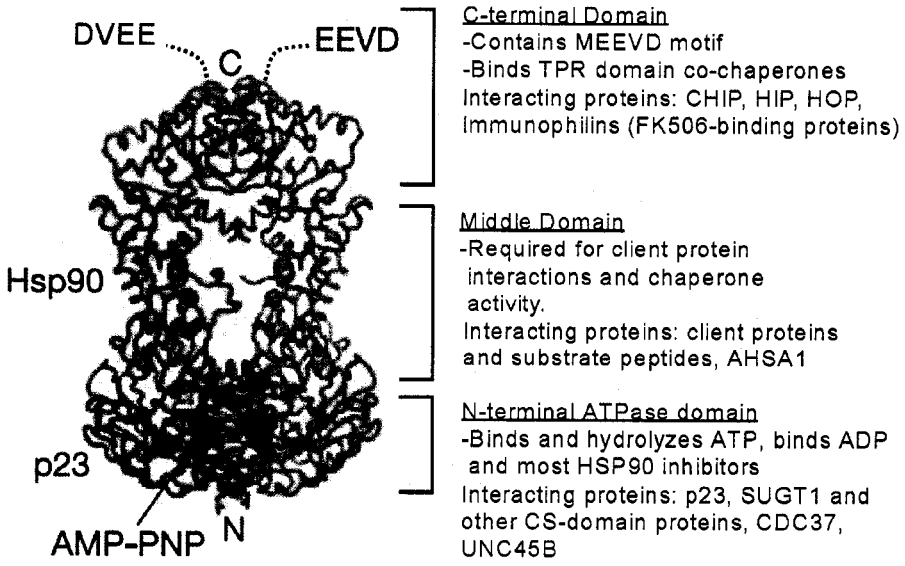

Adapted from Ali, et al (2006)

Figure 1. Crystal structure of the yeast HSP90 homolouge (Hsp82p binding the non-hydrolyzable ATP analog AMP-PNP in complex with the p23 homolougeue Sba1p (8). The domain structure is shown with a brief description of the function and selected binding proteins.

the first crystallographic studies of the ATPase domain conclusively showed the binding of ATP, ADP and the HSP90 inhibitor geldanamycin (9,10). ATPwas shown to be buried relatively deeply inside the active site with a loop of residues forming a "lid" structure much like that observed for DNA gyrase B. It is believed that this nucleotide "trapping" mechanism commits HSP90 to ATP hydrolysis once ATP is bound and nucleotide exchange is only possible after hydrolysis (11). The development of more sensitive assays allowed

several groups to report measurable and reproducible ATPase activities for HSP90. The *in vitro* ATPase activity is relatively weak, with a k_{cat} of 9×10^{-5} (12); in contrast, some ATPases are able to hydrolyze well over 200 molecules of ATP per second. However weak, the ability of HSP90 to bind and hydrolyze ATP is indispensable for its functions *in vivo*. Indeed, mutations that perturb the ATP binding or hydrolytic activity have been shown to be lethal in yeast (13-15).

Both genetic and biochemical studies have identified residues that are important for ATPase activity. To date, at least 20 point mutations have been reported that affect one or more aspects of HSP90 function (16). These mutants have proven useful in determining the effects of nucleotides on HSP90 interactions and were the first studies to functionally link ATPase activity to the binding and release of substrate proteins and co-chaperones. Two point mutants are particularly relevant to this work. The D93N (D79N in yeast) mutation destroys nucleotide binding through removal of a critical aspartic acid making hydrogen bonds with the N6 nitrogen in the adenine base of the nucleotide (15). This mutation was shown to be lethal in yeast and disrupts interactions with the co-chaperones, underscoring the importance of ATP binding in the overall function of HSP90 (16). Glutamic acid 47 in the ATPase site serves as a general base for the ATP hydrolysis reaction.

Mutation of this residue to aspartic acid is lethal in yeast and renders HSP90 unable to hydrolyze ATP; however, this mutant binds ATP with affinity comparable to the wild type enzyme (14,17,18). Similar activity was observed for the analogous mutation in the ATPase domain of the GHKL ATPase DNA gyrase B (19). The E47A mutant (E33A in yeast) can bind to substrate polypeptides but is deficient in release, suggesting that ATP hydrolysis is not required for substrate binding, but appears to facilitate release. This mutant was used as a kinetic trap for HSP90 interactors in a yeast two hybrid screen by virtue of its deficiency in releasing substrates (13).

Structural Effects of Nucleotides

Several investigations have focused on obtaining mechanistic data linking ATP binding and hydrolysis to the conformational changes believed to be responsible for the chaperone activity (20,21). It is hypothesized that the apo- (empty) and ADP-bound form assumed a free, relatively unrestrained conformation with the monomers joined only at the C-terminal dimer interface. Upon ATP binding, the N-termini are brought in close proximity and the structure becomes closed in a fashion likened to a "molecular clamp" (22-24). In support of this hypothesis, a low-resolution crystallographic model (3.8Å) has been obtained for the yeast HSP90 bound to the non-hydrolysable ATP

analog AMP-PNP (Figure 1) (8). This clearly shows HSP90 in a closed conformation with the two ATPase domains in close proximity producing a closed, clamp-like structure. It is this closed ATP-bound conformation that is predicted to interact with client proteins; however a structure of HSP90 in complex with a client protein substrate has not been determined. Recently, EM analysis of the *E. coli* HSP90 homolouge HtpG bound to ATP and ADP revealed significant conformational rearrangements dependent upon the nucleotide-bound state that differ from the yeast HSP90 crystal structure (Figure 2) (25). The ATP-bound form of HtpG assumes an extended, closed or open conformation that exposes hydrophobic surfaces known to interact with client proteins. The ADP bound form also assumes an open and closed conformation but these structures are much more compact than observed in the ATP-bound form and the hydrophobic regions are buried. The conformational changes that are thought to occur during ATP hydrolysis are thought to do the "work" of refolding client proteins. And finally, the unbound state assumes an open conformation presumably to allow for client protein loading. Similar structural evidence for full-length metazoan HSP90 is lacking with only one low-resolution study showing a linear antiparallel conformation without ligand, and a ring shape arrangement with ATP is bound suggesting a closed ATP-bound form (26). Despite the lack of high-resolution data on the specifics of the conformational changes associated with particular HSP90

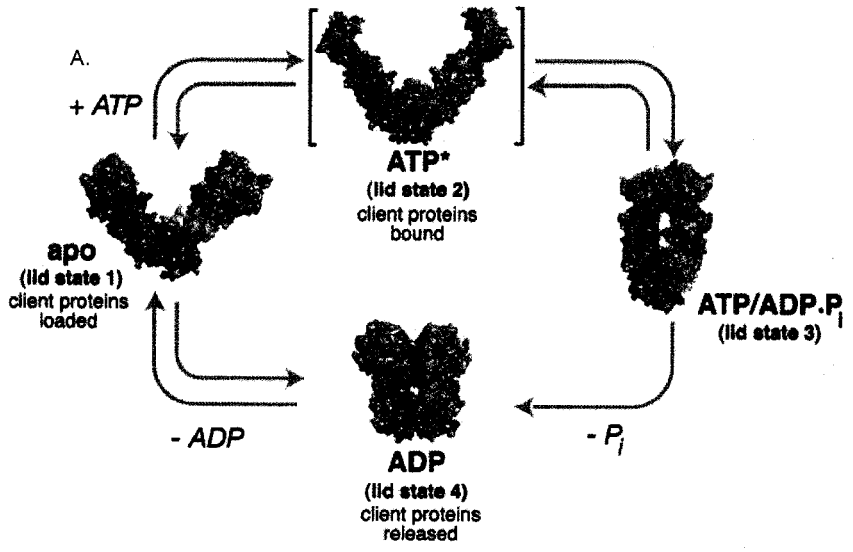

Figure 2. A schematic representation of the conformational changes observed for different nucleotide-bound states for the *E. coli* HSP90 homolouge HtpG. The ATP bound states are either open, or closed with hydrophobic regions in the middle domain exposed. The ADP-bound state is compressed, where the hydrophobic areas in the middle domain are buried and the dimer is closed. The apo state is open, yet still having a compressed middle domain as in the ADP-bound form.

ligands, it is becoming clear that distinct conformational states are induced by particular nucleotide ligands. A few important questions are: how do nucleotide-induced conformations affect interactions with client proteins or cofactors and how do HSP90 inhibitors affect these conformations? This information would begin to forge a link between the *in vitro* biochemical activities of HSP90 and its functions *in vivo*.

Mechanism of ATP hydrolysis- Several studies have focused upon understanding the mechanism of ATP hydrolysis. It was originally believed that the ATPase activities of the HSP90 monomers were cooperatively linked

and conformational changes allowing the two ATP-bound N-termini to come in contact was absolutely required for ATP hydrolysis. This hypothesis was modeled after the observed mechanisms for other GHKL ATPases whereby residues from the opposing monomer appear to be assisting in catalysis. However, this idea has been challenged by the observation that independent monomers of HSP90 that lack the C-terminal dimerization domain still retain a measurable, yet reduced ATPase activity- about ten-fold lower than the wild type dimer (27). This suggests that ATPase activity is not dependent upon interactions between the ATPase domains of monomers (12,23). Furthermore, heterodimers between mutants lacking the ATPase domain and full-length HSP90 are not completely devoid of ATPase activity (27,28). Interestingly, one study showed that a heterodimer composed of both wild type HSP90 and a mutant that is unable to bind ATP retains ATPase activity similar that of the wild type homodimer (27). This suggests that merely the presence of the ATPase domain is required for this cooperative effect and that ATP binding by both monomers is dispensable. Supporting evidence for this activity comes from early kinetic measurements of the ATPase activities from monomeric N-terminal fragments. In these experiments, k_{cat} was not dependent upon the concentration of the monomers, even at high concentrations used in single turnover experiments (11). This suggests that either the functional interactions between the ATP-bound N-terminal ATPase

domains are very weak and require the entropic restraint supplied by the dimeric interface, or interactions between these domains are not necessary for hydrolysis. Unfortunately, well-resolved crystallographic evidence for this apparent cooperative activity is currently lacking.

Much less is known about the effects of ADP binding. Early studies of the HSP90 ATPase domain revealed that ADP binds with a four to ten-fold higher affinity *in vitro* (11) and appears to inhibit ATP binding. This activity presented the possibility that HSP90 function may be controlled by fluctuations in intracellular ATP:ADP ratios. Indirect support for this hypothesis comes from one study showing that ATP depletion in cells caused dissociation of HSP90 from client proteins and their eventual degradation by the ubiquitin proteasome- a hallmark feature of HSP90 inhibition (29). It was impossible from these experiments to discern whether HSP90 was binding ADP and whether the degradation of client proteins was a direct effect of this interaction. In support of these observations, several studies have shown ADP to be an inhibitor of the interaction between HSP90 and the co-chaperone p23 (16,21,30,31), thus lending credence to the idea that ADP alters HSP90 function. These results, combined with the fact that many HSP90 clients are involved in energy sensing and metabolism introduces the intriguing possibility that HSP90 may function as an ATP sensor *in vivo*. With only a few

exceptions, it is still largely undetermined how nucleotide-induced conformations affect HSP90 interactions with co-chaperones and client proteins.

HSP90 Client Proteins and Pharmacological inhibition of ATPase Activity

The essential roles of HSP90 are underscored by the growing list of substrate proteins known as "client proteins" functioning in several biological processes such as cell division, metabolism, signal transduction and immune function. A nearly complete list of HSP90 interacting proteins can be found at the Picard Lab website (32). The stability of these client proteins has been shown to be dependent upon HSP90 and disruption of HSP90 activity either through mutation or pharmacological inhibition leads to proteolytic degradation of the client protein and subsequent collapse of the associated biological pathway.

Much less is known about the mechanism and the structural elements that control HSP90s interactions with client proteins. This is almost entirely due to the fact that HSP90 only transiently and weakly interacts with client proteins. Furthermore, because client proteins have no sequence commonalities it is not possible to discern HSP90 interaction elements through the use of bioinformatic tools. To date, only a few structural features have been

attributed to HSP90-client interactions, the most common being surface charge and hydrophobicity (33). Mutagenesis studies have localized client protein interactions to hydrophobic regions of the HSP90 middle domain but the mechanism for selectivity remains obscure (2,34,35). Recently, Citri and colleagues have identified a poorly defined surface feature common to all known kinase clients and postulate that neutral and negative charges in this region are responsible for HSP90 interactions (36). Several groups have identified CDC37 in complexes with HSP90 and kinase client proteins and have speculated that this protein acts as an adaptor molecule that supplies specificity for particular kinases. The possibility exists that this mechanism may be used on other client protein types; however, no additional co-chaperones have been identified that confer specificity in this way.

One common element of all client proteins is that they rely upon HSP90 ATPase activity for their stability and/or function. In most studies, client protein complexes are shown to be destabilized by pharmacological inhibition of the HSP90 ATPase activity and the client is then degraded through a ubiquitin proteasome pathway (for review, (37)). Temperature sensitive mutants of HSP90 have also been used to identify HSP90-dependent client proteins. It is generally thought that HSP90 clients are inherently unstable and assume misfolded, aggregated conformations in the absence of HSP90

activity. In the case of nuclear hormone receptors, however, HSP90 activity is required to bring the receptor in a conformation permissive to ligand binding and has less effect upon the overall stability of the protein *per se*. Furthermore, it is not understood how proteins is acquire functional interactions with HSP90. It has been proposed that mutations that slightly destabilize proteins allow for these proteins to serve as HSP90 substrates. Indeed, several mutated or chimeric proteins have been found to be chaperoned by HSP90 while their wild type counterparts are not (38,39). However, these interactions are contentious and only represent a small fraction of the HSP90 interactome, which is largely comprised of unmutated proteins. It has also been proposed that client proteins within critical biochemical pathways evolve dependencies upon HSP90 activity and that HSP90 then serves as a master regulator for these cellular functions and a capacitor for morphological evolution (40).

HSP90 has recently become an important target for anticancer therapies due to its role in the stability of proteins positioned at critical nodes of oncogenic pathways. HSP90 client proteins are involved in virtually every pathway associated with cancer including, but not limited to mitosis, CDK signaling and cell cycle progression, ATP metabolism, growth factor signaling, metastasis, angiogenesis, and cell motility. Accordingly, there is much interest and

investment in finding HSP90 inhibitors. The antibiotic Geldanamycin, named for its bright golden color, was the first HSP90 inhibitor to be identified. It was selected in a screen for compounds that revert the Src-transformed phenotype of cultured human cells (41,42). It was later determined that HSP90 is a selective inhibitor of the HSP90 ATPase (43). In the past 15 years several other small molecule HSP90 inhibitors have been discovered that represent several diverse chemical families. Geldanamycin proved to have poor pharmacokinetic properties and hepatic toxicity. However, analogues of geldanamycin are currently under investigation for several cancer types. 17-AAG and 17-DMAG are in government-sponsored clinical trials for patients with lymphoma and advanced solid tumors and for melanoma patients in the UK.

On a cellular level, the functional consequence of HSP90 inhibition is apoptosis arising from the degradation of client proteins essential for cell division and survival. Mounting evidence supports the idea that tumor cells are more sensitive to HSP90 inhibition than normal cells. One breakthrough paper by Kamal, et al. attempted to explain this phenomenon by showing that HSP90 exists in two states: one state is referred to as an "inactive state" existing in normal cells where HSP90 is in a low-affinity complex with HSP70 and client proteins and has a very low ATPase activity; the other state existing

in tumor cells is called the "activated state" where the ATPase activity is higher and HSP90 exists in a high-affinity complex with not only HSP70 and the client protein, but a cohort of other co-chaperones including HOP and p23 (44). This activated complex binds to geldanamycin with 50-fold higher affinity in tumor cells compared to the inactive complex found in normal cells. These results give a mechanistic basis for the selective killing of tumor cells by HSP90 inhibitors. Another perspective comes from the idea that tumor cells suffer from severe chronic stress: hypoxia, acidosis, nutrient deprivation, and mutation. It is this stressful condition that leads to a requirement for HSP90 activity; whereas normal cells do not encounter these stressors and therefore are less dependent upon the activity of stress proteins such as HSP90. A third concept is that tumor cells experience a condition termed oncogene addiction whereby the cell evolves in the context of activated oncogenes and thus becomes dependent upon their activities for survival. Because HSP90 controls the stability and activity of many oncogenes, inhibition of HSP90 therefore collapses the cells' lifeline. Very little is currently understood about the processes leading to HSP90 dependency and this remains to be a central question in this field.

Function of HSP90 Co-chaperones

It is well understood that HSP90 does not function in an isolated state. Rather, it forms transient interactions with several non-client protein co-factors termed co-chaperones. It has been proposed that interactions with these co-chaperones alter HSP90 activity and govern client protein interactions; however, the mechanisms are poorly understood. To date, HSP90 co-chaperones have been shown to either interact with the N-terminal ATPase domain, the middle domain or a highly conserved MEEVD motif located at the final 5 amino acids of the C-terminus (Figure 1).

One of the most widely studied co-chaperones binding to the HSP90 ATPase domain is the small acidic protein p23. p23 was first discovered as a member of nuclear hormone receptor complexes containing HSP90 (45). The HSP90-p23 complex binds to the unliganded receptor complex, holding it in a conformational state permissive for ligand binding. After hormone binding, the complex translocates to the nucleus to activate transcription (46). p23 is not required for interactions between HSP90 and the progesterone receptor; however, it is thought to stimulate hormone binding (47,48). It was originally believed that p23 was a specific co-chaperone for nuclear hormone receptors. However, p23 has since been identified in several complexes not found to

contain nuclear hormone receptors. Perhaps the best understood function of p23 is that it binds selectively to HSP90 in the ATP-bound form (14,30,49,50). This interaction is believed to inhibit the HSP90 ATPase activity, locking it in the ATP-bound conformation in complex with client proteins. In the case of nuclear hormone receptors, this conformation is predicted to be essential for full ligand-binding activity.

CS-domain Containing Co-chaperones

The CS (CHORD and SGT1 domain) proteins are predicted to bind the HSP90 ATPase domain based upon their homolougey to p23 (51). This new family of proteins referred to as CS domain-containing proteins (CDPs) was identified using hidden Markov models designed to detect distant homolougey (Figure 3) (51). Although identified as putative HSP90 interacting proteins, none of these CDPs were tested for interaction with HSP90 in biochemical assays in this study. These findings did, however, identify several previously known HSP90 interacting proteins and laid the foundation for further investigation. Indeed, several other novel CS domain-containing proteins have since been shown to interact with the HSP90 N-terminus- analogous to the p23 interaction. Structural evidence also supports the hypothesis that the CS domain confers HSP90 binding. The solution structures of the CS

domains from the known HSP90 interactors SUGT1, p23 (PTGES3), and SIP (CACYBP) are highly similar in overall structure with a RMSD of 1.6 Å and the HSP90 binding surfaces appear to share similar charge distribution (52). These observations strongly suggest that all CDPs interact with HSP90. Data presented in this chapter support the assertion that the CS domain is a *bone fide* HSP90 interaction domain.

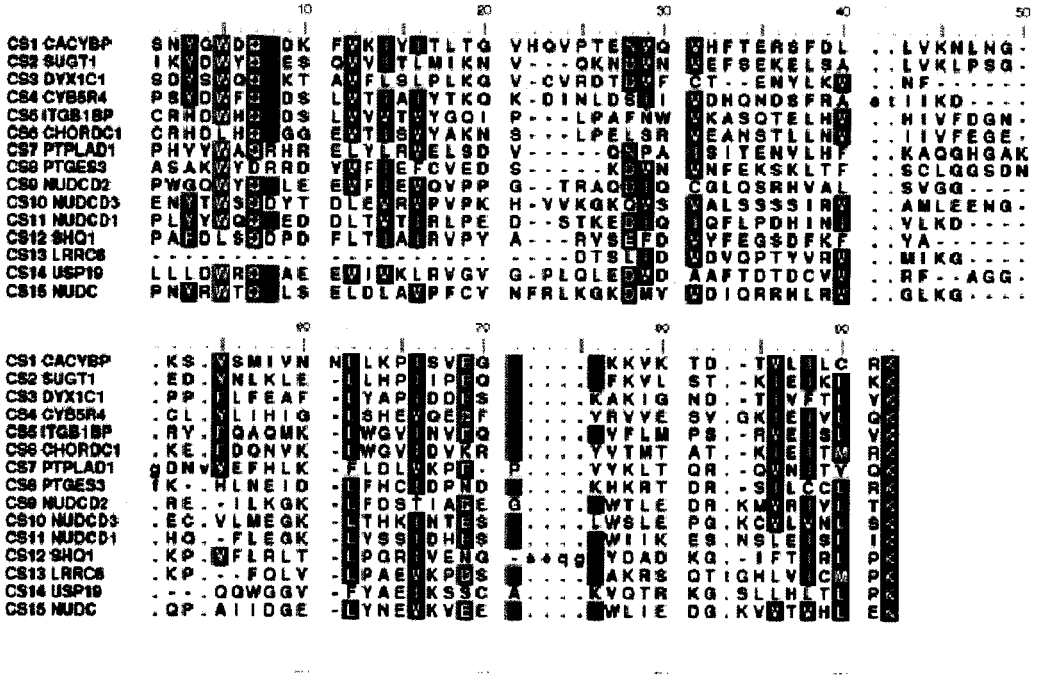

Figure 3. Protein alignment based upon alignment produced by Pfam.(53). CS domains from 15 CHORD domain-containing proteins aligned using hidden Markov models.

CS domain-containing proteins function in disparate biochemical pathways and cannot be grouped according to cellular function. The domain structure of these proteins is very diverse, with some members having enzymatic functions

such as phosphatase activity or NAD(P)H reductase activity (Figure 4 and Figure 5) . The only commonality amongst these proteins is their (putative) interaction with HSP90 through the CS domain. The CS-domain-containing protein SUGT1 (Sgt1p in yeast) interacts with HSP90 and this complex is believed to function in mitosis by linking kinteochore activation to proteolytic machinery via interactions with the SCF1 ubiquitin ligase (54-56). SUGT1 and HSP90 have also been shown to function in innate immunity against pathogenic infections (57-59). Another CS domain protein ITGB1BP2, or melusin functions in heart muscle to assist in recovery from mechanical stress (60,61). CYB5R4, a putative HSP90 interactor, is localized to the endoplasmic reticulum functions as a NAD(P)H reductase. CYB5R4 knockout mice are unable to manage antioxidant stress in pancreatic beta cells and develop early onset diabetes (62). Furthermore, NUDCD3 was recently shown to function as a chaperone for dynein (63). The fact that CS domain-containing proteins have such different functions introduces the possibility that these proteins have acquired HSP90 interactions for the purpose of recruiting HSP90 chaperone activity to specific cellular compartments, structures or complexes. The CS domain would therefore serve to anchor HSP90 to the site where chaperone activity is needed.

Despite possessing the conserved HSP90 interaction domain, it remains unclear whether CS domain-containing proteins behave similarly to p23 with respect to the nucleotide-bound state of HSP90. p23 has been shown by several groups to selectively interact with the ATP-bound HSP90. However, conflicting evidence exists for the influence of nucleotide or inhibitors on the HSP90-SUGT1 interaction. Catlett, et al determined that the presence of ATP disrupts SUGT1 interaction with HSP90 prepared from reticulocyte lysates. These experiments also showed, surprisingly, that inhibition of HSP90 by geldanamycin leads to increased binding of SUGT1 to HSP90 rather than disruption of the complex as would be expected from the inhibitory effects of geldanamycin on the p23-HSP90 interaction (54). However, in a separate study the HSP90-SUGT1 interaction was shown to be entirely independent of the nucleotide present in the lysates (55). A study using purified proteins showed that the HSP90-SUGT1 interaction was stimulated by ATP and demonstrated a weaker interaction without nucleotides (52). The CS domain-containing protein CHORDC1 (CHP-1) was also shown to be insensitive to ATP and HSP90 inhibition in assays using purified proteins (64). This raises the important question of whether p23 possesses unique structural elements

PTGES3 (p23)

TEBP_HUMAN[homo sapiens (human)] prostaglandin e synthase 3 (ec 5.3.99.3) (cytosolic prostaglandin e2synthase) (cpges) (telomerase-binding protein p23) (hsp90 co-chaperone) (progesterone receptor complex p23)
[160 residues]

Function: Binds HSP90 in ATP-dependent manner. Associates with HSP90-nuclear hormone receptor complexes and stimulates ligand binding.

CACYBP (SIP)

Q5R371_HUMAN[homo sapiens (human)] calcyclin binding protein (growth-inhibiting gene 5 protein)
[228 residues]

Function: Calcium-dependent Ubiquitylation. Associates with E3 ligases (SIAH).

SUGT1 (Sgt1)

SUGT1_HUMAN[homo sapiens (human)] suppressor of g2 allele of skp1 homolog (sgt1) (putative 40-6-3protein)
[365 residues]

Function: Interacts with HSP90 and directs interactions with SCF ubiquitin ligase and assists in kinetochore assembly.

DYX1C1

DYXC1_HUMAN[homo sapiens (human)] dyslexia susceptibility 1 candidate gene 1 protein
[420 residues]

Function: Unknown. Identified as a candidate gene for dyslexia.

CYB5R4

Q7L1T6_HUMAN[homo sapiens (human)] cytochrome b5 reductase 4. (cytochrome b5 reductase 4)
[521 residues]

Function: NAD(P)H reductase activity.

ITGB1BP2

ITBP2_HUMAN[homo sapiens (human)] integrin beta-1-binding protein 2 (melusin)
[347 residues]

Function: Contains CHORD domain. Required for recovery from mechanical stress in heart tissue.

CHORDC1

Q6IN49_HUMAN[homo sapiens (human)] cysteine and histidine-rich domain-containing protein 1
[332 residues]

Function: Contains CHORD domain. Binds to HSP90. Required for pathogen resistance in plants and possibly mammals.

Figure 4. Domain structures of all known CS-domain containing proteins. Members of this family have diverse functions. The graphical domain representations were created by Pfam (53). CS domains appear as green circles with the text "CS". Other functional domains are indicated.

NUDC

NUDC_HUMAN[homo sapiens (human)] nuclear migration protein nudc (nuclear distribution protein chomolog)
[331 residues]

Function: Binds to HSP90 via the CS domain. Required for end-on spindle attachment at the kinetochore in humans and nuclear distribution in fungi.

NUDCD1

Q9BVR5_HUMAN[homo sapiens (human)] nudc domain containing 1
[583 residues]

Function: Unknown

NUDCD2

NUDC2_HUMAN[homo sapiens (human)] nudc domain-containing protein 2
[157 residues]

Function: Unknown,

NUDCD3

NUDC3_HUMAN[homo sapiens (human)] nudc domain-containing protein 3
[361 residues]

Function: Required for dynein-mediated spindle attachments during mitosis.

LRRC6

LRRC6_HUMAN[homo sapiens (human)] leucine-rich repeat-containing protein 6 (leucine-rich testis-specificprotein) (testis-specific leucine-rich repeat protein)
[466 residues]

Function: Unknown.

USP19

UBP19_HUMAN[homo sapiens (human)] ubiquitin carboxyl-terminal hydrolase 19 (ec 3.1.2.15) (ubiquitinthioesterase 19) (ubiquitin-specific-processing protease 19)(deubiquitinating enzyme 19) (zinc finger mynd domain-containingprotein 9) (fragment)
[1371 residues]

Function: Has putative terminal ubiquitin thioesetease activity and may deubiquitylate proteins.

PTPLAD1 (B-ind1)

Q9P035_HUMAN[homo sapiens (human)] protein-tyrosine phosphatase-like a domain-containing protein 1 (butyrate-induced protein 1) (protein b-ind1)
[373 residues]

Function: Induced by sodium butyrate. Forms complexes with Rac1 and appears to regulate JNK signaling. Has putative phosphatase activity.

SHQ1

Q6PI26_HUMAN[homo sapiens (human)] protein shq1 homolog
[577 residues]

Function: Based upon homology to the *S. cerevisiae* this protein is required for rRNA processing.

Figure 5. Domain structures of all known CS-domain containing proteins. Members of this family have diverse functions. The graphical domain representations were created by Pfam (53). CS domains appear as green circles with the text "CS". Other functional domains are indicated.

either within or outside the CS domain that contribute to selectivity for the ATP-bound HSP90. Indeed, p23 contains an additional β-strand that is conserved amongst direct p23 homolouges in other species, but is not represented in other CS-domain containing proteins (52). The effects of nucleotides on CS proteins were not, however, conducted in tandem with p23 serving as a positive control, so no solid conclusions can be drawn. Notably, several experiments in this work test the ability of a panel of CS domain-containing proteins to bind HSP90 in the presence of ATP, ADP and geldanamycin where p23 is supplied as an internal reference.

CDC37, AHSA1, and UNC45A

The co-chaperone cdc37 was first discovered in early screens in yeast identifying proteins involved in cell cycle progression and was later shown to be required for cdc28 kinase activity. Subsequently, the human cdc37 (CDC37) homolougeue was found in complexes containing the tyrosine kinase v-Src and a 90 kDa protein later identified to be HSP90 (65). These discoveries laid the groundwork for further experiments that assigned cdc37 as a kinase-specific HSP90 co-chaperone. The crystal structure of the human CDC37 and yeast Hsp90 revealed a possible mechanism by which CDC37 binds to the lid structure of the Hsp90p ATPase site and inhibits ATPase

activity by hydrogen bonding a critical residue involved in ATP hydrolysis, E33 (E47 in human HSP90) (66,67). This is predicted to hold Hsp90p in a conformation permissive for loading kinase client proteins into the complex. CDC37 also makes contact with both HSP90 and kinase client proteins, forging a direct bridge between co-chaperone and client. The selectivity of the HSP90-CDC37 complex for kinase client proteins is rationalized by the physical interactions between the C-terminus of CDC37 and structural factors contained within the catalytic domain of the kinase. However, the HSP90-CDC37 complex does not bind all kinase clients, despite a high degree of conservation in the kinase domains. For example, CDK4 interacts strongly with CDC37, whereas CDK2 does not (68). It is still unknown how the HSP90-CDC37 complex is able to selectively bind certain kinases and not others, but is becoming clear that CDC37 serves as a kinase-specific co-chaperone for HSP90. Interestingly, despite its extensive interactions with the ATPase domain, the HSP90-CDC37 interaction does not change according to the nucleotide-bound state of HSP90 (69). Furthermore, pharmacological inhibition by the HSP90 ATPase inhibitor geldanamycin does not disrupt the HSP90-CDC37 interaction (69,70). It is currently unknown what role CDC37 has in the disruption of HSP90 complexes containing kinase clients.

Recently, AHSA1 was identified to be an activator of the HSP90 ATPase. Little is known about the cellular functions of AHSA1, but one study has shown a function for folding the mutant cyctic fibrosis transmembrane conductance regulator, implicating AHSA1 and protein folding in the pathology of this disease (71). AHSA1 binds the middle domain of HSP90 and positions a catalytic argenine residue from the middle domain into the ATPase active site (72-74). Some evidence supports a role for the ATPase activating function of AHSA1 in client protein activation (75). From the available literature, it is difficult to determine whether AHSA1 binds tighter to the ATP-bound HSP90 because this has not been tested directly. However, indirect evidence comes from a study where the yeast homolouge, Aha1p was shown to interact more strongly with the ATP-locked E33A mutant than wild type HSP90 in a yeast two hybrid assay (13). The activity of AHSA1 is controlled through competitive binding with CDC37, the co-chaperone HOP, p23 (75) and a recently identified HSP90 co-chaperone UNC45A (76,77). UNC45A was shown to inhibit HSP90 ATPase activity through binding to a novel TPR interaction surface at the N-terminus of HSP90. The effect of nucleotides on this interaction is currently unknown and the only known cellular function assigned to UNC45A is its role in myosin function (77).

TPR-domian Co-chaperones-

The C-terminus of HSP90 carries a highly conserved MEEVD motif known to interact with several co-chaperones containing TPR (tetratricopeptide repeat) domains. The TPR is a repeat of 34 amino acids appearing in various copy numbers and positions in a diverse group of proteins and known to act in protein-protein interactions and protein complex assembly. Remarkably, interactions at the C-terminus by TPR domain co-chaperones can affect the binding of co-chaperones at the N-terminus and *visa versa* (16) suggesting a mechanism by which structural affects of co-chaperone binding can be transmitted from one binding site to another.

Much like CS domain-containing proteins, TPR proteins often carry at least one of several functional domains such as a phosphatase or a peptidylprolyl isomerase domain and some TPR domain proteins carry chaperonin activity independent of their association with HSP90. It is not possible to predict HSP90 interactions simply based upon the presence of a TPR domain because not all TPR proteins interact with HSP90. SUGT1 carries a CS domain and a TPR domain, but interacts with HSP90 only through the CS domain (52). Furthermore, all TPR containing co-chaperones do not bind to HSP90 with similar affinities, suggesting a competitive model for co-chaperone

binding. It has been suggested that subtle variations in the sequence of the TPR domain govern binding affinity for HSP90. HSP90 interactions are not determined solely by the TPR domain, however. It has been shown that elements within and adjacent to the TPR domain can alter affinity for HSP90 (78).

One of the most studied groups of HSP90-binding TPR proteins is the immunphilin peptidylprolyl isomerases (FKBP4, 5 and CPR6). These proteins were first identified in complexes containing nuclear hormone receptors, however they are also observed in other HSP90-client protein complexes. The co-chaperone activity of these proteins is required for full maturation, ligand binding and nuclear translocation of hormone receptors. Interestingly, some studies show HSP90-hormone receptor complexes can exert selectivity for particular immunophilin co-chaperones, suggesting that selectivity determinants may originate from the receptor client protein rather than the co-chaperone. Little is known about how nucleotides and HSP90 inhibitors affect these interactions.

The TPR co-chaperone HOP (HSP70/HSP90 organizing protein), interacts with both HSP90 and HSP70 simultaneously through its multiple TPR domains and functions as a linker between the HSP70 and HSP90 chaperone systems.

It is believed that HOP, also known as STIP or Sti1, is believed to pass client proteins from HSP70 to HSP90 for completion of the final folding steps leading to activation (79-81). It has been established that HOP inhibits the ATPase activity of HSP90 and that this activity involves not only interactions with the C-terminal MEEVD motif of HSP90, but possibly residues in the N-terminal ATPase domain (82,83). Remarkably, the binding of HOP to HSP90 can displace geldanamycin from the ATPase site (82). This mechanism is believed to be non-competitive. The presence of HOP does not affect ATP binding, but inhibits conformational changes that stimulate ATP hydrolysis, namely the association of the N-terminal ATPase domains of the HSP90 dimer (83,84). Little is known about the effects of nucleotides on the HSP90-HOP interaction. In pure protein systems HOP has been shown to bind preferentially to the ADP-bound HSP90 and the presence of ATP inhibits this interaction (83,85). The yeast HOP (Sti1p) does not show any preference for the nucleotide-bound state of wild type HSP90 when complexes were purified from whole cell lysates (16). However, the HSP-HSP90 interaction was reduced in the ATP-locked E33A mutant which binds ATP, but lacks the ability to hydrolyze it. These results suggest a role for ATP hydrolysis and/or ADP binding in the destabilization of the HSP90-HOP interaction.

CHIP (c-terminus of HSC70-interacting protein) is an E3 ubiquitin ligase that associates with the MEEVD motif at the C-terminus of both HSC70 and HSP90 (86). This interaction is mediated through a TPR domain situated at its C-terminus. It is hypothesized that CHIP functions in protein quality control to ubiquitylate proteins that are chronically associated with chaperones due to severe folding defects. CHIP is thought to be a switch that turns a protein from a futile refolding pathway to a degradation pathway. One of the best studied CHIP substrates is the glucocortocoid receptor (GR). When CHIP binds to the C-terminus of HSP90, p23 is displaced from GR complexes and the receptor is concurrently ubiquitylated and degraded. In addition, CHIP displaces the TPR domain co-chaperone HOP by competitively binding the MEEVD motif at the C-terminus of HSP90, supporting yet another mechanism of receptor deactivation(87). Other important CHIP substrates are HSP90 client proteins: p53, erbB2 (88). Geldanamycin treatment causes increased binding of CHIP to HSP90 leading to ubiquitylation and proteosomal degradation of client proteins such as erbB2. However, the activity of CHIP cannot totally account for the proteolytic effects of HSP90 inhibition as the client protein ErbB2 is still degraded by geldanamycin in CHIP-/- cells (88).

Chapter 1: A proteomic investigation of Ligand-dependent HSP90 complexes

Systems Biology Investigations of the HSP90 interactome

It is very apparent that the multitude and complexity of HSP90 interactions requires tools designed to identify and monitor the constituents of dynamic protein complexes. Several attempts to catalog the HSP90 interactome have been made using systems biology tools. The first approach to studying HSP90 interactions was a heroic effort by Zhao and colleagues that combined tandem affinity purification, yeast two-hybrid, and genetic and chemical interaction studies to produce a comprehensive interaction map of the yeast HSP90 homolougeue (89). This study identified 198 physical interactions and 451 genetic or genetic/chemical interactions and presented a new role for HSP90 in several biological pathways such as chromatin remodeling. Concurrently, another group conducted a yeast two-hybrid interaction screen using a kinetically-trapped yeast HSP90 mutant to identify several new HSP90 Interactors, several of which appear to interact selectively with the ATP-bound HSP90 (13). Remarkably, there appears to be very little overlap in the proteins identified from these two independent screens despite using similar methods. However, the commonalities between the two are valuable as they may represent the most robust of HSP90 interactions.

The yeast HSP90 interactome studies are important because the use of multiple comprehensive genome/proteome-scale techniques provides a level of resolution currently unavailable to researchers studying the human proteome. However, protein homologueies and analogous biochemical pathways are limited between yeast and human cells, so direct comparisons are rare. Furthermore, the idea that HSP90 and its interacting proteins co-evolve (90,91) suggests that these interactions may be dependent upon the specific natural histories of the species under investigation. Several groups have attempted proteomic investigations of the human HSP90 interactome in tumor cell lines using purified HSP90 complexes and mass spectrometry. Before these studies, HSP90 interactions from human cells were identified un-systematically, usually through the identification of HSP90 as a member of other complexes under investigation.

The first proteomic experiment in human cells reported by Falsone, et al utilized an antibody-based purification technique where HSP90 complexes were immunoprecipitated and interacting proteins were identified from 1D polyacrylamide gel slices (92). This attempt identified very few known HSP90 interacting proteins and was enriched for glycolytic and ribosomal proteins. These results provided a case for HSP90s involvement in energy metabolism

and protein synthesis; however, ribosomal proteins and glycolytic enzymes are commonly considered to be contaminants in immunoprecipitates partly because of their great abundance in cells. Furthermore, the in-gel isolation technique used in this study, while being adequate for identification of particular protein species, does not give a comprehensive inventory of protein complexes. Rather, this method is much more biased toward proteins of interest to the researcher based upon discretionary criteria such as appearance or abundance of particular protein species in the gel.

Another group used similar methods to identify several new HSP90 interacting proteins (93). This study used immobilized HSP90 antibodies and high salt washes to purify complexes. 2D gel electrophoresis was then used to gain increased separation of the interacting proteins. This method was much more successful in identifying several known HSP90 interactors such as the immunophilin FKBP52, HOP, PIH1 and the CS domain-containing proteins SUGT1 and NUDC. This study did not identify a significant number of known HSP90 client proteins, however. The majority of identifications were co-chaperones. This is not surprising considering these proteins are the most abundant proteins in HSP90 complexes. Client proteins, on the other hand, are bound by HSP90 only transiently and are probably not abundant enough in HSP90 complexes to be visible on gels.

Falsone, et al recently published another proteomic method that focused specifically upon identifying client proteins of HSP90 (94). This method capitalized on the fact that many HSP90 client proteins are ubiquitylated before being degraded after treatment with HSP90 inhibitors. HSP90 and the proteasome were simultaneously inhibited in cultured cells and the insoluble, ubiquitylated protein fraction was purified and subjected to 2D electrophoresis and tandem mass spectrometry. This experiment indirectly identified several putative HSP90 interacting proteins; however, the data lacked the majority of known HSP90 client proteins such as receptor tyrosine kinases, IkB kinases, and transcription factors. It is not possible to discount the possibility that these proteins are ubiquitylated as a secondary affect of HSP90 inhibition or proteasome inhibition and not due directly to the loss of HSP90 binding. A complementary study was recently published showing proteome-wide changes in protein abundance in cells treated with geldanamycin (95). This method used a method of isotopic labeling called ICAT to quantify proteins up and down regulated by HSP90 inhibition from whole cell lysates. Ideally, the two reports would show some overlap in identified proteins. One would expect some ubiquitylated proteins identified in the Falsone, et al study would be reported in this study as proteins downregulated after treatment with geldanamycin. Remarkably, these studies did not identify a single protein in

common. It should not be overlooked that these two studies were conducted under very different conditions and in different cell lines and therefore would be expected to differ to some degree. Furthermore, the methods currently used for proteomic analysis are only able to identify peptides from a small fraction of proteins present in a sample, so proteins common to both experiments may have been overlooked.

The above efforts have produced variable results depending upon the method used and at best have only produced a static picture of the HSP90 interactome. While developing a comprehensive list of proteins that interact with HSP90 is certainly an important goal, there is still much to be learned about the functions of these interactions. One outstanding question in this field is how the various constituents of HSP90 complexes change according to the nucleotide-bound state of HSP90. One study published during the preparation of this dissertation reported a comprehensive analysis of the yeast HSP90 interactions with the yeast HOP (Sti1p), p23 (Sba1p) and immunophilin CYP40 (Cpr6p) (16). This study looked at the dynamics of HSP90 interactions when these complexes were purified in the presence of nucleotide ligands. This study showed that the dynamics of HOP and CYP40 binding to HSP90 are not affected similarly with respect to the nucleotide-bound state of HSP90 despite the fact that these TPR-domain containing proteins have both been

shown to bind the C-terminal MEEVD motif of HSP90. CYP40 seems to bind HSP90 only when bound by ATP (AMP-PNP), whereas the HOP interaction appears to be nucleotide independent. While these experiments started to define the dynamics of the HSP90 interactome, it was focused only on a small subset of HSP90 interactors. The development of quantitative proteomic tools has opened the opportunity to observe the effects of nucleotides and other ligands on broader spectrum on HSP90 interactions. These observations may allow us to see the HSP90 interactome as a dynamic signaling network responsive to environmental conditions and biochemical stimuli on a proteome-wide scale. This dissertation presents data and interpretations from a proteomic investigation of the dynamics of the HSP90 interactome in response to altered nucleotide pools and pharmacological inhibition.

Results

Proteomic identification of HSP90 interactions altered by nucleotides and pharmacological inhibition

Several groups have reported proteomic studies of the HSP90 interactome; however, these studies were focused on documenting HSP90 interactions under a single experimental condition and were not designed to study how the dynamic interactions of this chaperone complex are influenced by HSP90 ligands. The recent advances in quantitative proteomics allow for comparison

of protein abundance changes under several experimental conditions; therefore, we used TAP purification (tandem affinity purification) and the label-free quantitative proteomics method of spectral counting to observe alterations in the human HSP90 interactome when complexes were purified in the presence of excess ATP, ADP or the HSP90 inhibitor geldanamycin.

We stably expressed a TAP-tagged wild type human HSP90α cDNA (referred to henceforth as HSP90) in the kidney epithelial cell line HEK293T and purified HSP90 complexes in the presence of the above HSP90 ligands. In addition to the wild type HSP90α, we chose to use the E47A mutant that is unable to hydrolyze ATP, yet able to bind nucleotide with affinities comparable to the wild type protein (14,17,18). This mutant has been shown to strengthen interactions between HSP90 and misfolded substrate peptides *in vitro* and is predicted to function as a kinetic trap to detect interactions with client proteins and co-chaperones *in vivo*. Indeed, Milson et al, demonstrated in a yeast two-hybrid screen that the analogous mutation in yeast strengthened the interaction between Sba1p (the yeast p23 homolouge) and HSP82- an interaction known to be reinforced when HSP90 is in the ATP-bound state (13). In addition to p23, several other HSP90 interactions were detected in this study that are known to be selective for HSP90 in the ATP-bound state; therefore, E47A is predicted to serve as a suitable probe in this system to

identify HSP90 interactions that are particularly strengthened by HSP90 in the ATP-bound state. TAP purifications were performed in three independent replicate experiments containing the following five experimental groups: 1) Empty vector control with ATP (VO-ATP); 2) wild type HSP90 with ATP (WT-ATP); 3) ADP (WT-ADP); 4) geldanamycin (WT-GA); and 5) HSP90 E47A with ATP (E47A-ATP). Purified complexes were then subjected to LC-MS/MS and spectral counting was used as a label-free method for quantifying differences in protein abundances amongst experimental groups (96,97). (see materials and methods).

To deplete contaminating ADP or ATP from cell lysates, the initial cell lysis and the streptavidin binding step was performed in the presence of an ATP regeneration system composed of phosphocreatine and creatine kinase (RS) for ATP groups or an ATP depletion system composed of glucose and hexokinase (Hex) for ADP groups respectively (see Materials and Methods). This approach has been used successfully to identify interactions with *E. coli* ATPase chaperones (98). As a precautionary measure, we monitored ATP levels in lysates during the 8-hour streptavidin pull-down step to ensure there was no significant depletion of ATP in the ATP groups (Figure 6). We found that ATP was not depleted with or without the RS. In fact it appeared that ATP was actually increased over time in the absence of the RS. This was

observed several times and may be due to ATP being freed from intracellular compartments. We did, however, detect slightly increased ATP levels in the presence of the RS. This may account for cellular ADP being enzymatically converted to ATP. We considered the ATP levels in this assay to be stable enough to perform these experiments using the RS in only the first step as a precautionary measure.

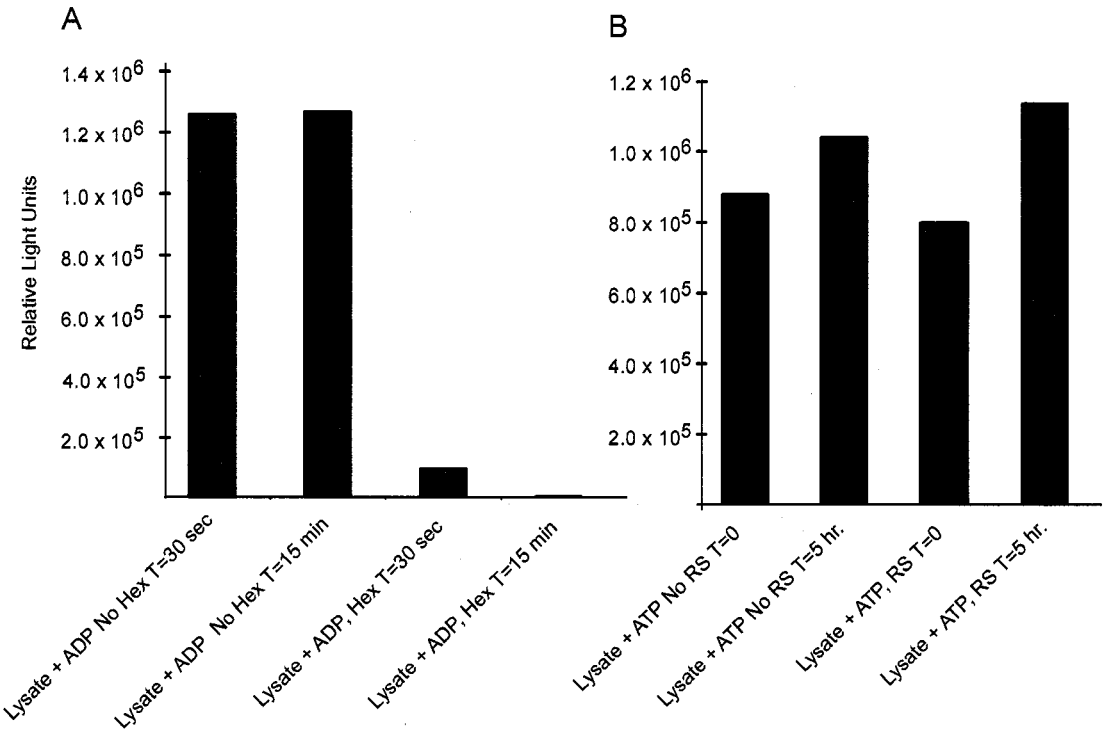

Figure 6. ATP assay from HSK293T whole cell lysates showing the effect of the effects of A) an ATP depletion system and B) an ATP regeneration system.

It is important to note that in preliminary experiments we determined that GA was only able to fully disrupt known HSP90 complexes if the intact cells were pretreated with drug (Figure 7a). We purified HSP90 complexes containing endogenous NUDC (known HSP90 interactor) with and without pretreatment with GA (5 μM and 10 μM). HSP90-NUDC complexes are predicted to be disrupted by geldanamycin treatment based upon their homologuey to p23. Vector only (VO) and DMSO are used as controls. We show that HSP90-NUDC complexes are disrupted only when the cells are pretreated with drug. If geldanamycin is added after lysis only, the complexes remain intact. This suggests that the drug has limited solubility in the lysis buffer or it is unable to efficiently bind and inhibit HSP90 after cell lysis. Therefore cells were pretreated with drug for two hours before lysis for all purifications containing geldanamycin.

A sample from each full-scale TAP purification was loaded onto 4-20% SDS-PAGE gel and silver stained to detect proteins (Figure 7b). HSP90-TAP and endogenous HSP90 appear to form a dimer with approximately 1:1 stoichiometery and these dimers are present in all purifications, suggesting little effect of nucleotides on HSP90 dimerization. In addition, several proteins appear to be differentially represented in these complexes according to the experimental condition. Most notably, the E47A mutant preparation appears

to contain more protein species than other preparations, as judged by the increased number of silver stained bands. This is expected based upon previous studies using the analogous E33A mutant of the yeast HSP90. In this case, the mutant was able to detect more interactions and with higher affinity than the wild type chaperone (13).

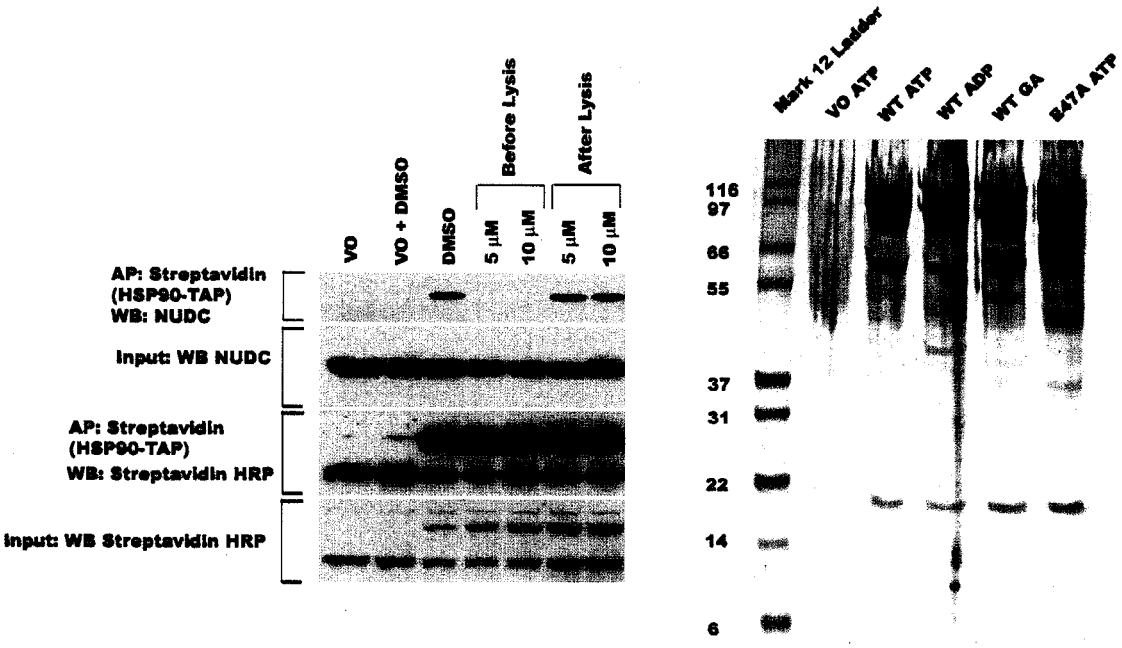

Figure 7. a) Left panel. Geldanamycin disrupts NUDC complexes. Western blot of affinity precipitations of endogenous NUDC with TAP-tagged HSP90 showing stability of complexes treated with geldanamycin before lysis and after lysis. b) Right panel. Silver stained HSP90 TAP complexes. 20 µL of TAP purified HSP90 complexes from each experimental condition were run on a 4-20% PAGE gel and silver stained. Molecular weight marker is shown in the first lane.

After the LC-MS/MS procedure, the resulting raw spectra were subjected to X!Tandem scoring and database searching. The IPI protein database (release Feb 22, 2007) was searched and the resulting peptide sequences were analyzed by ProteinProphet for the assignment of proteins. A pseudo-reversed database was also used in a target-decoy strategy to estimate the false discovery rate (FDR) associated with these searches (99). These data were then entered into the CPAS system and the protein identifications were compared across technical replicates and experimental groups using the *Compare* function (see materials and methods for complete analysis methodology and references). We filtered our dataset to reject proteins where the average spectral count for any experimental group was not greater than 5-fold in excess of the vector only control group (VO). To account for spurious identifications where only single peptides were counted in each run, we included only proteins that had a total of 4 or more peptides across each replicate for at least one experimental group. Redundant protein assignments were eliminated. When one protein identification was found to be a subset of another (splice isoform) peptides matched to these proteins were manually checked for likeness and spectral counts were combined into one protein. The length of the longest splice isoform was used to represent the protein group. We first normalized all spectral counts from all runs to account for any variation in sampling depth by the spectrometer amongst runs as in Xia, et al

(100). To gain a relative measure of the spectral abundance amongst interacting proteins across experimental groups we needed to account for the fact that longer proteins have more tryptic cleavage sites than shorter proteins. Each peptide from a long protein contributes less to the whole than a peptide from a short protein. We employed a normalization technique called the spectral abundance factor (SAF) (101,102). All spectral count totals for a particular protein were divided by the number of amino acids in that protein. A complete record of spectral counts, protein and peptide certainty values and other statistics for each identified protein are submitted in the appendix of this work. A spreadsheet was created with hyperlinks to the Entrez Gene webpage for all proteins and is submitted in the appendix under the file: HSP90 interactors.xls. For simplicity, all IPI accession numbers for the final list of interacting proteins were converted to the corresponding Entrez gene name associated with the protein.

Identification of Known and Novel HSP90 Interactions

In addition to 33 known HSP90 interacting proteins (Table 1), we identified 54 putative novel interactions (Table 2). GO (gene ontology) terms for biological process (level 3) were retrieved using the FatiGO web-based GO search engine (103). Of the known interactors, we found 6 chaperones, 17 co-

chaperones and 9 client proteins and one protein, RPAP3, where the functional interaction with HSP90 is unknown. Interestingly, HSP90α/HSP90α homodimer appears to be 2-fold lower in abundance than the HSP90α/HSP90β heterodimer. If the dimers were equally abundant in the cell lysates, we would expect an approximately 3:1 ratio of spectral counts from HSP90α to HSP90β using HSP90α as bait and both endogenous HSP90 isoforms interacted equally with a single monomer of TAP-tagged HSP90α. Rather, we observe approximately 2:1 ratio. This could be either due to the possibility that HSP90α preferentially dimerizes with HSP90β, or the endogenous HSP90α is expressed at a lower level and is therefore less untagged HSP90α monomers available for dimerization with HSP90β. The later is in agreement with the widespread understanding that the constitutively expressed HSP90β isoform is expressed at a higher level in cells than the stress-inducible HSP90α isoform (104,105). The fact that we see no statistically-significant variation in the levels of HSP90α or HSP90β amongst experimental groups suggests that the nucleotide or drug-bound state of HSP90 does not affect the isoform content of HSP90 complexes. Furthermore, both the endogenous HSP90α and HSP90β are well known to be induced by geldanamycin treatment. We did not observe any noticeable increases of HSP90α or β in our experiment. We attribute this to the fact that

we harvested geldanamycin treated cells 2 hours after treatment and these effects may not have been realized in protein abundance. In addition to these chaperones, we identified 17 co-chaperones including 6 containing TPR domains- an established HSP90 interaction domain. Furthermore, we identified 5 CS domain-containing co-chaperones including SUGT1, PTEGS3 (p23), CHORDC1 and NUDC, and CACYBP. Our experiment also identified 10 known client proteins or proteins with putative status as client proteins. While these interactions are not novel discoveries, they do stand to validate our system as an effective probe for identifying new HSP90 interacting proteins.

We identified one novel chaperone subunit (CCT2) and two novel CS domain-containing co-chaperone interactions (USP19 and NUDCD3). The CCT2 identification, agrees with Falsone, et al (92) where another subunit of this complex, CCT1, was identified as a HSP90 interacting protein. This provides further evidence that HSP90 may associate with the CCT complex (Chaperone Containing and TCP1, also known as TRiC). However, this interpretation is confounded by the fact that the CCT complex is composed of 8 different subunits and no other subunit of this complex was present in our final list of HSP90 interacting proteins. This opens the possibility that CCT1 and CCT2 are HSP90 client proteins whereby HSP90 may regulate the folding

Known interactons

Graph #	Entrez Gene Name	Entrez Locus ID	Description	Biological Process (GO)
	Chaperones			
1	HSP90AA1	3320	HSP90 Alpha	Protein folding
2	HSP90AB1	3326	HSP90 Beta	Protein folding
4	HSPA8	3312	Heat shock 70kDa protein 8	Protein folding
5	HSPA1A	3303	heat shock 70kDa protein 1A	Protein folding
6	HSPA2	3306	Heat shock 70kDa protein 2	Protein folding
7	HSPA9	3313	Heat shock 70kDa protein 9 (mortalin)	Protein folding
	Co-chaperones			
10	CDC37	11140	Cell division cycle homolog 37 (CDC37)	Protein folding, regulation of CDK activity
22	BAG2	9532	BCL2-associated athanogene 2	Protein folding, apoptosis
27	UNC45A	55898	Unc-45 homolog A (SMAP1)	Protein folding, muscle development
39	PIH1D1	55011	PIH1 domain containing 1 (PIH1p, NOP17)	Metabolism, preRNA processing
18	AHSA1	10598	Activator of heat shock protein ATPase homolog 1 (AHA1)	Protein folding, response to stress
	TPR domain co-chaperones			
17	PPP5C	5536	Protein phosphatase 5, catalytic subunit	Mitosis, transcription
3	STIP1	10963	Stress-induced-phosphoprotein 1 (Hsp70/Hsp90-organizing protein- HOP)	Response to stress
8	STUB1	10273	STIP1 homology and U-Box containing protein 1 (CHIP)	Ubiquitination, protein folding
9	FKBP5	2289	FK506 binding protein 5 (FKBP54)	Protein folding
11	FKBP4	2288	FK506 binding protein 4, 59kDa (FKBP52)	Protein folding
34	DNAJC7	7266	DnaJ (Hsp40) homolog, subfamily C, member 7 (TPR2)	Protein folding
29	ST13	6767	Hsp70 interacting protein (HIP)	Protein folding
	CS Domain Co-chaperones			
50	CACYBP	27101	Calcyclin binding protein (SIP)	Ubiquitination
13	CHORDC1	26973	Cysteine and histidine-rich domain (CHORD)-containing 1 (CHP1)	N/A
14	SUGT1	10910	SGT1, suppressor of G2 allele of SKP1	Ubiquitination, Mitosis
19	NUDC	10726	Nuclear distribution gene C	Mitosis
23	PTGES3	10728	Prostaglandin E synthase 3 (p23)	Protein folding, signal transduction
	Client Proteins			
61	CDK7	1022	Cyclin-dependent kinase 7 (MO15 homolog, Xenopus laevis, cdk-activating kinase)	Cell cycle, regulation of transcription
33	CDC2L2	728642	Cell division cycle 2-like 2 (CDK11)	Cell cycle
51	INOC1	54617	INO80 Complex homolog 1	[Chromatin remodelling]
73	TOMM70A	9868	Translocase of outer mitochondrial membrane 70 homolog A	[Mitochondrail protein translocation]
38	PPP3R1	5534	Protein phosphatase 3, regulatory subunit B, alpha isoform (Calcinurin)	[Stress response, cell cycle]
49	EF2	1938	Eukaryotic translation elongation factor 2	Protein biosynthesis
57	CHUK	1147	Conserved helix-loop-helix ubiquitous kinase (IKBKA)	Immune response
70	IKBKG	8517	Inhibitor of kappa light polypeptide gene enhancer in B-cells, kinase gamma (NEMO)	Regulation of transcription
76	NR3C1	2908	Nuclear receptor subfamily 3, group C, member 1 (glucocorticoid receptor)	Regulation of transcription
	Unknown			
36	RPAP3	79657	RNA polymerase II associated protein 3	Transcription

Table 1. Known HSP90 interacting proteins TAP purified in the presence of HSP90 ligands ATP, ADP and geldanamycin. Proteins are categorized by the literature –defined functional interaction with HSP90.

Novel interactions

Graph #	Entrez Gene Name	Entrez Locus ID	Description	Biological Process (GO)
	Chaperones			
63	CCT2	10576	Chaperonin containing TCP1, subunit 2 (beta)	Protein folding
31	PFDN6	10476	Prefoldin subunit 6	Protein folding
42	PFDN2	5202	Prefoldin subunit 2	Protein folding
46	C19orf2	8725	Chromosome 19 open reading frame 2 (unconventional prefoldin RPB5 interactor)	Protein folding, regulation of transcription
35	PDRG1	81572	p53 and DNA damage regulated 1 (Prefoldin complex)	Protein folding
	Co-chaperones			
48	USP19	10869	Ubiquitin specific protease 19	Ubiquitination
21	NUDCD3	23386	NudC domain containing 3	N/A
	Other/Unknown			
26	NSUN5C	260294	NOL1/NOP2/Sun domain family, member 5C	N/A
37	C10orf137	26098	Erythroid differentiation-related factor 1 (EDRF1)	Regulation of transcription
53	PTOV1	53635	Prostate tumor overexpressed gene 1	Protein biosynthesis
59	TRIM38	10475	Tripartite motif-containing 38	Ubiquitination
64	FBXO38	81545	F-box protein 38	Ubiquitination
72	SPAG1	6674	Sperm associated antigen 1	Fertilization
74	DYNC1LI2	1783	Dynein, cytoplasmic 1 light intermediate chain 2	N/A
78	CAD	114010	Carbamoyl-phosphate synthetase 2, aspartate transcarbamylase, and dihydroorotase	N/A
80	FLJ20294	55626	Hypothetical protein FLJ20294	N/A
81	BCOR	54880	BCL6 co-repressor	Regulation of transcription
84	TTF2	8458	Transcription termination factor, RNA polymerase II	Transcription termination
86	TTN	7273	Tintin	Response to stress
20	TTC9C	283237	Tetratricopeptide repeat domain 9C	N/A
32	PPP2R1A	5518	Protein phosphatase 2 (formerly 2A), regulatory subunit A , alpha isoform	Cell cycle
43	MARCKS	4082	Myristoylated alanine-rich protein kinase C substrate	N/A
45	Similar to MAGE-10	N/A	gi|17485686| similar to melanoma antigen, family A, 10 (Discontinued Record)	N/A
24	CSNK1A1	1452	Casein Kinase 1, alpha 1	[Wnt Signaling]
25	PLCE1	51196	Phospholipase C, epsilon 1	Ras protein signal transduction
52	CNOT6	57472	CCR4-NOT transcription complex, subunit 6	Regulation of transcription
54	PRPF8	10594	PRP8 pre-mRNA processing factor 8 homolog	mRNA splicing
55	CDH5	1003	Cadherin 5, type 2, VE-cadherin (vascular epithelium)	Cell adhesion
56	CXorf57	55086	Chromosome X open reading frame 57	[Possible ssDNA binding (Pfam)]
58	ASCC3L1	23020	Activating signal cointegrator 1 complex subunit 3-like 1	RNA splicing
60	LRRC1	55227	Leucine-rich repeat-containing 1	N/A
62	OGDHL	55753	OGDHL oxoglutarate dehydrogenase-like	Metabolism, glycolysis
65	SCRIB	23513	Scribbled homolog	N/A
66	C22orf30	253143	Chromosome 22 open reading frame 30	N/A
67	KLHL15	80311	Kelch-like 15	N/A
68	MOV10	4343	Mov10, Moloney leukemia virus 10, homolog	Development
69	SKP2	6502	S-phase kinase-associated protein 2 (p45)	Ubiquitination, cell cycle
71	DYNC1H1	1778	Dynein, cytoplasmic 1, heavy chain 1	Microtubule-base movement
75	FLII	2314	Flightless 1 homolog	Regulation of transcription
77	CUL3	8452	Cullin 3	Ubiquitination, cell cycle
79	ANAPC1	64682	Anaphase promoting complex subunit 1	Ubiquitination, mitosis
82	SALL2	6297	Sal-like 2	Regulation of transcription
83	YTHDC2	64848	YTH domain contining 2	N/A
85	SYNE1	23345	Spectrin repeat containing, nuclear envelope 1	Golgi organization and biogenesis
12	MYLK2	85366	Myosin light chain kinase 2, skeletal muscle	Protein amino acid phosphorylation
15	CCDC117	150275	Coiled-coil domain containing 117	N/A
16	TOMM34	10953	Translocase of outer mitochondrial membrane 34	Protein folding, protein-mitochondrial targeting
28	POLR2E	5434	Polymerase (RNA) II (DNA directed) polypeptide E, 25kDa	Transcription from RNA polymerase II promoter
30	FAM83H	286077	Family with sequence similarity 83, member H	N/A
40	HNRPAB	3182	Heterogeneous nuclear ribonucleoprotein A/B	mRNA editing
41	MAP3K7IP1	10454	Mitogen-activated protein kinase kinase kinase 7 interacting protein 1	Activation of MAPKKK activity
44	EFTUD2	9343	Elongation factor Tu GTP binding domain containing 2	protein biosynthesis, nuclear mRNA splicing
47	LRRIQ2	79598	Leucine-rich repeats and IQ motif containing 2	N/A

Table 2. Putative novel HSP90-interacting proteins TAP purified in the presence of HSP90 ligands ATP, ADP and geldanamycin. Proteins are categorized by their literature –defined functional interaction with HSP90.

and stability of certain components of the CCT complex. We also identified two interactions with the CS domain-containing proteins USP19 and NUDCD3 that had not been previously described. These represent two novel additions to the growing list of CS domain-containing HSP90 interactors and provide support for the CS domain as a *bone fide* HSP90 interaction domain. Notably, we identified 3 kinases forming novel HSP90 interactions (TTN, CSNK1A1, and MYLK1). The presence of the known HSP90 client kinase CHUK and the kinase-specific CDC37 in our purifications further strengthen the possibility that these kinases may be HSP90 client proteins. However, it must be addressed that several kinase client proteins are absent from our data. There are two major reasons for this observation: 1) the sensitivity of this procedure may not be high enough to detect client proteins- HSP90 interactions with client proteins are known to be very transient; 2) the detection of particular proteins may be dependent upon their expression levels and some HSP90 interactors may be expressed conditionally or not expressed in the renal epithelium (HEK293T cells).

Identification of proteins that vary in spectral abundance according to HSP90 ligands- It is well established that some interactions with co-chaperones and client proteins are dependent upon the nucleotide or drug-bound state of HSP90. We sought to identify new ligand-dependent interactions and to

observe effects of ligands on the dynamics of the HSP90 interactome. We searched our dataset to identify proteins that increased in spectral abundance in one ligand-bound state over the others by subjecting the spectral abundance factors (SAFs) for each protein to ANOVA analysis. We identified 59 proteins that were above the ANOVA p-value cutoff of 0.05 (Table 3). These represent more than half of the total protein identifications, suggesting that HSP90 complexes are particularly sensitive to the ligand present. As expected, our bait protein HSP90α did not pass the ANOVA cutoff (ANOVA= 0.2336), indicating good precision of the purification process and LC-MS/MS procedure amongst groups. We then subjected these data from all four conditions to a t-test and used the lowest p-value to determine the particular experimental group responsible for the observed variation. Values are presented in Table 3. The average SAF and standard deviation are represented graphically in Figure 8 Figure 9 Figure 10. All proteins represented in these graphs are numbered and this number will be referenced with the gene name.

ATP-dependent Interactions

We speculated that the use of the E47A mutant would increase the strength of interaction between HSP90 and ATP-dependent interacting proteins as has

been observed in Millson, et al. with the yeast HSP90 mutant HSC82p E33A (13). Under this assumption, we expected that proteins identified in the E47A ATP group would also be represented in the WT ATP group, albeit at a lower abundance. Consistent with this idea, we found that 13 proteins identified in the E47A ATP complexes were also present in the WT ATP complexes at a reduced abundance. (Figure 8, Figure 9 and Figure 10: FKBP5 #9, SUGT1 #14, AHSA1 #18, NUDC #19, NUDCD3 #23, PTGES3/p23 #23, CSNK1A1 #24, FAM83H #30, UNC45A #27, HNRPAB #40, MAP3K7IP1 #41, FBXO38 #70, FLII #75). However, proteins with abundant spectra in the E47A ATP group were often not identified in any WT ATP runs. This may be due to the fact that client protein and co-chaperone release is known to be coupled to ATP hydrolysis (17). WT HSP90 is an active ATPase and may not sustain the ATP-bound state *in vivo* and therefore ATP-dependent interactions may not be represented in these complexes. It is also possible that E47A mutation may alter structural elements in the ATPase domain such that spurious interactions may occur exclusively with this mutant. Furthermore, we cannot eliminate the possibility that clonal effects may influence the interactions identified with the E47A mutant. The stable clonal selection of the E47A-TAP construct may have influenced the cellular abundance of particular proteins in the E47A mutant cells and therefore may have had a concomitant effect on the abundance of these proteins in HSP90 complexes. However, known HSP90

Group Overabundant*	Entrez Gene Name	Graph Ref. #	Entrez Locus ID	Description	Association with HSP90	t-test (p-value)
WT ATP	STIP1	3	10963	Stress-induced-phosphoprotein 1 (Hsp70/Hsp90-organizing protein- HOP)	TPR domain co-chaperone	9.48E-08
	STUB1	8	10273	STIP1 homology and U-Box containing protein 1 (CHIP)	TPR domain co-chaperone	3.32E-04
	PLCE1	25	51196	Phospholipase C, epsilon 1	Unknown	1.09E-06
	OGDHL	62	55753	OGDHL oxoglutarate dehydrogenase-like	Unknown.	3.68E-04
	SYNE1	85	23345	Spectrin repeat containing, nuclear envelope 1	Unknown	4.74E-05
	MYLK2	12	85366	Myosin light chain kinase 2, skeletal muscle	Unknown	2.27E-07
	CCDC117	15	150275	Coiled-coil domain containing 117	Unknown	1.10E-04
WT ADP	CHORDC1	13	26973	Cysteine and histidine-rich domain (CHORD)-containing 1 (CHP1)	CS Domain Co-chaperone	5.01E-06
WT Geldanamycin	HSPA8	4	3312	Heat shock 70kDa protein 8	Chaperone	4.98E-07
	HSPA1A	5	3303	heat shock 70kDa protein 1A	Chaperone	0.00E+00
	HSPA2	6	3306	Heat shock 70kDa protein 2	Chaperone	1.41E-06
	HSPA9	7	3313	Heat shock 70kDa protein 9 (mortalin)	Chaperone	2.03E-06
	FKBP4	11	2288	FK506 binding protein 4, 59kDa (FKBP52)	TPR domain co-chaperone	7.40E-04
	BAG2	22	9532	BCL2-associated athanogene 2	Co-chaperone	1.44E-03
	PIH1D1	39	55011	PIH1 domain containing 1 (PIH1p, NOP17)	Co-chaperone	1.07E-04
	DNAJC7	34	7266	DnaJ (Hsp40) homolog, subfamily C, member 7 (TPR2)	TPR domain co-chaperone	1.06E-02
	ST13	29	6767	Suppression of tumorigenicity 13 (colon carcinoma) (Hsp70 interacting protein- HIP)	TPR domain co-chaperone	1.08E-03
	PPP3R1	38	5534	Protein phosphatase 3, regulatory subunit B, alpha isoform (Calcineurin)	Client	5.20E-05
	EF2	49	1938	Eukaryotic translation elongation factor 2	Client	8.05E-03
	NR3C1	76	2908	Nuclear receptor subfamily 3, group C, member 1 (glucocorticoid receptor)	Client	5.47E-04
	CCT2	63	10576	Chaperonin containing TCP1, subunit 2 (beta)	Chaperone	9.59E-05
	CXorf57	56	55086	Chromosome X open reading frame 57	Unknown	2.76E-03
	ASCC3L1	58	23020	Activating signal cointegrator 1 complex subunit 3-like 1	Unknown	1.25E-03
	MOV10	68	4343	Mov10, Moloney leukemia virus 10, homolog	Unknown	2.14E-02
	YTHDC2	83	64848	YTH domain containing 2	Unknown	1.47E-04
	TOMM34	16	10953	Translocase of outer mitochondrial membrane 34	Unknown	1.37E-06
	POLR2E	28	5434	Polymerase (RNA) II (DNA directed) polypeptide E, 25kDa	Unknown	6.12E-04
	PFDN6	31	10476	Prefoldin subunit 6	Unknown	6.48E-03
	RPAP3	35	79657	RNA polymerase II associated protein 3	Contains TPR Domain	1.71E-03
	PFDN2	42	5202	Prefoldin subunit 2	Unknown	3.10E-04
	EFTUD2	44	9343	Elongation factor Tu GTP binding domain containing 2	Unknown	8.82E-03
	C19orf2	46	8725	Chromosome 19 open reading frame 2 (unconventional prefoldin RPB5 interactor)	Unknown	1.98E-03
E47A ATP	UNC45A	27	55898	Unc-45 homolog A (SMAP1)	Co-chaperone	1.45E-05
	AHSA1	18	10598	Activator of heat shock protein ATPase homolog 1 (AHA1)	Co-chaperone	2.77E-06
	FKBP5	9	2289	FK506 binding protein 5 (FKBP54)	TPR domain co-chaperone	1.97E-03
	SUGT1	14	10910	SGT1, suppressor of G2 allele of SKP1	CS Domain Co-chaperone	2.17E-04
	NUDC	19	10726	Nuclear distribution gene C	CS Domain Co-chaperone	3.74E-05
	PTGES3	23	10728	Prostaglandin E synthase 3 (p23)	CS Domain Co-chaperone	1.75E-02
	CHUK	57	1147	Conserved helix-loop-helix ubiquitous kinase (IKBKA)	Client	5.47E-03
	IKBKG	70	8517	Inhibitor of kappa light polypeptide gene enhancer in B-cells, kinase gamma (NEMO	Client	5.84E-04
	NUDCD3	21	23386	NudC domain containing 3	CS Domain Co-chaperone	1.04E-05
	CSNK1A1	24	1452	Casein Kinase 1, alpha 1	Unknown.	1.83E-04
	CNOT6	52	57472	CCR4-NOT transcription complex, subunit 6	Unknown	4.49E-04
	PRPF8	54	10594	PRP8 pre-mRNA processing factor 8 homolog	Unknown	3.84E-03
	CDH5	55	1003	Cadherin 5, type 2, VE-cadherin (vascular epithelium)	Unknown	4.21E-03
	LRRC1	60	55227	Leucine-rich repeat-containing 1	Unknown	1.26E-03
	SCRIB	65	23513	Scribbled homolog	Unknown	4.48E-05
	C22orf30	66	253143	Chromosome 22 open reading frame 30	Unknown	4.31E-04
	KLHL15	67	80311	Kelch-like 15	Unknown	1.75E-03
	SKP2	69	6502	S-phase kinase-associated protein 2 (p45)	Unknown	5.84E-04
	DYNC1H1	71	1778	Dynein, cytoplasmic 1, heavy chain 1	Unknown	1.55E-03
	FLII	75	2314	Flightless 1 homolog	Unknown	2.45E-02
	CUL3	77	8452	Cullin 3	Unknown	5.84E-04
	ANAPC1	79	64682	Anaphase promoting complex subunit 1	Unknown	2.57E-06
	SALL2	82	6297	Sal-like 2	Unknown	5.84E-04
	FAM83H	30	286077	Family with sequence similarity 83, member H	Unknown	3.75E-07
	HNRPAB	40	3182	Heterogeneous nuclear ribonucleoprotein A/B	Unknown	7.90E-03
	MAP3K7IP1	41	10454	Mitogen-activated protein kinase kinase kinase 7 interacting protein 1	Unknown	5.20E-03
* (ANOVA p=.05)	LRRIQ2	47	79598	Leucine-rich repeats and IQ motif containing 2	Unknown	2.94E-03

Table 3. Table of HSP90 interacting proteins that are overrepresented in a particular experimental group (ANOVA= 0.5). Proteins categorized according to the ligand present in the purification and the associated t-test p-value is listed to the right.

interacting proteins were also identified exclusively in the E47ATP group: CDK7 #61, IKBKG #70, SKP2 #69, CACYBP #50) so it is improbable that this is true for every protein of this type. Surprisingly, we also identified PLCE1 (Phospholipase C type E1) as a protein that behaves conversely to this pattern. It appears to be highly abundant in all groups except for the E47A mutant. In this case, we cannot rule-out the effects of clonal selection or any biochemical effects specific to the E47A mutant.

ADP-dependent interactions

We were able to identify the CS domain-containing co-chaperone CHORDC1 (Figure 8 #13) as the sole ADP-dependent HSP90 interactor (t-test p= 5.01×10^{-6}). This result was surprising based upon the observation that the HSP90 binding interactions of other CS domain-containing proteins are apparently ATP-dependent (PTGES3, SUGT1, CACYBP, NUDC, NUDCD3 with USP19 being an exception). Based upon this striking binding interaction, we selected this protein for further study and the results of this investigation are presented in the sections below.

Geldanamycin-dependent interactions

Most evidence supports the hypothesis that HSP90 inhibition by pharmacological agents prevents the ability of HSP90 to bind client proteins and some co-chaperones like p23. Indeed, in most cases we show that known and novel HSP90 interacting proteins are excluded to varying degrees from HSP90 complexes treated with geldanamycin (see: Figure 8, 9 and 10 protein #s 13, 14, 19, 21, 23, 26, 41, 86). It is well established, however, that a complex between HSP90 and HSP70 is formed in response to treatment with geldanamycin (106,107). Consistent with these findings, we identified 4 distinct HSP70 family chaperones exclusively in the WT GA group (see Figure 8, protein #s 4-7). Several proteins known to form complexes with HSP70 were also identified in this group including FKBP4 #11, BAG2 #22, POL2RE #28 and ST13 (HIP) #29 suggesting that these proteins constitute a HSP70 complex that becomes associated with HSP90 in response to geldanamycin treatment. FKBP4 binding is increased after geldanamycin treatment whereas the highly homolougeous FKBP5 (#9) is most abundant in the E47A ATP group. In support of this observation, it has been previously shown that FKBP4 (alternatively known as FKBP52) binding to HSP90 is increased after treatment with geldanamycin (108). Furthermore, the increase in FKBP4 in these HSP90 complexes is associated with a concomitant

increase in NR3C1 (glucocortocoid receptor) (Figure 10, protein #82). It has been shown that geldanamycin treatment does not disrupt HSP90-GR complexes and in some cases has been shown to stabilize this interaction (17,109).

We present evidence for the existence of several novel HSP90 interactions that are specifically induced after treatment with geldanamycin (Table 3). Interstingly, these complexes are enriched for proteins known to function in basic processes of RNA metabolism including POL2RE (RNA polymerase II subunit), C19orf2 #28 (a transcriptional co-repressor known to associate with POL2RE, (110,111)), ASCC3L1#58 (RNA helicase), RPAP3 #36 (RNA polymerase binding element containing two TPR domains) and PIH1D1 #39 , (hypothesized to be involved in pre-rRNA processing). The discovery of PIH1D1 is supported by evidence that the yeast HSP90 interacts with the yeast PIH1D1 homolougeue Pih1p, however this interaction was not observed to be geldanamycin-dependent (89). TTF2 #84, (a transcription termination element), was also identified only in the WT GA group; however the variance between replicates was too great to pass our ANOVA testing criteria.

A recent publication by Jeronimo and colleagues presented a proteomic investigation of the components of the human transcriptional apparatus (112).

Notably, several components of transcription complexes identified in this study were also identified in our geldanamycin-dependent HSP90 complexes, including HSP90, HSP70 and the prefoldin chaperone subunits PFDN2 #42 and PFDN6 #31, RPAP3 #36, c19orf2 #46, PIH1D1 #39, and EFTUD2 #44. The proteins PDRG1 #35 and ANAPC1 #79 were also identified in these transcriptional complexes; however, their abundance appeared to not be geldanamycin-dependent in our experiments. These findings suggest the interesting possibility that HSP90 may be intimately involved in regulating transcription at several levels and geldanamycin treatment may alter fundamental transcriptional processes.

In addition, several components of chaperone systems were specifically increased in geldanamycin-dependent complexes including components of the hexameric prefoldin complex (PFDN2, PFDN6) and the unconventional prefoldin C19orf2. The enrichment of these chaperones suggests a few possibilities: 1) HSP90 inhibition causes the compensatory recruitment of several distinct protein folding machineries in the absence of HSP90 activity; 2) HSP90 inhibition is causing a blockade in the passage of protein substrates from the prefoldin/HSP70/TRiC complexes (known to function early in the protein folding pathways) to the HSP90 complex (known to function later in protein folding pathways). This blockade may cause an accumulation of these chaperone components in HSP90 complexes; or 3) these prefoldin subunits

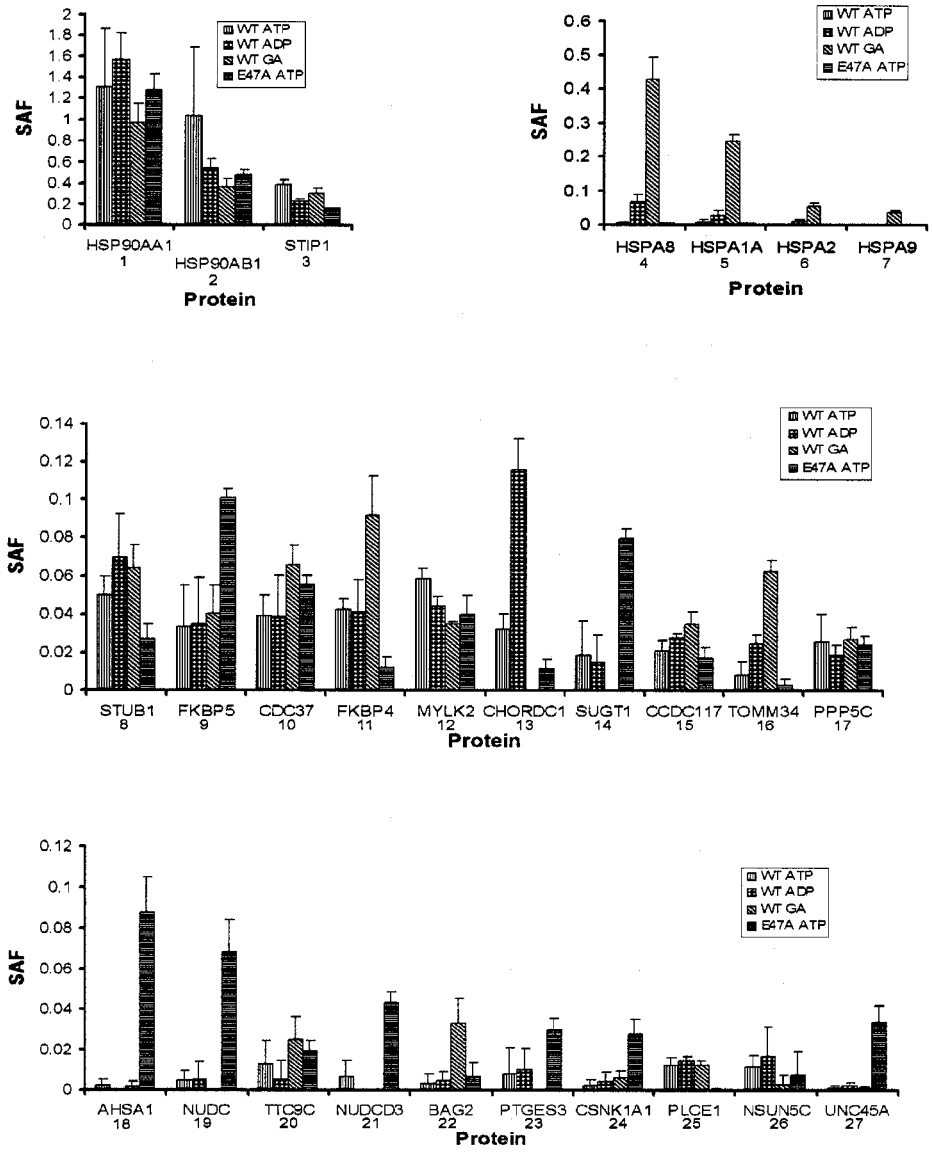

Figure 8. Spectral abundance for HSP90 proteins across experimental groups. Column graph of average SAF values calculated for HSP90 interacting proteins identified in this experiment. Error bars represent the SD for three technical replicates. Proteins are presented in the order of their relative spectral abundance. The data appear in the following order: WT ATP vertical bars, WT ADP checker pattern, WT GA (geldanamycin) left diagonal bars, E47A ATP horizontal bars. All proteins are indexed with a number referencing the corresponding data from Table 1, Table 2, and Table 3 above.

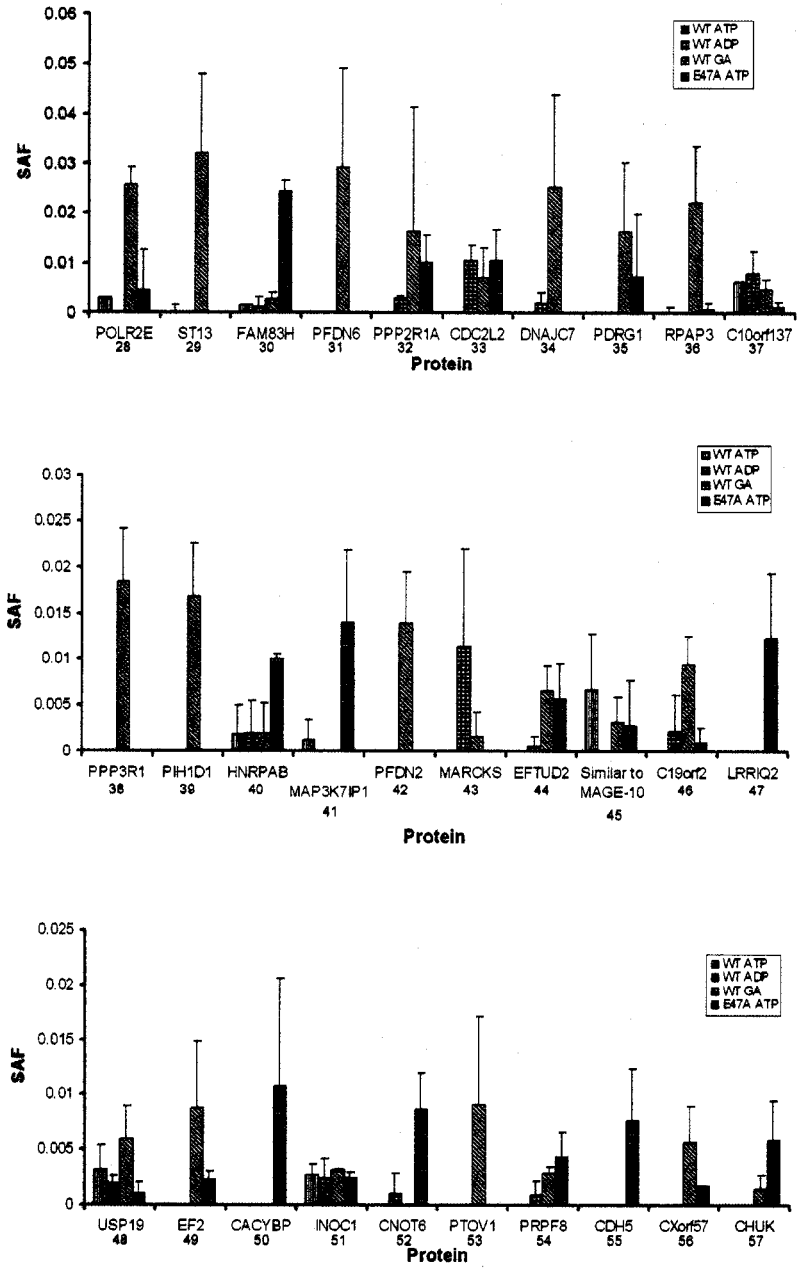

Figure 9. Spectral abundance for HSP90 proteins across experimental groups. Column graph of average SAF values calculated for HSP90 interacting proteins identified in this experiment. Error bars represent the SD for three technical replicates. Proteins are presented in the order of their relative spectral abundance. The data appear in the following order: WT ATP vertical bars, WT ADP checker pattern, WT GA (geldanamycin) left diagonal bars, E47A ATP horizontal bars. All proteins are indexed with a number referencing the corresponding data from Table 1, Table 2, and Table 3 above.

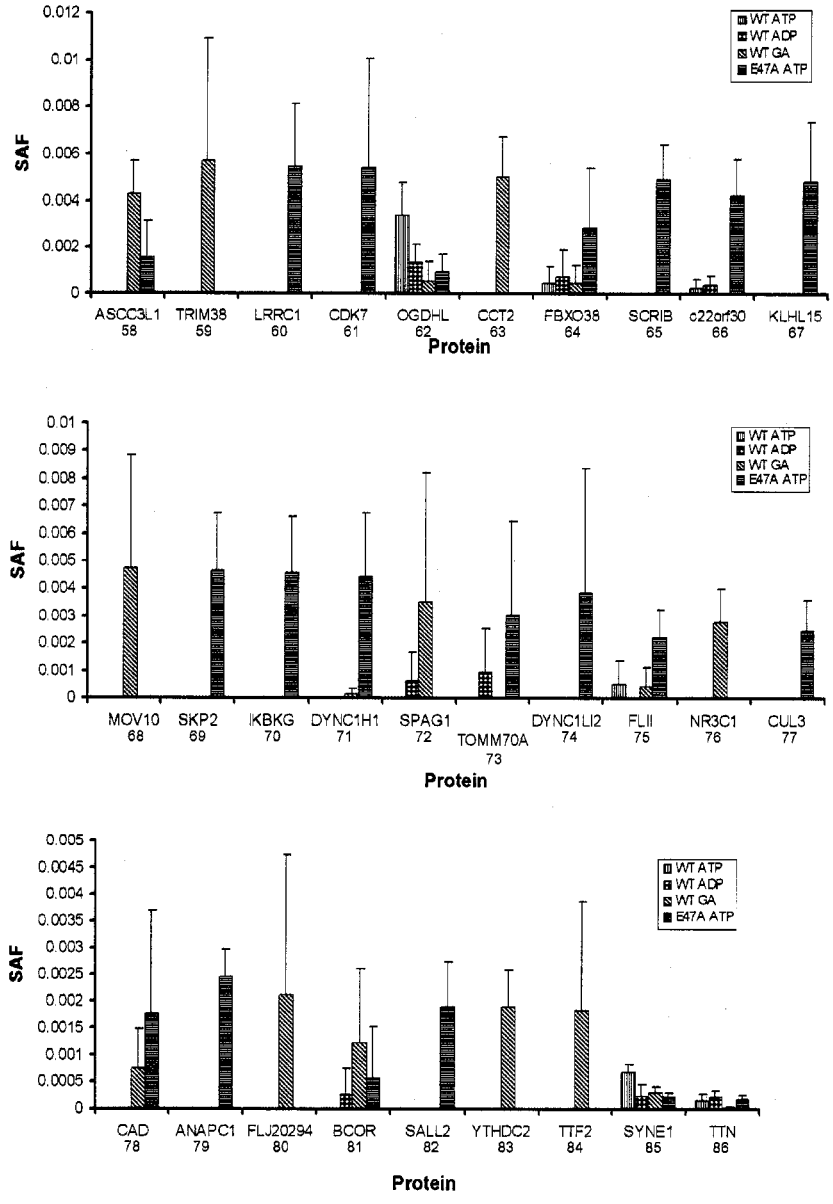

Figure 10. Spectral abundance for HSP90 proteins across experimental groups. Column graph of average SAF values calculated for HSP90 interacting proteins identified in this experiment. Error bars represent the SD for three technical replicates. Proteins are presented in the order of their relative spectral abundance. The data appear in the following order: WT ATP vertical bars, WT ADP checker pattern, WT GA (geldanamycin) left diagonal bars, E47A ATP horizontal bars. All proteins are indexed with a number referencing the corresponding data from Table 1, Table 2, and Table 3 above.

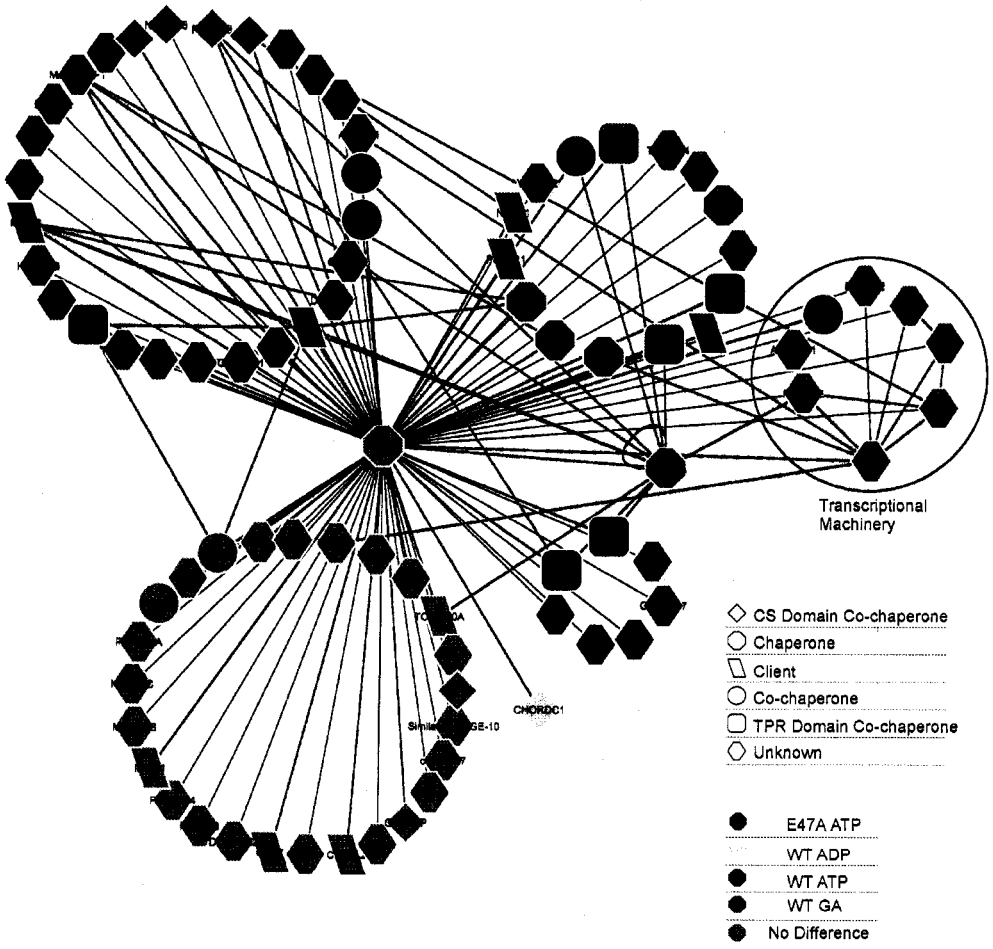

Figure 11. Ligand-dependent HSP90 interaction map. Protein interaction nodes are grouped according to the experimental group with the greatest spectral abundance. E47A ATP (blue), WT ATP (red), WT ADP (yellow), WT GA (green) and no significant difference (grey). The shape of the node represents the known functional interaction with HSP90: chaperone (octagon), co-chaperone (circle), TPR domain co-chaperones (square), CS domain co-chaperone (diamond), client protein (rhombus), unknown association (hexagon). Edges are color-coded for known interaction (black) or novel interactions (red).

are integral parts of the transcriptional complexes associated with HSP90 after geldanamycin treatment, and as such, are co-purifying with this complex.

An interaction diagram was created to depict all the HSP90 interactions identified in this study The APID (Agile Protein Interaction Database) (113). The dataset form Jeronimo, et al (112) was used to identify known HSP90 interactions existing in our dataset as well as any associations amongst these HSP90 interactors. APID uses the following databases: BIND (114), DIP (115), HPRD (Human Protein Reference Database) (116), IntAct (Database system and analysis tools for protein interaction data) (117,118), and MINT (Molecular Interactions Database) (119,120). APID filters all results to include only experimentally defined protein-protein interactions that have literature-based sources. This interaction data was loaded into Cytoscape software to visualize the network (121). For simplicity, all HSP90 isoforms were considered functionally equivalent and combined into one node called HSP90. Protein nodes were arranged to reflect any ligand-dependent interactions. Several proteins appear to serve as hubs of interaction amongst HSP90 interactors. HSP70 (HSPA1A) makes 12 interactions between HSP90-interacting proteins identified in this study, while RPAP3 makes 9 interactions-mainly with components of transcription machinery identified in geldanamycin-dependent complexes. RPAP3 contains two TPR domains which are known in several proteins to be the structural feature responsible for interaction with the C-terminal MEEVD motif on HSP90. Therefore, both RPAP3 and HSP70 appear to be good candidates for direct interactions the HSP90 in the

geldanamycin-dependent complexes and may serve as a bridge between HSP90 and the transcriptional apparatus. We do realize that these interpretations may be biased due to the lack of in-depth protein-protein interaction data for all proteins in this network; however, these protein interactions may give some information about the effects of nucleotides or geldanamycin on HSP90 complexes.

HSP90 Complexes are Dynamic and Sensitive to Geldanamycin Treatment and Nucleotide Ligands

We have shown that tandem affinity purified HSP90 complexes exposed to ATP, ADP or the pharmacological inhibitor geldanamycin are dynamic with respect to these ligands. Apparently, ATP and ADP have only subtle effects that may be largely undetectable in our system; however, the geldanamycin treatment and the expression of the ATP-locked E47A mutant and has more striking effects on these complexes. One explanation for this phenomenon is the possibility that catalytically-competent wild type HSP90 (WT) is not saturated with the exogenously-provided nucleotide after cell lysis. This process may occur, but over a long enough timescale that interactions cannot be made or sustained *in vitro* during the first step of the purification procedure. This possibility is supported by the observation that HSP90 complexes known to be disrupted by geldanamycin are not altered if geldanamycin is simply

added to the lysate and purification buffers (Figure 7a). Furthermore, ADP apparently has limited effect on the interaction of PTGES3 (p23) with HSP90 in our system. Our proteomic data shows no significant difference in the spectral counts for PTEGS3 between WT ATP and WT ADP (Figure 8, #23). Whereas several groups have published that the addition of ADP partially disrupts this interaction with a breif incubation at 30°C. These two pieces of evidence suggest that HSP90 from cell lysates is not efficient at binding exogenous ligands *in vitro*. We did, however, discover one very selective ADP-dependent HSP90 interaction with CHORDC1 which is investigated further in the next section.

Characteristics of HSP90 Interactions with CS Domain-containing Proteins

There is a growing body of evidence that the CS domain is a *bone fide* HSP90 binding domain that interacts with the N-terminal ATPase domain. Indeed, several CS domain-containing proteins (CDPs) have been shown to interact with the HSP90 ATPase domain in biochemical assays (8,51,52). It has also been demonstrated *in vitro* and in a yeast two-hybrid system that PTGES3 (p23) and SUGT1 show a degree of selectivity for interacting with HSP90 in the ATP-bound state (14,30,49,50,52). The HSP90 inhibitor geldanamycin has also been shown in some cases to disrupt complexes between HSP90

and CDPs (31,122). Wu, and coworkers showed that the interaction between purified CHORDC1 and HSP90 was independent of ATP and insensitive to geldanamycin treatment. Importantly, the effects of ADP were not tested in this study (64). Our proteomic data presented above supports the notion that despite the presence of a CS domain, CDPs do not bind HSP90 homogeneously with regard to nucleotide or drug ligands. SUGT1, NUDC, NUDCD3, PTEGS3, and CACYBP1 (Figure 8, protein #s14, 19, 21, 23 and , #50, respectively) appear to bind selectively to the ATP-bound HSP90, as evidenced by their overabundance in the E47A ATP group. These proteins all appear to be absent from the geldanamycin treated group, suggesting that HSP90 inhibition disallows these interactions. However, the presence of a CS-domian in CHORDC1 (Figure 8 protein #13) does not seem to confer similar HSP90 binding properties, as this protein appears to bind HSP90 selectively when ADP is present in the purification reactions and does not bind in the presence of geldanamycin. Furthermore, USP19 (, protein #48) is present in all purifications and does not seem to be influenced in a statistically significant way by any ligands studied (ANOVA p= 0.07323).

Systematic Characterization of the Effects of Nucleotides and Geldanamycin on CDPs

While in several instances the CS domain appears to be necessary for interactions with HSP90, it has not been determined whether this domain contains elements that confer specificity to this binding interaction with regard to the nucleotide-bound state of HSP90. The influence of ligands on binding interactions between CDPs and HSP90 has not been studied comprehensively under identical conditions. Therefore, due to a lack of a controlled basis for comparison, the information we have about the role of the CS domain in nucleotide-dependent HSP90 interactions is limited.

In order to investigate the possibility that CDPs may have unique HSP90 binding properties with respect to nucleotide and geldanamycin, we co-expressed and affinity precipitated a nearly complete panel of HA-tagged CDPs with a C-terminal TAP-tagged wild type HSP90 and the HSP90 E47A mutant with ATP, ADP or geldanamycin (GA) added to the lysis buffer. As before, cells were pretreated cells with GA in culture two hours before lysis. Importantly, to maintain consistency amongst experimental groups and minimize variation due to liquid-handling error, we utilized a high-throughput method for affinity precipitations where lysates were incubated, washed and eluted together in 96-well plates (see Materials and Methods).

In these experiments, all CDPs tested interacted with HSP90 to varying degrees (Figure 12). We were, however, able to identify three distinct groups of CDPs based upon their interactions with HSP90 in the presence of nucleotides and GA. The first group consisted of two proteins, CHORDC1 and ITGB1BP2, the only proteins in the human proteome known to contain two tandem CHORD domains (123). Both of these proteins appeared to form complexes with HSP90 exclusively in the presence of ADP and bound to the HSP90 E47A mutant stronger than wild type. It is possible that ADP has an increased affinity for HSP90 E47A over the wild type protein and this leads to a stronger interaction with CHORDC1 and ITGB1BP2. However, the cause of this phenomenon was not determined in these experiments. Unlike CHORDC1, we were not able to detect increased binding of ITGB1BP2 to wild type HSP90 in the presence of ADP over other ligands. However, a robust signal was obtained using ADP with the E47A mutant. These results suggest that the CHORD domain may confer an ADP-dependent interaction with HSP90.

The second group contained proteins with weak or undetectable interactions with wild type HSP90, but had strong interactions with the E47A mutant (CACYBP1, SUGT1, PTEGS3, NUDC, NUDCD3, NUDCD2). These interactions did not show any selectivity for ATP over ADP. As mentioned

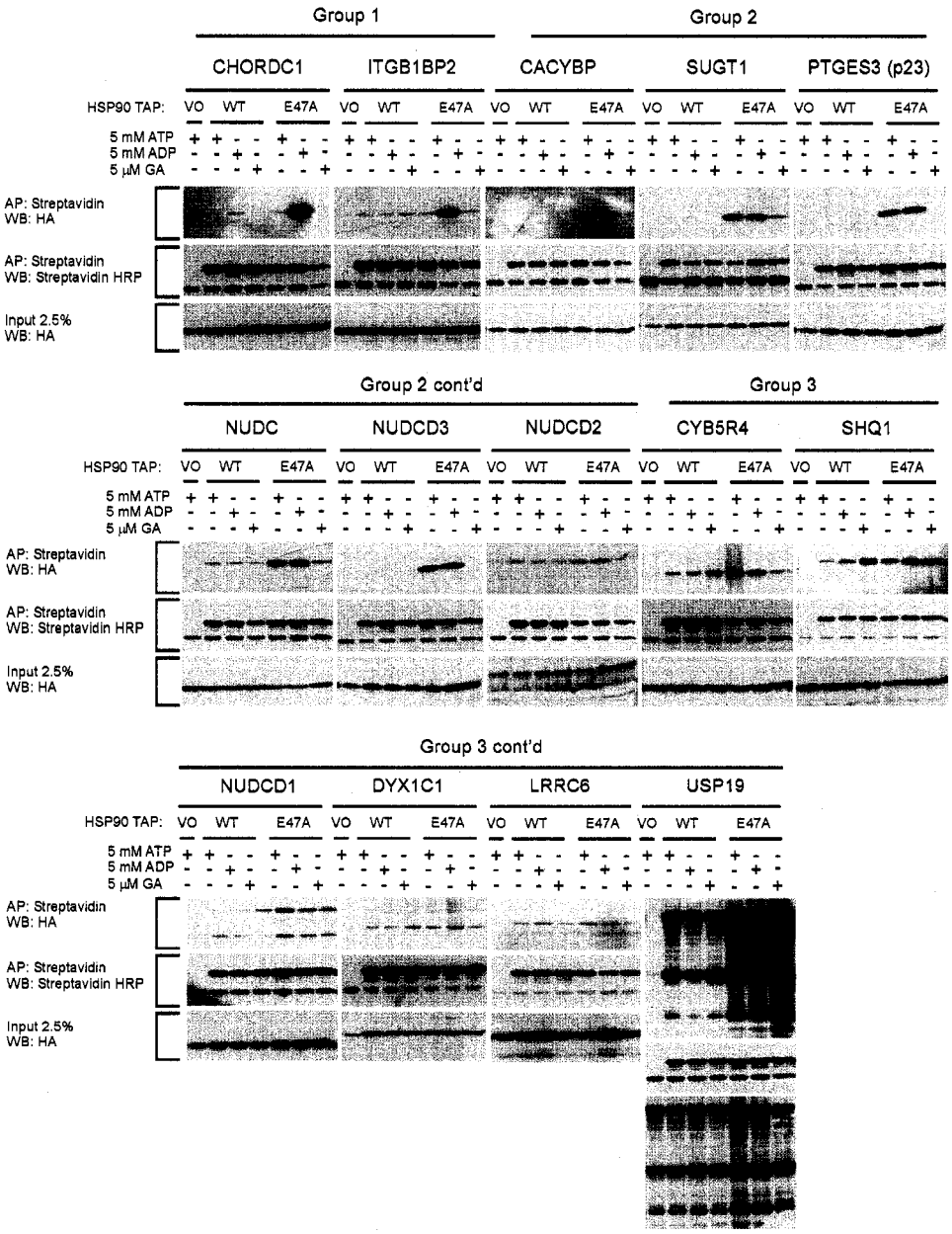

Figure 12. CS domain-containing proteins (CDPs) are influenced by nucleotides and geldanamycin. 14 proteins containing CS domains were HA tagged and co-affinity precipitated with TAP-tagged HSP90 in the presence of ATP, ADP or geldanamycin (GA) and the resulting complexes were western blotted. Results are arranged according to the effects of these ligands: ADP-dependent interactions (group 1); interactions where the CDP binds strongest to the HSP90 E47A mutant and the interactions are disrupted by geldanamycin treatment (group 2); and ligand-independent interactions (group 3).

earlier, previous *in vitro* experiments have shown the co-chaperone PTEGS3 (p23) will form higher affinity interactions with the ATP-bound HSP90 than the ADP-bound form. Under these conditions we were unable to observe any inhibitory effect of ADP upon this interaction with the E47A mutant even when lysates were incubated for 30 minutes at 30°C, conditions shown to be permissive to nucleotide exchange *in vitro* (21) (data not shown). Johnson, et al. (2007) showed that the yeast HSP90 E33A mutant has a sustained, however reduced, interaction with Sba1p (PTEGS3) in the presence of ADP, so we do not expect to see a total loss in PTEGS3 binding to the E47A mutant in our assays. It is not possible to exclude the possibility that nucleotide exchange is not efficiently occurring in the HSP90 ATPase site after cell lysis and endogenous ATP remains bound despite the presence of ADP in the lysis buffer. Notably, all of these interactions showed some sensitivity to geldanamycin, suggesting that pretreatment with drug is permissive for ligand exchange. This finding is consistent with previous experiments showing HSP90 complexes containing NUDC, SUGT1, and PETGS3 to all be disrupted in the presence of GA.

The third group of interactions consisted of CDPs that bound to both wild type and mutant HSP90, had no selectivity for nucleotide and the interactions were not significantly disrupted by geldanamycin. Notably, USP19 Figure 9, #48)

behaved similarly in this experiment as in our proteomic experiment. However, in this case there is a detectable increase in the amount of USP19 associating with the HSP90 E47A mutant over the wild type protein. This can be explained by the possibility that our proteomic assay is not sensitive to two-fold changes in abundance or there are undetectable expression differences between the WT and E47A mutant in these co-expression experiments.

These results taken together strengthen the hypothesis that the CS domain is a *bone fide* HSP90 interaction domain. And based upon these results, the nature of the HSP90 interaction with respect to nucleotide and geldanamycin is not necessarily governed simply by the presence of the CS domain; but perhaps conferred by either subtle amino acid variations within the CS domain or by other as yet undetermined elements residing elsewhere in these proteins.

Characterization of an ADP-dependent HSP90 Interaction

Based upon the spectral counting and affinity precipitation data presented above, we decided to further investigate the novel ADP-dependent HSP90 interaction with CHORDC1. We first wanted to determine whether this interaction was dependent upon high ADP:ATP ratios or simply the presence

of ADP. To this end, we performed affinity precipitations and Western blots using a C-terminal HSP90 TAP-tag fusion and an N-terminal HA-tagged CHORDC1 cDNA coexpressed in HEK293T cells. Cells were lysed directly into TAP lysis buffer containing increasing amounts of ADP or decreasing ratios of ADP:ATP holding the concentration of ADP constant. HSP90 was then affinity precipitated with streptavidin beads, washed with lysis buffer containing the appropriate nucleotide ratios and the bound proteins were Western blotted. Empty vector constructs (VO) were used to control for nonspecific binding to the streptavidin beads. The 37 kDa HA-CHORDC1 band began to appear when ADP alone was added in as little as 1 μM and reached a maximal intensity at 1 mM (Figure 13a, lanes 3-7). Importantly, no interaction was detected where ADP was not added suggesting that this interaction requires ADP and is not occurring because the reaction is lacking ATP (Figure 13a, lanes 2 and 13). Because both ATP and ADP are known to bind HSP90 and influence client protein and co-chaperone interactions, we therefore sought to determine whether the ADP:ATP ratio, and not solely the presence of ADP, was governing this interaction. To answer this question, ATP was titrated into the lysis buffer while holding the ADP concentration constant at the sub-saturating concentration of 100 μM. Interestingly, the addition of ATP began to disrupt the interaction at 1 μM. At 100 μM ATP (1:1 ADP:ATP ratio) the interaction was completely abolished, demonstrating an

inhibitory effect of ATP on the stability of this complex (Figure 13a, lanes 8-13). Densitometry was then performed to produce a relative quantitation of the western blot signal (Figure 13a, bottom). It must be noted that we were unable to use an ATP depletion system in this experiment because of the necessity to titrate ATP into the reaction. We can therefore assume that endogenous ATP is present in small amounts in the lysates and could cause a relatively small underestimation of the ADP:ATP ratios reported here. To further verify that the position of the TAP tag had no bearing on the interaction, affinity precipitations of HA-CHORDC1 were performed with both N- and C-terminal HSP90 TAP tag constructs in the presence of 5 mM ATP or 5 mM ADP. The 37 kDa HA-CHORDC1 band was only visible in the presence of ADP regardless of the position of the TAP tag (data not shown).

The CHORDC1-HSP90 interaction has been implicated in innate immune response signaling via its role in the stability of NOD1 (124). NOD1 serves as a cytoplasmic sensor for bacterial components such as peptidoglycan and LPS (125). The ADP used in this study is purified from a bacterial source, so we considered the possibility that traces of bacterial components could be positively influencing the CHORDC1-HSP90 interaction. To test this possibility, we repeated these affinity precipitations in the presence of synthetic ATP and ADP and obtained the same results. We conclude that this

effect is in fact due to the presence of ADP and not a contaminant of bacterial origin. Furthermore, the use of ADP that was enzymatically converted from ATP using glucose and hexokinase was as effective as commercially available ADP at producing this ADP-dependent CHORDC1-HSP90 interaction.

Role of Nucleotide Binding in the ADP-dependent HSP90-CHORDC1 Interaction

It is well established that the binding and hydrolysis of ATP in the N-terminal ATPase domain of HSP90 induces conformational changes that influence the client protein and co-chaperone constituents of HSP90 complexes. Furthermore, the binding of ADP has also been demonstrated to alter the binding properties of proteins in the core HSP90 complex (83,85). CHORDC1 is among a family of proteins containing a domain homolougeous to the HSP90-interaction domain of p23 and SGT1 and both interact with the N-terminal ATPase domain of HSP90 (8,51). Based upon this homolougey, CHORDC1 is predicted to bind the N-terminal ATPase domain similarly. In support of this hypothesis, the HSP90 ATPase domain was shown to be necessary and sufficient to bind CHORDC1 in a yeast two-hybrid assay where nucleotides are presumed to be at physiological ratios (64,124). Because high ADP:ATP ratios appear to be stimulating the HSP90-CHORDC1 interaction, we wanted to determine what structural elements of HSP90 are specifically

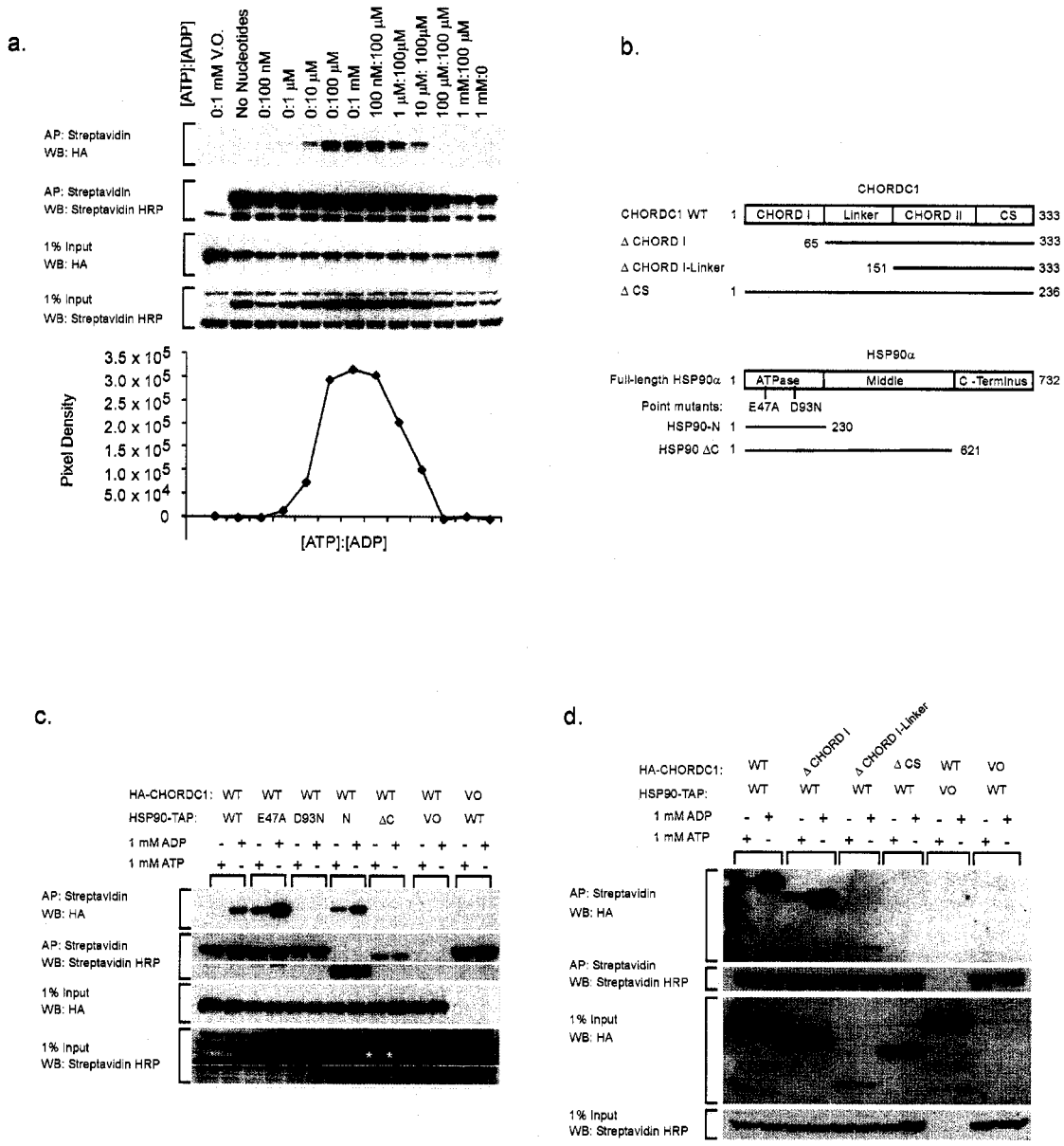

Figure 13. CHORDC1 is an ADP-dependent HSP90 interacting protein. Panel a) shows a western blot of affinity precipitated HSP90 and CHORDC1 and accompanying densitometry data. Precipitations were performed in buffers containing varying amounts of ADP or varying ratios of ADP:ATP. Panel b) shows the domain structure and location (in amino acids) of truncation and point mutants utilized in experiments presented in panels c) and d). Panel c) is a western blot of affinity precipitation reactions performed on HSP90 truncation and point mutants in the presence of either ATP or ADP. Panel c) is a western blot of affinity precipitations performed on CHORDC1 truncation mutants in the presence of ATP or ADP.

responsible for this activity. We tested whether 1) the ADP-dependent binding of CHORDC1 is dependent upon the presence of the HSP90 N-terminus in which the ATPase domain resides; 2) whether nucleotide binding to HSP90 is necessary for this interaction; 3) whether the ATPase activity of HSP90 is essential for this ADP-dependent interaction and 4) whether elements at the C-terminus or HSP90 dimerization confer this interaction. To this end, we co-expressed and affinity precipitated wild type HA-CHORDC1 with a panel of C-terminal TAP-tagged HSP90 mutants consisting of only the N-terminal ATPase domain (HSP90-N), or with the C-terminal 110 amino acid residues deleted (HSP90 ΔC), a point mutant lacking ATP hydrolysis but retaining nucleotide binding (HSP90 E47A) (14,17,18), or a mutant lacking both nucleotide binding and hydrolysis (HSP90 D93N) (15). A schematic of the domain structure of both HSP90 and CHORDC1 is presented in Figure 13b. An attempt was made to construct an HSP90 mutant with the ATPase domain deleted; however this construct was not tested due to undetectable expression. Chen, et al. (1998) also observed decreased expression of an *in vitro* translated N-terminal ATPase domain deletion mutant of HSP90 (126). To test the effects of these mutations on the nucleotide dependence of this interaction these affinity precipitation reactions were performed in lysis buffer containing either 1 mM ATP or 1 mM ADP (Figure 13c).

As observed in the preceding experiments HSP90 E47A mutant precipitated more CHORDC1 than the full-length wild type protein in the reactions containing ADP despite equivalent expression levels of all proteins (Figure 1c, compare lanes 1 and 2 with 3 and 4). We were able to observe some interaction in the presence of ATP; however, the E47A mutant showed increased binding to CHORDC1 in the presence of ADP, much like the wild type protein. Notably, the HSP90 D93N mutant failed to interact with CHORDC1 in either the ATP or ADP reaction despite robust protein expression. This suggests that CHORDC1 is unable to bind the apoenzyme form of HSP90 and that nucleotide binding is necessary. The isolated ATPase domain of HSP90 (HSP90-N) interacted with CHORDC1 in both ATP and ADP reactions. Compared to full-length wild type HSP90, however, the ATPase domain alone (HSP90-N) appeared to interact with less specificity for ADP as evidenced by the CHORDC1 band appearing in the ATP-containing reaction (compare Figure 13c, lanes 1 and 2 with lanes 7 and 8). This suggests that elements outside the ATPase domain may reinforce the selectivity for ADP-dependent binding. It is, however, possible that this result may be due to the ATPase domain being expressed in greater abundance than the full-length WT protein in these cells. The HSP90ΔC mutant failed to interact with HA-CHORDC1 in this assay, perhaps because deletion of the C-terminal 110

amino acids leads to about 10-fold lower expression of this mutant compared to wild type HSP90 (Figure 13c, lanes 9 and 10 white asterisks). We tested several separately cloned HSP90ΔC constructs for expression and obtained the same result (data not shown). Because the C-terminus is responsible for dimerization, these results suggest that an intact HSP90 dimer is required for the HSP90-CHORDC1 interaction as has been shown for p23 (24).

The CHORDC1 protein is composed of two tandem zinc-binding CHORD domains separated by a 90 AA linker region and a C-terminal CS domain (CHORD-containing protein and Sgt1) homolougeous to the HSP90 binding domain of p23 and the human SUGT1 (123). Wu and others have shown subsections of the CHORD domain to be essential for CHORDC1 binding to HSP90 in yeast two-hybrid assays (64,124). Specifically, the N-terminal CHORD domain (CHORDI) was shown to be dispensable for binding HSP90; however, the linker region and the C-terminal CHORD domain (CHORDII) are necessary for the full binding interaction. We wanted to determine which elements of CHORDC1 were involved in producing this novel ADP-dependent interaction with HSP90 and whether deletion of a particular domain would destroy selectivity for ADP. We created N-terminal HA-tagged truncation mutants of CHORDC1 either by deleting the first CHORD domain (ΔCHORDI), deleting CHORDI with the intervening linker region (ΔCHORDI-Linker), or

deleting the C-terminal CS domain (ΔCS) (Figure 13b). We also attempted to test the binding of a CHORDC1 mutant consisting of only the C-terminal CS domain, but this construct failed to express (data not shown). As before, we co-expressed these constructs with wild type full-length HSP90 in HEK293T cells and performed affinity precipitations on lysates containing either 1 mM ATP or 1mM ADP (Figure 13d).

Deletion of the CHORDI domain had no effect on either HSP90 binding or nucleotide selectivity. The amount of ΔCHORDI precipitating with HSP90 was equivalent to the full-length protein suggesting that the CHORDI domain is dispensable for both HSP90 binding and ADP selectivity. These findings are in accordance with previous studies showing CHORDI to be dispensable for this interaction. Interestingly, deletion of the linker region in addition to the CHORDI domain caused the loss of selectivity for ADP. Despite lower protein expression both ATP and ADP reactions precipitated equivalent amounts of CHORDC1 (Figure 13d, lanes 5-6). This raises the possibility that the linker region may play a role in conferring nucleotide selectivity to the CHORDC1-HSP90 interaction. Deletion of the CS domain, however, completely abolished the interaction regardless of nucleotide composition of the reaction (Figure 13d, lanes 7-8). This result is in agreement with previous yeast two-hybrid data showing the CS-domain to be necessary for HSP90 interactions (64).

Notably, in this experiment we were able to detect a basal level of CHORDC1 in the HSP90 wild type reactions containing ATP. We interpret this to be the minimal, ADP-independent interaction between HSP90 and CHORDC1 detected in a previous report identifying CHORDC1 as a HSP90 interacting protein (64).

Depletion of ATP from cells using ATP metabolism blockades has been shown to alter HSP90 function (29). Because CHORDC1 appears to bind HSP90 with higher affinity when ADP ratios are high, we were interested in whether the ADP-dependent HSP90-CHORDC1 interaction could be produced in the same manner. We co-expressed HSP90 and CHORDC1 as above and treated cells with 5 nM rotenone (Rot) and100 nM Antimycin A (AA) at 24 hours post-transfection in media containing the glycolosis inhibitor 2-deoxyglucose (2-DOG). This treatment inhibits both oxidative phosphorlylation and glycolosis, thereby quickly depleting ATP in cells to about 1% of controls within 1 hour (Figure 14, panel a). After treatment with drugs for 20 minutes, 1 hour and 4 hours, cells were lysed and affinity precipitated and analyzed as above except exogenous nucleotides were left out of the lysis buffer and washes. We observed no increase in the CHORDC1-HSP90 complex over the 5 mM ATP control. (Figure 14, panel b). We assume this is due to a severe dilution of ADP when the cells were lysed.

It is possible that the interaction was produced within the intact cells but could not be supported by the low concentrations of ADP in the lysate. Further experiments utilizing *in vivo* protein-protein interaction assays must be performed to verify this interaction in a physiological context.

Discussion

We have presented proteomic and biochemical data that identify several novel HSP90 interacting proteins and go further to characterize an ADP-dependent interaction between CHORDC1 and HSP90. This was the first study employing a proteome-wide analysis of human HSP90 interacting proteins using tandem affinity purification and LC-MS/MS. Previous studies used gel-based identifications which tend to be more robust to protein quantitative measurements and completeness of peptide identifications, but suffer from lack of sampling breadth- leaving many interacting proteins unidentified. Our dataset was enriched for proteins that function as chaperones or HSP90 co-chaperones (24 out of 87 proteins- 28%) and these proteins generally tended to be in the greatest spectral abundance most likely due to their strong, direct interactions with HSP90. However, we did not detect any significant enrichment for known HSP90 client proteins. We consider this to be due mainly to the fact that interactions between HSP90 and client proteins are

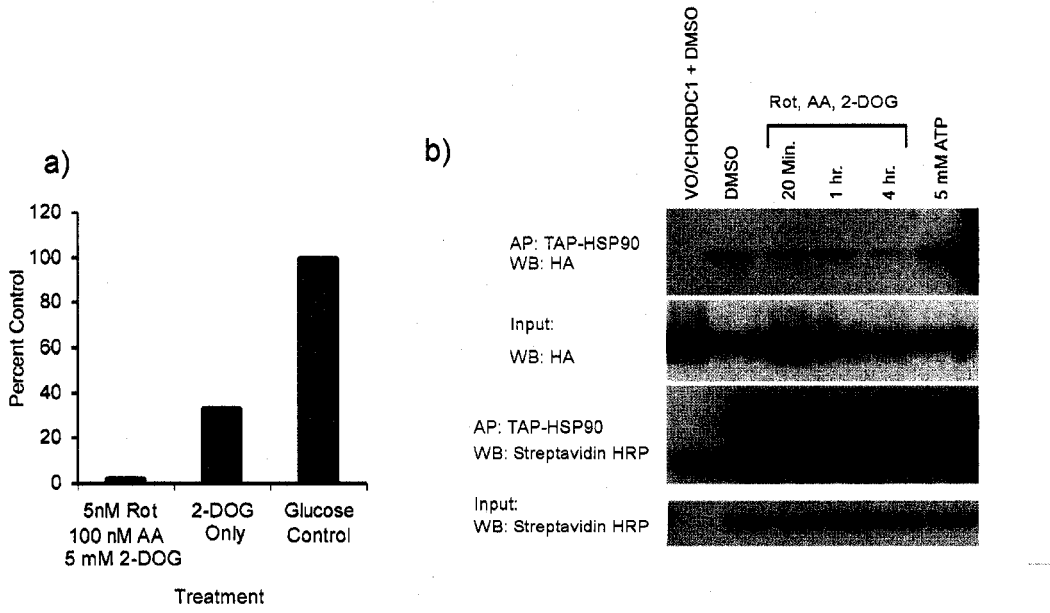

Figure 14. ATP depletion in cells does not sustain the ADP-dependent HSP90-CHORDC1 interaction. a) Rotenone (Rot), antimycin A (AA) and 2-deoxyglucose (2-DOG) were used to inhibit ATP production by both oxidative phosphorylation and glycolosis and cell lysates were assayed for relative ATP concentration after 1 hour. Data are shown relative to control (Glucose only). b) Western blot of CHORDC1-HSP90 complexes affinity precipitated from cell lysates. Drug concentrations were as in panel a) and cells were harvested after the indicated times. 5 mM ATP was supplied without drug treatment as a control.

known to be weak, and transient. The purification and LC-MS/MS technology used in this study may not be sensitive enough to identify these interactions. We are unable to qualify any of the novel HSP90 interacting proteins identified in this study as client proteins based solely upon sequence or predicted structure. Currently, no consensus sequences on client proteins have been shown to confer interactions with HSP90 as has been shown for co-chaperones (TPR and CS-domain). Rather, interactions between HSP90 and

client proteins have been attributed to a set of generalized features common to misfloded or unstable proteins such as areas of solvent-exposed hydrophobicity (33). The observation that only a specific subset of proteins interact with HSP90 creates a complicated problem: What are the specific set of requirements that influence HSP90 interactions with client proteins?

The relative lack of known HSP90 client proteins in our dataset may also be due to the purification procedure itself. We did not enrich our cell lysates for any particular cellular compartment such as membrane fractions or organelles; several known HSP90 client proteins are membrane-bound receptors. We also did not selectively harvest cells in any particular stage of the cell cycle. Several HSP90 clients show cell cycle coordinated expression patterns such as Aurora B. We did identify the cell cycle kinase Aurora B as an interactor in our unfiltered dataset; however, peptides matching this protein were not abundant enough to pass our filtering criteria showing only one peptide in two out of three runs of the E47A ATP group and one peptide total in three WT ATP runs. It is important to mention that these peptides were unique to this kinase and showed high PeptideProphet scores. It would be interesting to see if Aurora B and other cell cycle regulated client proteins are enriched in HSP90 complexes purified from metaphase arrested or synchronized cells. This

method would also identify other cell cycle-dependent HSP90-interacting proteins.

HSP90 Complexes are Sensitive to Nucleotide and Drug Ligands

This study also demonstrates that HSP90 complexes are dynamic with respect to nucleotide and drug ligands. This was the first whole proteome-level study demonstrating that the constituents of HSP90 complexes are influenced by nucleotides and geldanamycin. One striking result is the observation that HSP90 complexes from geldanamycin treated cells are highly enriched for components of transcriptional machinery (Figure 11). These data present the possibility that disruption of HSP90 ATPase activity may either lead to alterations in fundamental transcriptional programs or may actually buffer against stress-induced perturbations of transcriptional processes. Some clues come from a study by the Workman lab where cDNA microarray and proteomic analysis (2D-electrophoresis) was performed on whole cell lysates treated with the closely-related geldanamycin analog 17-AAG (127). Several components of transcriptional machinery were shown to be altered by 17-AAG, lending further evidence to the notion that fundamental transcription process are altered by HSP90 inhibition. Additionally, several chaperones including HSP90α, HSP90β, HSPA1A (HSP70) and HSP27, were increased in

expression after 17-AAG treatment. The co-chaperones AHSA1 and ST13 (HIP) also showed increased expression. These findings present the possibility that the increase of these components in the geldanamycin-dependent HSP90 complexes may be a result of increased expression of these factors and not necessarily indicative of some direct structural or biochemical effect of geldanamycin binding. Interestingly, the majority of transcription-related genes (splicing factors and snRNPs, and hnRNPs) identified in this study were actually down-regulated, including HNRPAB- a novel HSP90 interacting protein described in this work. In our experiment, HNRPAB did not show any significant change in abundance in the WT GA group. The fact that several known HSP90 interacting proteins upregulated after 17-AAG treatment were not found to be increased in geldanamycin-dependent complexes confounds the idea that a protein's expression level is directly related to its membership in HSP90 complexes. However, this idea deserves further testing. Overexpression of components of the geldanamycin-dependent complex and affinity precipitation of HSP90 complexes with and without geldanamycin treatment could determine whether protein level alone influences the constituents HSP90 complexes and whether geldanamycin treatment is required for these effects. However, direct comparison between these microarray/ protein expression experiments and our proteomic data is complicated by the fact that the first sample of protein and mRNA in the

Workman study was taken for analysis 8 hours after 17-AAG treatment, so these effects may be indirect or a consequence of a cell cycle blockade known to be elicited by 17-AAG treatment. In our experiment, cells were harvested at 2 hours after treatment in efforts to observe early affects of geldanamycin treatment and minimize secondary effects such as cell cycle arrest or apoptosis.

ATP-dependent Interactions

The HSP90 E47A mutant appears to function as a kinetic trap for HSP90 interactions. We were able to identify 41 proteins interacting with this mutant 18 of which are known HSP90-interacting proteins. Furthermore, several of these proteins appear to selectively bind the ATP-locked E47A mutant. We propose that these are putative ATP-dependent HSP90 interacting proteins. However, this assertion needs further *in vitro* testing with purified proteins. Among the proteins identified with the E47A mutant were 7 CS domain-containing proteins (CDPs) including the known ATP-dependent interacting co-chaperone PTGES3 (p23). 6 out of 7 of these proteins bound to HSP90 homogenously to with regard to HSP90 E47A (Figure 12, group 1), strongly suggesting an ATP-dependent binding mechanism. In addition, several putative novel HSP90-interacting proteins appear to bind to selectively to the

E47A mutant in this manner. Further biochemical analysis of these interactions is necessary; however, it is tempting to speculate that these proteins may represent new HSP90 client proteins or co-chaperones. It should be noted that our filtering criteria excluded several known HSP90 complex members. Among those filtered was SKP1, a member of a complex containing HSP90 and SGT1 (54,55). Other known HSP90-interacting proteins filtered were CNSK2A1, S100A7, SFRS1, two HSP40 homolouges and HSPA1L, a HSP70 homolouge. Perhaps further optimization of the purification procedure such as performing reciprocal purifications such that the calmodulin purification was performed first, before the streptavidin step. We realize that forgoing the use of TEV for free-biotin (see materials and methods) may have increased the background in the vector only preparation. However, as judged by the silver staining of our TAP preparations we believe that the background protein content in the vector only group is minimal (Figure 7).

Insights into the Function of HSP90

This study has presented data that suggests a functional role for HSP90 in fundamental transcription processes and provides the basis for a new mechanism of action geldanamycin on a cellular level. Geldanamycin and radicicol are natural product antibiotics with antifungal and antimalarial

activities. Many antibiotics target fundamental cellular processes such as transcription and translation. It is tempting to speculate that one fundamental function of these antibiotics is to inhibit or alter transcription.

Our results do not point directly to HSP90 functioning as an energy sensor *per se*. This is supported by the observation that addition of ADP to the lysis buffer during purification of HSP90 complexes has relatively little effect. We would expect to see more effects on proteins with direct metabolic functions such as ATP synthesis or glycolytic processes. We did not find any enrichment for metabolic enzymes in these experiments. However, we cannot formally exclude the possibility that HSP90 may regulate energy production or be sensitive to fluctuations in physiological ATP:ADP ratios. Further experiments utilizing inhibitors of oxidative phosphorylation to deplete ATP in living cells would re-test this idea and perhaps bring different results.

The CS Domain Confers Heterogeneous Ligand-regulated Interactions with HSP90

We also presented biochemical interaction data confirming a nearly complete panel of CS domain-containing proteins from the human proteome to be HSP90 interacting proteins. These data strengthen the hypothesis that the CS domain is a *bone fide* HSP90 interaction element. However, the presence of

the CS domain alone did not confer homogeneous interactions amongst CS domain-containing proteins with respect to nucleotide or the pharmacological HSP90 inhibitor geldanamycin. One protein ITGB1BP2, or melusin, was shown here to have an ADP-dependent complex formation similar to CHORDC1; however, we were only able to show interaction with the HSP90 E47A mutant with ADP. The observation that in addition to CHORDC1, ITGB1BP2 is stimulated to bind HSP90 E47A by ADP strengthens the assertion that the CHORD domain may be an ADP-dependent HSP90 binding element. However, with these data we are unable to explain why ITGB1BP2 binding to wild type HSP90 is not stimulated by ADP as with CHORDC1. Perhaps sequences outside the CHORD domains affect the affinity of this interaction, or perhaps because of subtle differences in the structure between the two CHORD domains. Further experiments using purified proteins and mutational analysis of conserved residues in the CHORD domains are needed to resolve the biochemical details of this interaction.

These results also define a group of CHPs that appear to interact weakly or not at all with wild type HSP90 while interacting relatively strongly with the hydrolysis-deficient E47A mutant. These complexes are disrupted by pretreatment with geldanamycin, but are insensitive to the addition of ATP or ADP to the lysates. This finding is not consistent with *in vitro* evidence that the

interaction of PTEGS3 (p23) with HSP90 is inhibited by ADP (16,21,30,31). In our study it may be possible that our purification conditions were not permitting ATP/ADP exchange. This possibility is supported by the fact that addition of geldanamycin to the lysis buffer alone without pretreatment of the cells in culture does not disrupt the HSP90-NUDC interaction (Figure 7a). It has been proposed that once HSP90 binds ATP, a "lid" structure closes over the bound nucleotide and commits the complex to ATP hydrolysis (11). If very little *in vitro* ligand exchange occurred in the wild type HSP90, the nucleotide bound in the cell would not change throughout the affinity precipitation procedure barring the conversion of a small amount of ATP to ADP from the residual ATPase activity. In whole cell lysates, there may be several factors present in HSP90 complexes that prevent ATP-ADP exchange that are not present in reactions containing purified components. This provides some interesting questions into the molecular basis of the ADP-dependent HSP90 interaction with CHORDC1. Under our experimental conditions, it is not possible to discount the possibility that nucleotides may be binding another co-purifying factor and this forms the interface between CHORDC1 and HSP90.

Surprisingly, several CS domain-containing proteins appear to have no nucleotide selectivity and are insensitive to disruption by geldanamycin (see Figure 12, group 3). These data suggest that geldanamycin does not disrupt

all HSP90 interactions with CDPs. In the case of USP19, both proteomic and supplementary immunoblotting experiments support the assertion that this interaction is insensitive to HSP90 inhibition. Interestingly, USP19 contains a C-terminal MEEVD motif homolougeous to that found at the C-terminus of HSP90 and HSP70. This motif may provide an additional interaction interface for other TPR domain containing proteins including co-chaperones. It remains to be tested whether particular sequence variations in the CS domain are responsible for variable ligand-dependent HSP90 binding amongst the CS domain family members.

CHORDC1 and Innate Immunity

Several studies have established the role of the plant CHORDC1 homolouge RAR1 in innate immunity and host response to pathogenic infection (128,129). RAR1 mutants are defective in the host response to pathogenic invasion by the powdery mildew *Blumrtia sp.* and other plant pathogens. Like CHORDC1, the *Arabidopsis* RAR1 contains two tandem repeated CHORD domains and binds to the *At*HSP90 ATPase domain. This interaction appears to be required for the stability of RPS2, a pathogen resistance protein (R protein) in plants with homolougey to the metazoan Toll-like receptors. Hahn, et al (124) presented evidence that CHORDC1 may function analogously in human

innate immunity. In this work, purified HSP90 complexes were shown to contain both CHORDC1 and NOD1, member of mammalian proteins functioning similarly to the R proteins in plants.

Because the presence of ADP in cell lysates stimulates the CHORDC1-HSP90 interaction, we propose the possibility that the ADP-dependent HSP90-CHORDC1 interaction may also function in innate immunity. In support of this hypothesis, perturbations in the ATP:ADP ratios occur when cells undergo necrosis in response to bacterial toxins and this process leads to inflammatory signal activation. *Streptococcus pyogenes* transmits an NADase to the host cell which depletes cellular NAD, and as a result, ATP levels drop (130). Furthermore, the phenomenon known as cytopathic hypoxia elicited by sepsis is marked by a drop in the cells ability to utilize molecular oxygen in ATP synthesis, suggesting mitochondrial damage (131). ATP can also be depleted through direct damage of mitochondrial membranes during *shigella* (132) *B henselae* (133) infections. These findings suggest the intriguing possibility that CHORDC1-HSP90 interaction may be stimulated in cells experiencing these pathogenic insults. It remains to be tested whether microbial infection or pharmacological ATP depletion can stimulate the HSP90-CHORDC1 interaction *in vivo.*

Materials and Methods

Plasmids

Expression vectors for proteomic analysis were derived from the parental TAP expression vector pGlue (Angers, et al 2006). N-terminal TAP fusions of the wild type HSP90α and E47A mutant were created by PCR amplification from cDNAs and verified by sequencing. Subsequent biochemical analysis was performed using pCS2+ parental vectors for all C-terminal HSP90-TAP constructs and the pSPORT6 backbone (Invitrogen, Carlsbad, CA) for expression of all HA-tagged CHORD domain-containing proteins (CHPs). CHORDC1 cDNA was created from RNA isolated from HEK293T cells and PCR amplified. All other CHPs were derived from cDNA clones obtained from the IMAGE collection (Open Biosystems, Huntsville, AL). Clone ID numbers and the position of the HA tag is supplied in supplemental information.

Cell culture

Low passage number HEK293T cells (ATCC #CRL-1573) were used in all experiments. Cells were grown in high-glucose DMEM containing 10% FBS,

penicillin and streptomycin, and 2 mM supplemental L-glutamine (Invitrogen, Carlsbad, CA). All incubations were at 37°C with 5% CO_2.

Nucleotide and Geldanamycin Stocks

Stocks of 250 mM ATP were made in 50 mM HEPES, 5mM $MgCl_2$ (pH 8.0) and treated with 50mM phosphocreatine and 50 μg/mL creatine kinase (Roche Applied Science, Indianapolis, IN) for three hours at 20°C. Stocks of ADP were made in 50 mM HEPES, 5mM $MgCl_2$ (pH 8.0) with 100mM glucose and 20 U/mL Hexokinase (Roche Applied Science, Indianapolis, IN) and incubated for three hours at 20°C. Both stocks were then subjected to ultracentrifugation at 4°C using YM-3 (3,000 Da cutoff) filters (Millipore, Billerica, MA) to remove enzymatic activities. 20mM geldanamycin stock (NCI, Bethesda, MD) was made by suspending purified drug in 100% DMSO.

ATP depletion in Cells and ATP Assay.

Cultured cells were washed gently 3 times with PBS at 37°C and complete media was replaced with media lacking glucose and containing 5mM 2-Deoxyglucose, 5nM Rotenone and 100nM Antimycin A (Sigma-Aldrich) . Cells were incubated for the indicated time, washed 3X with warm PBS, and

harvested with TAP lysis buffer (see below). Lysates were diluted 1000-fold in cold PBS. 100 μL diluted lysate was then added to 100 □L Cell Titer Glo ATP assay reagent (Promega, Madison, WI) in a black plastic opaque 96-well assay plate and incubated at room temperature for 30 minutes. Luminosity was determined using a Topcount NXT (PerkinElmer, INC., Waltham, Massachusetts).

Affinity Purifications and Mass Spectrometry

Affinity purifications were adapted from Angers, et al (134). 7.5×10^8 HEK293T cells were grown to 100% confluence on 15 cm coated plates (Nunc, Roskilde, Denmark. Cat No. 168381). Two hours before lysis, the cells were treated with 5 μM geldanamycin in 0.1% DMSO where indicated or left untreated. The cells were gently washed twice on the plates with ice cold PBS and subsequently detached from the plate by aspiration in PBS and centrifuged for 2 minutes at 4°C in a clinical centrifuge. All further procedures were conducted at 4°C unless otherwise noted. The supernatant was replaced with 7.5 mL of TAP lysis buffer containing 50 mM HEPES-KOH (pH 8.0), 10% glycerol, 0.1% NP-40, 150 mM KCL, 5 mM $MgCl_2$, 2 mM DTT and EDTA-free protease inhibitor cocktail tablet (Roche Applied Science, Indianapolis, IN). Before lysis, the lysis buffer was supplemented with either 5 mM ATP

including an ATP regeneration system (50mM phosphocreatine and 50 μg/mL creatine kinase) (135), 5 mM ADP with an ATP depletion system (100mM glucose and 20 U/mL Hexokinase), (136), or 5μM geldanamycin (GA) with 0.1% DMSO total. Lysates were cleared by centrifugation and supernatant was added to 200 μL packed Streptavidin beads (GE Healthcare, Piscataway, NJ) that were pre-washed three times and equilibrated in 300 μL TAP lysis buffer. The remaining steps were conducted essentially as in (137) with the following exceptions: TEV protease cleavage was eliminated as free biotin alone eluted most of the HSP90; ATP, ADP and GA were supplemented to all buffers except the elution step. Protein complexes were finally eluted from calmodulin beads 3 times in 300 □L for a total of 900 μL. Each sample was adjusted to 50 mM ammonium bicarbonate and the disulfide bonds were reduced with 5 mM dithiolthreitol for 1 hour. The proteins were digested overnight with modified porcine trypsin (V5111, Promega, Madison, WI) at 37°C. The resulting peptide mixtures were concentrated to 100 □L volumes, desalted using C18 ZipTips (Millipore), dried to completion and resuspended in dH_2O with 0.1% formic acid.

Each digested protein mixture was analyzed by automated microcapillary liquid chromatography-tandem mass spectrometry (LC-MS/MS). A 75 μm i.d.

PicoFrit silica capillary nanospray emitter (New Objective, Woburn, MA) was slurry-packed with 20 cm of 5 μm C18AQ (100 Å.) packing material (Michrom Bioresources, Auburn, CA) using a pressure bomb. The column was placed inline with a guard column created from a 100 μm i.d. IntegraFrit column (New Objective) packed with 1.5 cm of 5 μm C18AQ (200 Å) packing material. The column setup was connected inline to an Eksigent 2D nanoLC (Eksigent Technologies, Dublin, CA) and interfaced to a LTQ-FT ion trap mass spectrometer (ThermoFisher Scientific, San Jose, CA).

The mobile phase for the HPLC separation was 0.1% formic acid in water (Buffer A) and 0.1% formic acid in acetonitrile (Buffer B). The LC-MS/MS experiments consisted of a 100 minute HPLC run where the HPLC gradient started at 2% buffer B for 5 minutes, ramped to 10% buffer B over 3 minutes, then ramped to 40% buffer B over 60 minutes followed by washing between samples at 80% buffer B for 12 minutes and re-equilibration at 2% buffer B for 20 minutes.

The LTQ-FT mass spectrometer was operated in the data-dependent acquisition mode using the Xcalibur 2.0SR2 software. The experiment consisted of a single full-scan mass spectrum in the FT (400 - 1800 m/z, 100K resolution at m/z 400) followed by 5 data-dependent MS/MS scans in the ion

trap at 35% normalized collision energy. The mass spectrometer was set to only perform MS/MS on ions with identifiable charge states of +2 or +3. The dynamic exclusion parameters were as follows: Repeat Count = 1; Repeat Duration = 30; Exclusion List = 100; and Exclusion Time = 45.

Raw Data Analysis and Database Searching

The MS/MS scans from each LC-MS/MS run were converted from the .RAW file format to .mzXML files using the program ReAdW.exe (v. 1.1) with the default parameters. The database search program X!Tandem (v. 2005.12.01.1) (138), bundled in the CPAS (Computational Proteomics Analysis System) data analysis system (v. 2.1)(139), was used for peptide identification of the MS/MS spectra. The Comet scoring function (K-Score) was used in place of the default X!Tandem scoring function (140). The following parameters were used in the database search: Full trypsin enzyme specificity; Missed cleavages allowed = 2, Peptide mass tolerance = 2.0 Da; Fragment ion tolerance = 0.5 Da; Monoisotopic molecular weight for both peptide and fragment ion masses, b/y ion search, and Variable modification at M = +15.995, Q = -17.027 only if on the peptide N-terminus and E = -18.011 only if on the N-terminus.

The MS/MS spectra were searched against a custom database created by combining the IPI Human database (v. 3.26, released Feb, 21, 2007; 67665 sequences and 3 bovine/porcine trypsin sequences with a pseudo-reversed version of each protein sequence (135336 sequences total) for the purpose of estimating the false discovery rates (FDR). The pseudo-reversed sequences were created by identifying all the tryptic protein cleavage sites and holding all terminal lysine and arginine residues static while reversing all other amino acids present within the internal peptide sequences of the protein (5). The .mzXML peak lists were filtered by X!Tandem during the database search with the following parameters: maximum charge state +4, minimum peptide mass 600 Da, maximum peptide mass 4000 Da, and the minimum number of allowed fragment peaks was 6. The MS/MS database search results were then analyzed using PeptideProphet (v. 3.0 April 1, 2004 (TPP v2.9 GALE rev.9, Build 200703221424)) and ProteinProphet (v. Insilicos_LabKey_C++ (TPP v2.9 GALE rev.9, Build 200703221424)) both under default settings. The final results were then organized in the CPAS system.

Comparison, Normalization, Protein List Filtering, and Statistical Analysis

Peptide spectral counts from all the identified proteins were compared using the *Compare* function in CPAS. The following filtering protocol was used:

First, proteins having less than a 5-fold spectral abundance over the vector control in all experimental groups were considered to be contaminants and were eliminated. Secondly, proteins with less than 4 spectra total (pre-normalization) for the three replicates were also eliminated. The total spectral count for all proteins from each run was then determined individually and used to normalize all runs. The spectral abundance factor (SAF) was then determined by dividing the normalized spectral count for an individual protein by the length of the protein in amino acids (102,141). This calculation accounts for the fact that longer proteins contain more tryptic sites than shorter proteins and forms a basis for determining relative protein abundance (102,141). Thirdly, the list was then searched for common contaminants such as keratin, and these proteins were eliminated. At this stage, any redundant protein identifications were identified and spectral counts were combined into one entry. Where several splice variants were identified, the spectra for all variants were combined and redundant peptides (single peptides matching two variants) were only counted once. This was determined using the scan numbers for spectra from individual runs. The amino acid number for the longest protein isoform was used to determine the SAF for these proteins. The resulting list of interacting proteins was then subjected to ANOVA to determine whether variances were due to any particular experimental condition. A coupled t-test then determined p-values for all 4 experimental

conditions. A secondary g-test (3 degrees of freedom) was performed on proteins with more than 25 total spectral counts (pre-normalization) (96,100). All computations were performed using the R statistical analysis software.

Transfections, Affinity Precipitations and Western Blotting

1.3×10^6 HEK293T cells were plated in 60 cm plates 24 hours before transfection by calcium chloride precipitation. Media was changed 18 hours post- transfection and cells were allowed to recover 24 hours before lysis. Drug treatments were as described above. Lysates were prepared in 500 μL TAP lysis buffer, cleared by centrifugation, incubated with 5 μL streptavidin beads for 5 hours in a 1.5 mL deep well 96-well plate and transferred to Orochem OF1100 fritted 96-well plate for washing. The bead solution was centrifuged briefly to remove supernatant, washed 4 times by centrifugation with 250 μL TAP lysis buffer containing the appropriate nucleotide or drug and eluted with 20 μL hot 1.2x SDS PAGE loading buffer. Western blotting was performed using anti-HA (Covance, Emeryville, CA. Cat No. MMS-101R) and HRP-conjugated streptavidin (GE Healthcare, Piscataway, NJ). ImageJ was used to collect all densitometry data.

Chapter 2: Validation of Human Ribonucleotide Reductase as a Target for Mismatch Repair-Deficient Cancers

Introduction

Although DNA replication is necessary for life, the process is inherently mutagenic. Fortunately, cells have employed proofreading and repair mechanisms to ensure mutagenic events are kept within a range that supports the crucial balance between viability of the individual and evolution of the species. One such repair mechanism termed mismatch repair (MMR) functions to resolve mutations caused by replicating polymerases and recombination events. The importance of the MMR pathway in cancer is underscored by the prevalence of genomic instability in tumor cells that lack MMR activity. Increased genomic instability is believed to arise from errors in DNA replication that remain unrepaired due to defects in MMR. These mutations propagate in subsequent rounds of replication and eventually lead to cancer. Currently there are no options for specifically and effectively treating tumors deficient in mismatch repair, which makes the study of MMR-deficient cancers scientifically intriguing and clinically relevant. We have focused on studying the genetics of MMR-deficient cancers and are directly applying this knowledge to identify and develop novel chemotherapeutic

agents that selectively target MMR-deficient cancers. We have identified several genes in the yeast *S. cerevisiae* that are synthetic lethal with MMR-deficiency having direct sequence and functional homologues in humans. One gene encodes the catalytic subunit for the enzyme responsible for *de novo* dNTP synthesis- ribonucleotide reductase (RNR).

Experiments in this chapter attempt to validate RNR as a target for anticancer agents that selectively kill MMR-deficient cancers. To this end, we designed human RNR mutants analogous to those found in the yeast RNR and expressed them in a human matched-pair MMR+/MMR- cell line to determine whether similar synthetic lethal effects are observable. These mutants are recessive, and no synthetic lethal phenotype was observed. As an alternative strategy, we attempted to identify synthetic lethal alleles of the human RNR in *S. cerevisiae*. We identified one recessive double point mutant and attempted unsuccessfully to identify dominant alleles using a modified screen. Finally, we attempted to eliminate endogenous wild-type RNR activity from the human matched-pair cell line using shRNA technology as a strategy to observe the synthetic lethal phenotype of the previously identified recessive synthetic-lethal RNR alleles. We were unable to reduce RNR expression in these cells using this approach. We conclude that due to technical difficulties in obtaining suitable conditions to test our hypothesis,

the human RNR is currently not a valid target for human MMR-deficient cancers.

Background

The DNA mismatch repair pathway (MMR) functions to correct base-base mismatches and short insertion and deletion loops (IDLs) of less than 15 mismatched bases. These errors can arise spontaneously during replication and recombination or through the effects of genotoxic agents. MMR activity prevents the propagation of these errors to progeny cells by first sensing the DNA mismatch then discriminating between the wild type template DNA and the mutated, newly synthesized strand (142,143). After a series of signaling events, the lesion is excised by endonucleases and correct nucleotides are incorporated. The newly repaired DNA strand is then re-ligated. This pathway is perhaps the most thoroughly understood in *Escherichia coli* MutHLS system; however much is being discovered about the conserved functions of MMR genes in eukaryotic organisms (for review see (142)). Many genes are highly homologous in the MutHLS pathway in *E. coli*, and consequently many MMR genes have orthologs in multiple species. The complex employed to sense replication errors and signal their repair in eukaryotic cells consists of two functional classes of proteins that share both

sequence and functional homology to their prokaryotic counterparts (Figure 15 A). The MutS homologues, MSH1-6 in *S. cerevisiae* and hMSH2-6 in humans are responsible for sensing mismatched or unpaired DNA lesions and subsequently function in concert with the MutL homologues to activate downstream repair machinery (MLH1-3, PMS1 in *S. cerevisiae* and hPMS1&2, hMLH1&3 and humans) (Figure 15 B). Because the functions of these homologues are virtually identical between these organisms distinctions between species will only be made only when major departures in function are notable.

MutS Complexes

The MutS proteins Msh2, Msh3 and Msh6 are the primary MutS proteins involved in the sensing of DNA mismatches and the subsequent signaling to downstream repair proteins during mitotic growth in both yeast and humans. These proteins form heterodimeric complexes composed of Msh2p and either Msh6p (MutSα complex) or Msh3p (MutSβ complex). Although MSH2 and hMSH2 are able to bind heteroduplexed DNA as homodimers *in vitro* (144-146), genetic (147,148) and biochemical data (149-153) confirm that heterodimers of MSH2 with MSH3 or MSH6 are in fact the

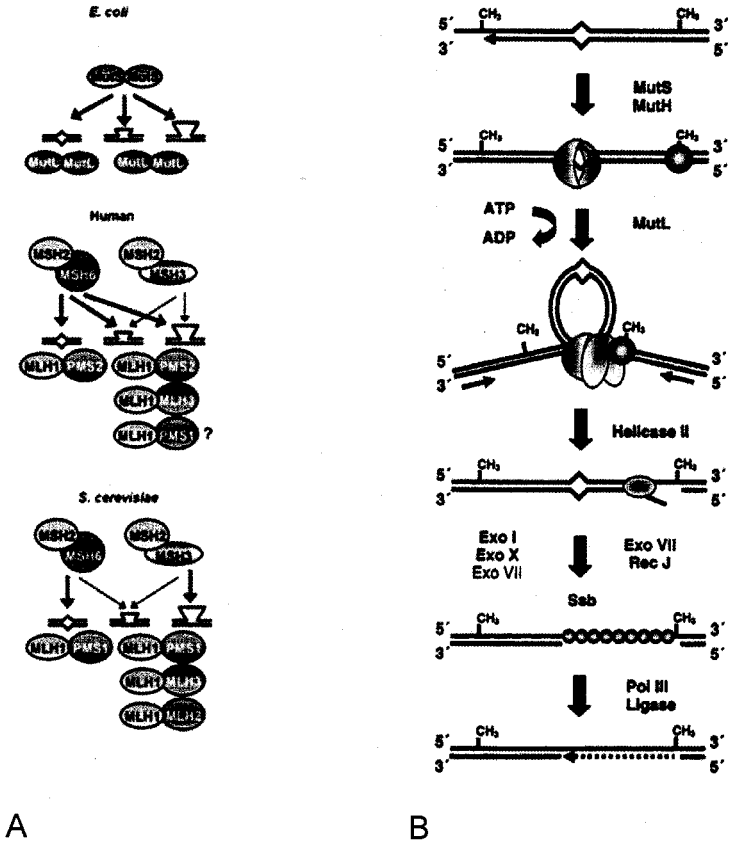

Figure 15. Comparison of the componenets of MMR pathways form *E. coli*, *S. cerevisiae*, and humans. Arrows indicate activity toward DNA mismatch heterologies. B) General progression of mismatch recognition to repair as exemplified in *E. coli*. Images from Marti, et al 2002.

Physiologically relevant complexes required for MMR activity. The MutS heterodimeric complexes form sliding clamps that encircle the DNA and translocate along DNA duplexes- apparently scanning for DNA mismatches (154,155). The MutSα heterodimer (MSH2-*MSH6*) exclusively identifies single mismatched bases and short loops consisting of fewer than 8

nucleotides while the MutSβ heterodimer (MSH2-MSH3) recognizes larger loops consisting of 8-14 nucleotides (142,152,156). Early genetic experiments set fourth the idea that MutSα and MutSβ had redundant and overlapping activities for insertion/deletion loops (IDLs) of moderate length consisting of loops of 4 and 12 unpaired nucleotides, though the yeast MutSα seems to have a more restricted substrate range with respect to loop size. The *msh2Δ* mutant gave rise to a marked increase in single base mismatches and IDLs from one to several nucleotides while *msh6* single mutants have an increased prevalence of mutagenic IDLs consisting of several nucleotides. Although the degree to which each complex binds a particular substrate may vary amongst reports, a definite pattern exists: MutSα binds single mismatches and MutSβ binds larger IDL structures while having little affinity for single mismatched bases (148). With these findings in mind, the MSH2p component of the complex is believed to act as a scaffold or adaptor protein for interactions with other MMR factors while MSH3p or MSH6p supply the complex with specificity toward particular heteroduplex structures (148). As a result, loss of function mutants in MSH2p have a completely inactivated MMR system (147,157,158).

MutL Complexes

Little is known about the signaling mechanisms involved in MMR downstream of MutS activities, though genetic data have confirmed that similar to prokaryotic MMR, eukaryotic MutL homologues are involved in the signaling of downstream repair machinery through physical interactions with the lesion-sensing MutS complexes. In both humans and yeast, MutL proteins are heterodimeric with Mlh1p (hMLH1 in humans) being present in every known MutL-containing complex. Deletion of this gene causes a dramatic increase in mutation rates and leads to a generalized genomic instability phenotype caused by a total loss of DNA MMR activity. The predominant MMR signaling complex involving MutL proteins is MutLα composed of a heterodimer of hMLH1 and hPMS2 in humans (159) or *MLH1* and *PMS1* in *S. cerevisiae* (160).

Cancer and MMR

Persistent genomic instability caused by the loss of MMR function can ultimately lead to the development of cancer in humans. A heritable disease called HNPCC (*H*ereditary *N*onpolyposis *C*olon *C*ancer) is an autosomal recessive disorder also known as Lynch syndrome, caused by a inactivating germline mutation in one allele of either hMLH1, or hMSH2 coupled with a

somatic inactivation of the other wild type allele (161). Mutations in hPMS2 are also present in HNPCC populations, but to a lesser extent. Although HNPCC accounts for only about 3% of the total colon cancer incidence, individuals with germline mutations in MMR have an 80% chance of developing cancer (162,163). Inactivation of the MMR system can lead to widespread genomic instability measured by increases in point mutations caused by single base misincorporations and larger insertions and deletions caused by unrepaired IDLs. Alone, a inactivating mutation in one allele of hMLH1 or hMSH2 is not sufficient to cause genomic instability; mutation rates increase only when this germline mutation is accompanied by the eventual loss of the other functional allele. Several somatic defects in the second allele can occur with promoter hypermethylation being very common (164). The loss of MMR is generally thought to be an early step for HNPCC tumor formation. MMR defects lead to secondary mutations in growth controlling tumor suppressor genes which drive tumor growth (165,166). In addition to HNPCC, MMR mutations can lead to several types of sporadic cancers such as gynecological, lung and non-HNPCC colon cancers. Approximately 15-25% of these sporadic tumors display genomic instability indicative of MMR defects, such as microsatellite length instability (167,168).

Understandably, the increase in genomic instability arising from MMR defects coupled with increased proliferation rates serves as a means for developing metastatic potential and resistance to chemotherapeutic agents. DNA-damaging chemotherapeutic agents such as streptozocin (*N*-methyl-*N'*-nitro-*N*-nitrosoguanidine), temozolomide (*N*-methyl-*N*-notrosourea), cisplatin, and 6-thioguanine require functional MMR for anticancer function. These DNA intercalating agents can also often cause selection for MMR-defects in non-tumor cell populations, leading to secondary tumors. For example, MMR is required for toxicity of O6-methylguanine because lesion-bypassing polymerases incorporate Thymidine across from *O*6-methylguanine creating a structure that is bound by MutSα. During re-synthesis of the mismatch thymidine is once again incorporated across form the methylated guanine and this is once again recognized by the MMR system. This reiterative process eventually leads to cell death. One of the most common and most effective treatments for MMR-deficient colon cancers is the florinated uracil derivative 5-fluorouracil (5-FU) used in conjunction with methotexate, but is criticized for having significant toxicity to normal cells.

MMR Synthetic Lethal Genes

Since many conventional anticancer chemotherapeutics cause damage to otherwise healthy tissues, the development of anticancer agents that selectively kill MMR-deficient tumors is of high priority. One approach is to identify genes are essential to tumor growth and survival, but have little to no essential role in the functions of healthy tissues. When these genes are mutated, tumor cells die, while leaving normal cells intact- a phenomenon known as synthetic lethality. Moreover, pharmacological alteration of these targets will be toxic to tumor cells while leaving normal cells intact. With these goals in mind, we conducted a screen in the model organism *S. cerevisiae* to identify mutant alleles that are lethal exclusively to cells lacking MMR while allowing wild type cells to grow unaltered, a phenomenon referred to in this work as mismatch repair synthetic lethality (*msl*). *S. cerevisiae* was employed for this screen because the yeast MMR pathway is highly similar to that of humans, therefore it was likely that any mutant alleles identified would have direct human homologues and the *msl* phenotype in yeast may therefore be reproducible in genetically analogous human cancers. In this screen, the MMR pathway was disabled in wild type yeast by deleting the *MLH1* gene. Effectively, this deletion causes an elevated mutation rate and genomic stability similar to that seen in human cancers

(169,170); therefore we believe these yeast serve as a suitable model for human cancers lacking MMR. Mutant alleles of three genes were isolated including a point mutatant of the catalytic subunit of Ribonucleotide Reductase *RNR1* (J. Pincus, et al. (2008), in preparation). The other two mutations identified were in the exonuclease domains pol δ and ε affecting functions integral to the proofreading activities of these enzymes. Importantly, Rnr1p has a direct functional and sequence homologue in the human genome called RRM1. The function of this enzyme has been known for decades and many studies have probed its molecular mechanics, but relatively little is known about its genetic interactions. To further understand the relationship between *RNR1* and the MMR pathway on a molecular scale, a secondary screen employing mutagenic PCR of the *RNR1* gene later identified several additional synthetic lethal alleles (J. Pincus, et al. (2008), in preparation).

Ribonucleotide Reductase

Ribonucleotide reductase RNR is an essential enzyme catalyzing the rate-limiting step in deoxynucleotide synthesis through reduction of the 2' hydroxyl of ribonucleotide diphosphates. These dNTP precursors are quickly phosphorylated non-specifically in a single step by nucleoside

diphosphokinase to become deoxynucleotide triphosphates. The primary functional unit of RNR is an $\alpha_2\beta_2$ heterodimer consisting of a dimer of a large catalytic subunit generally referred to as R1 and a radical-supplying dimeric subunit called R2 (171). Although recent studies have presented models for hexameric quaternary structures (172), much of the structure-function information is based upon dimeric forms of the subunits. R1 contains the active site where ribonucleotides are reduced, and two distinct allosteric activity sites, one governing the rate of reaction and one controlling the specificity of NDP substrate species to be reduced (Figure 16). The R2 dimer supplies the energy to R1 for the reduction reaction through an organic free radical.

Ribonucleotide Reductase Allosteric Regulation

RNR required for the *de novo* synthesis of all four deoxynucleotides and must produce a balanced pool of these nucleotides for accurate DNA replication. Therefore, it is not surprising that this enzyme is extensively regulated. The α_2 dimeric R1 catalytic subunit contains two distinct allosteric regulatory sites dependent upon feedback of the dNTP products (Figure 17). One site termed the "activity site" binds ATP to stimulate the overall reductase activity of the enzyme while binding of dATP decreases overall

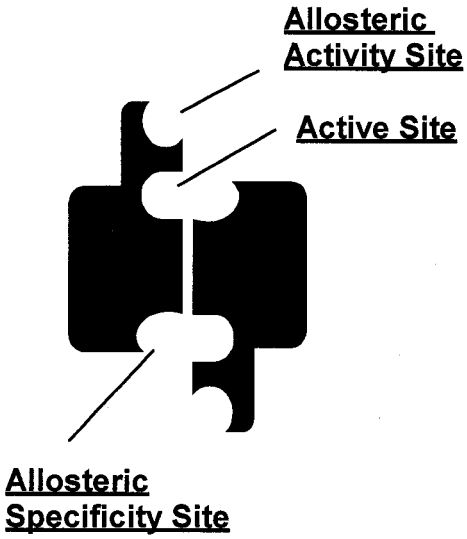

Figure 16. Schematic representation of the R1 dimer based upon the *S. cerevisiae* crystal structure. Individual antiparallel dimers are shown in red and blue.

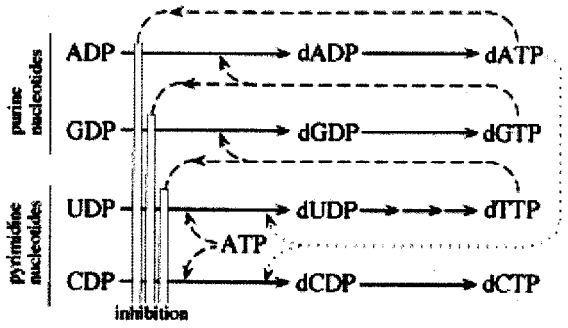

Figure 17. Allosteric regulation of class 1a RNRs. The products of NDP reduction feedback to regulate production a balanced deoxynucleotide pool. Dashed lines pointing toward vertical bars indicate negative regulation and dashed lines pointing toward horizontal solid lines indicate positive regulation. Eklund, et al. 2002.

activity using a product feedback inhibition mechanism thought to inactivate the radical transfer chain from the R2 subunit (173). RNR produces a balanced deoxynucleotide pool through a second mechanism of allosteric regulation where a particular dNTP product will feed back to regulate

ribonucleotide substrate specificity. This unique function causes ribonulcleotides to be reduced in a specific order in a process referred to as sequential transformation. The reactions proceed as follows (Figure 17): The binding of ATP to the overall activity site stimulates the reduction of the pyrimidine ribonucleotides CDP and UDP; dUDP is then modified to dTTP, which upon binding to the specificity site induces reduction of GDP (dCTP has no affect at physiological concentrations); and finally dGDP nucleotides feedback to induce reduction of ADP. dATP will then feed back to inhibit the enzyme at the activity site.

The exact mechanism governing this unique activity is not known, although several observations have led to speculation about how the dNTP effectors binding at the specificity site illicit changes in substrate binding at the active site. Largely, the extent of our knowledge of allosteric regulation comes from highly conserved residues that interact with the nucleotide effector; However, the crystal structure of the *E. coli* and yeast R1 dimer with nucleotide effectors bound to the specificity site and nucleotide diphosphates bound in the active site has given insight into new possibilities (173-175). The monomers are arranged anti-parallel with a four-helix bundle constituting the dimer interface. The active site and the specificity site are 24 Å apart in the monomer, but the specificity site on one monomer is only 15 Å away from the

active site on the other monomer. This has raised the idea that the binding of the allosteric effector in the specificity site on one monomer may affect substrate specificity in the active site on the other monomer through inter-protein signaling.

Ribonucleotide Reductase Inhibitors and Cancer

Several pharmacological inhibitors of ribonucleotide reductase have been identified and have been used to treat various cancers in humans (176). Hydroxyurea (HU), a well-known inhibitor of RNR, destabilizes the iron center of the enzyme, thereby destroying the tyrosine free radical essential for enzyme activity. Deferoxamine also strongly inhibits RNR through chelating the ferric ion. Gemcitabine and other nucleoside analogues that funtion to inhibit RNR in the active site. All these inhibitors block DNA synthesis via RNR, but this property seems to have little selectivity toward killing MMR-deficient cancer cells.

Identification and characterization of msl RNR1 alleles Our goal was to determine whether mutants of the human ribonucleotide reductase can induce the *msl* (mismatch repair synthetic lethal) phenotype in human cancer cells lacking MMR as it does in *mlh1Δ S. cerevisiae*. This finding would

validate the human ribonucleotide reductase as a chemotherapeutic target in MMR-deficient cancers and provide a novel platform for developing drug therapies for cancers that are presently refractory to treatment.

Preliminary Results

In work performed by co-worker Jeff Pincus a series of *msl* mutant alleles of the yeast *RNR1* were identified in a screen employing an *mlh1Δ* strain and its isogenic wild type parent. These alleles specifically kill *mlh1Δ* yeast, but do not greatly affect wild type growth. The strongest of these alleles are *rnr1* S269P and *rnr1* S610F (Figure 18). Using the structure of the *S. cerevisiae* R1 subunit, Ser269 was mapped to the specificity site of Rnr1p and Ser610 to the active site of the enzyme (174). These two residues do not appear to be directly involved in reaction chemistries, but mutations proximal to these sites may alter the allosteric regulation. Therefore, we hypothesize that disabled regulatory mechanisms in these mutants may lead to the *msl* phenotype in yeast by skewing the otherwise balanced deoxynucleotide pools. Pincus, et al (2007- in process) found that yeast *msl rnr1* mutants are altering the *in vivo* ratios of dNTPs such that pyrimidine deoxynucleotides are significantly overrepresented in the dNTP pool relative to wild type cells (Figure 19). It is well understood that altered nucleotide pools lead to

increased mutation rates due to misincorporated deoxynucleotides during DNA synthesis and repair (for review see reference (177). It is therefore possible that mutation rates are low in MMR+ cells carrying *msl rnr1* alleles because these mutations are effectively repaired by the intact MMR pathway. However, in MMR- cells the mutation rate increases to reach a threshold level where essential genes are deactivated by mutations caused by misincorporated nucleotides. This leads to the hypothesis that deoxypyrimidine overproduction or deoxypurine underproduction may play an important role in the *msl* phenotype.

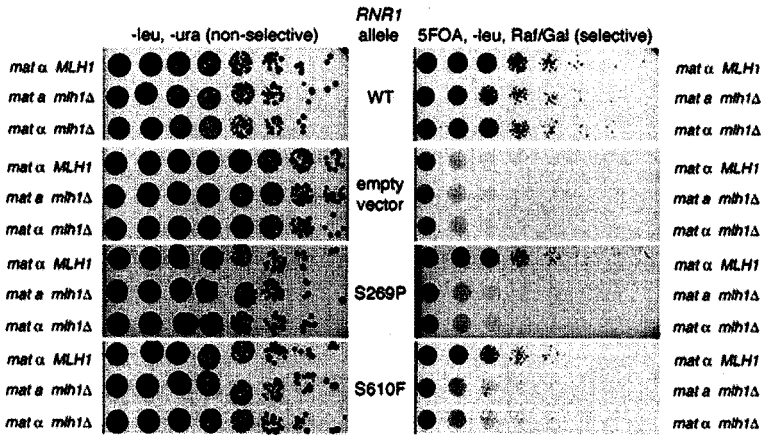

Figure 18. Mutant *rnr1* S269P and S610F induce a synthetic lethal phenotype in MMR- cells (*msl*). All strains are *rnr1Δ*, *rnr3Δ*. MMR+ cells have wt*RNR1* on a *URA3* covering plasmid. MMR- strains have an additional deletion of *MLH1* with wt*MLH1* and wt*RNR1* on a *URA3* covering plasmid. Mutant *rnr1* S269P and the wt *RNR1* control construct are expressed under the Gal1 promoter on a *LEU2* vector. Plating on 5-FOA selects against retention of the URA3 plasmids, leaving the *RNR1* allele on the LEU2 vector as the only source of ribonucleotide reductase activity. (J. Pincus, et al. (2008), in preparation).

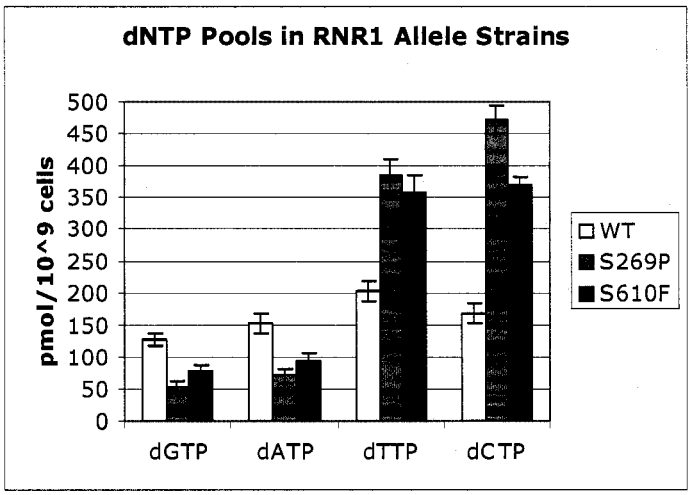

Figure 19. Alteration of endogenous dNTP pools in yeast carrying *msl rnr1* mutations. Deoxynucleotide levels in extracts from log-phase cells were measured using a PCR-based radioactive dNTP incorporation assay. (J. Pincus, et al. (2008), in preparation).

Results

Testing Human RNR Mutations in Tumor Cells

The full-length yeast Rnr1p is 66.8% identical to the human homologue RRM1 and *msl* residues identified in yeast Rnr1p either align directly in highly conserved domains, or align with small gap. It was therefore likely that the *msl* mutations in the yeast Rnr1p could be recreated in the human sequence and could reproduce the *msl* phenotype observed in yeast in a human cell line lacking hMLH1. To test this hypothesis, we created point mutations in the human RRM1 cDNA to mimic the mutations in the yeast *msl* alleles using site-directed mutagenesis. Other candidate mutations identified from the literature were also created to investigate their function. D57N was

identified in a screen in cultured murine lymphocytes for resistance to deoxyguanosine (178) and created a constitutively active mouse R1 that conferred a dominant mutator phenotype. G217S was isolated from a screen in *S. cerevisiae* for genes that increase the weak mutator phenotype in *exo1Δ* cells (179). We hypothesized that these mutations could create the *msl* phenotype in human cancer cells by virtue of their direct conservation amongst species and the mutator phenotypes they produced. All mutant alleles were virally expressed in MMR-deficient and MMR-proficient isogenic cell lines with hMLH1+/- hMLH1-/- genotypes respectively. The hMLH+ cell line was created by reintroduction of a large segment of chromosome 3 carrying a wild type copy of hMLH1 into the hMLH1-/- colon cancer cell line HCT116 (180). HCT116 was also transfected with an arm of chromosome 2 which has no affect on MMR activity. This cell line serves as a control for chromosomal reintroduction. The viral vector also carried the eGFP marker gene so the ratio of eGFP+ cells to eGFP- cells was measured by fluorescence activated cell counting to monitor the viability of the cells in culture over a period of 14 days. Any detectable effect on viability would be shown by a dercrease in eGFP+ cell population over time. No detectable difference was seen between hMLH1+/+ (MMR+) hMLH1-/- (MMR-) cells over the time period monitored (Figure 20). Tentatively, I conclude that these alleles were either completely recessive to the endogenous wild type

enzyme, were non-functional, were weak *msl*, or had wild type activity and therefore were not synthetic lethal with MMR defects in human cells.

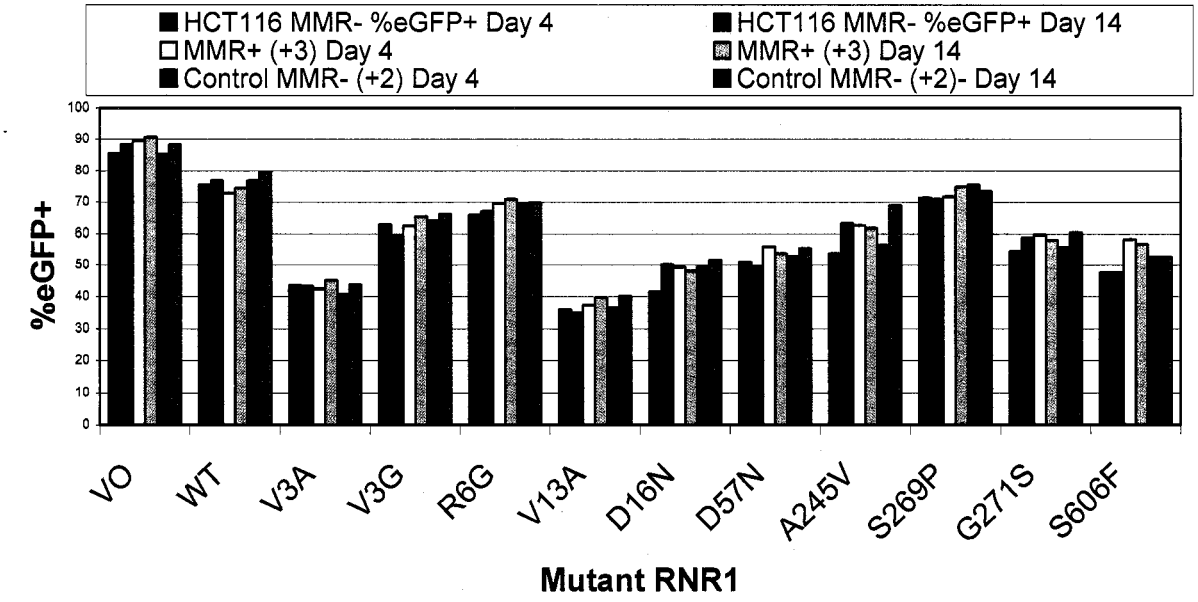

Figure 20. Effect of putative *msl* mutations in human tumor cells. Viral constructs carrying mutant alleles of RRM1 and the eGFP reporter gene were transduced into the MMR- cell line HCT116 and MMR+ cell line HCT116 (+3) and control cell line HCT116 (+2). Viability was then monitored monitored over a 14 day period.

MSL Screen for Human RNR1 Alleles in *S. Cerevisiae*

We then employed a secondary approach to creating *msl* alleles of the human RRM1 by creating a screen in yeast with the human RRM1 and RRM2 subunits. We hypothesized that the human RNR holoenzyme would rescue *rnr1Δ* yeast and therefore could be used to directly screen for *msl*

alleles of RRM1 in yeast. To test this hypothesis, the human cDNAs for both RRM1 and RRM2 under the control of the Gal1 promoter were transformed into haploid *rnr1Δ/rnr3Δ* yeast with the wild type *RNR1* on a *URA3* covering plasmid. Rnr3p is a non-essential RNR catalytic subunit present after DNA damage known to have only 1% activity relative to Rnr1p and was therefore expected to interfere with the screen (181). Subsequent plating onto media containing 5-fluoroorotic acid (5-FOA) selected against the *URA3* palsmid carrying the wild type *RNR1*. Figure 21 shows that only the human RNR holoenzyme composed of RRM1 and RRM2 will complement the RNR deletion in yeast. This strain relies completely upon the human RNR holoenzyme for *ne novo* deoxynucleotide production and grows very similarly to its wild type parent.

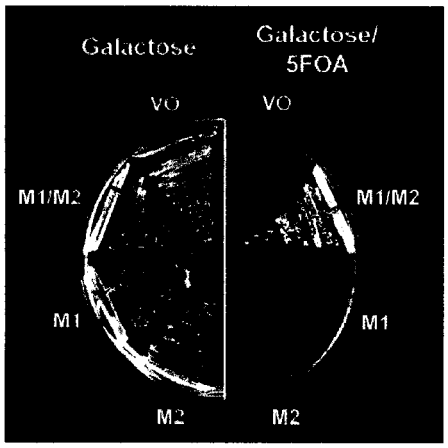

Figure 21. Human RRM1 and RRM2 rescue *rnr1Δ/rnr3Δ* yeast. RRM1 (M1) and RRM2 (M2) are the human homologues to *RNR1* and RNR2 in *S. cerevisiae*. The strains on the left half of the plate contain both yeast *RNR1* and components of the indicated components of the human ribonucleotide reductase holoenzyme. The yeast on the right side are living exclusively on the human RNR holoenzyme consisting of RRM1 and RRM2.

Based upon the results this complementation experiment, we devised a two-step screen to identify *msl* RRM1 alleles (Figure 22). The overall screen proceeds as follows: A yeast a *rnr1Δ/rnr3Δ/mlh1Δ* strain was constructed that expressed the human holoenzyme with wild type RRM1 on a *URA3+* covering plasmid under the control of the native yeast *RNR1* control elements and RRM2 genomically inserted into the *RNR2* locus. Wild type *MLH1* was expressed from a Cen/Ars *TRP1+* plasmid under the native elements. Yeast were then transformed with a PCR mutagenized RRM1 cDNA library under control of the Gal1 promoter on a Cen/Ars plasmid and plated to medium containing galactose to express the mutant proteins. Subsequent replica plating to 5-FOA expelled the wild type RRM1. Growth of these cells on 5-FOA indicated the presence of wild type RRM1 or mutant RRM1that were functional in a *MLH1+* background. These colonies were then replica plated to medium containing 5-fluoroanthranilic (5-FAA) to select against the *TRP1+* linked *MLH1* gene. The counter-selective drug 5-FAA is converted into the toxin 5-fluorotryptophan by the tryptophan biosynthetic pathway (182). Any colonies unable to grow on 5-FAA were considered to be *msl* alleles of RRM1 and were tested further.

A preliminary screen of 40,000 colonies was performed and two colonies displayed an *msl* phenotype where growth defects were only observed in the

presence of 5-FAA (Figure 11). Plasmids were recovered and re-transformed to confirm this phenotype. Sequencing revealed that *msl* M1 plasmids recovered from this screen carried the same mutations K180R and D327N. The mutant allele was named *msl* M1-1. The crystal structure of the *S. cerevisiae* Rnr1p was used to map these mutations (Figure 24). K108R is a conservative mutation mapping to a region not associated with any *RNR1* function, and is not expected to contribute to the *msl* phenotype. However, D327N maps to a region proximal to the $R1_2$-$R2_2$ dimer interface. The surrounding residues G326 and R329 are conserved 80% amongst class 1a RNRs. Importantly, biochemical evidence shows the R1-R2 dimer interaction to be both controlling and sensitive to allosteric effector binding to the specificity site (171). Because this residue is positioned between the allosteric effector of one monomer and the substrate nucleotide of the other monomer, it is possible that this residue may be involved in communicating information about the identity of the bound effector in one monomer to the active site of the other monomer. The D327N mutation was found to be recessive by plating cells with both WT RRM1 and *msl*M1-1 directly on 5-FAA to select against the *MLH1-TRP1* plasmid, bypassing the initial WT RRM1-*URA3* counterselection step. The *msl* M1-1 cells grew as well as wild type cells, indicating a recessive phenotype (data not shown).

If our hypothesis is correct and the *msl* mutants are skewing the ratios of deoxynucleotides *in vivo*, any endogenous wild type RNR activity is expected to correct this imbalance via its functional allosteric regulation. The human HCT116 MMR proficient/MMR deficient matched pair cell lines are both diploid and expresses the endogenous wild type RNR; therefore, any *msl* M1 alleles expressed in these cell lines must be dominant to observe the *msl* phenotype. We believed the approach with the best possibilities of obtaining *msl* alleles of M1 that would show the *msl* phenotype in human cells would be to identify dominant *msl* M1 alleles in a diploid yeast background. No *msl* allele isolated to date has been dominant over the wild type enzyme, due partly to the screening procedure used. In all our previous screens, the first wild type enzyme to complement the *msl* phenotype. While this step does not *exclude* the possibility of isolating dominant mutants, it does not specifically select for them. Importantly, the literature has reported dominant mutants of mammalian RNRs (183); however, according to our screening in yeast, recessive mutants are much more common. for counterselection with 5-FOA. We elected to not use the TRP plasmid for selection against *MLH1* as in the previous screen because the slow growth phenotypes associated with 5-FAA treatment made for problematic selection. We then co-transformed this strain with a PCR-mutagenized RRM1 library and a linearized *URA3* Cen/ARS plasmid to obtain recombinant plasmids

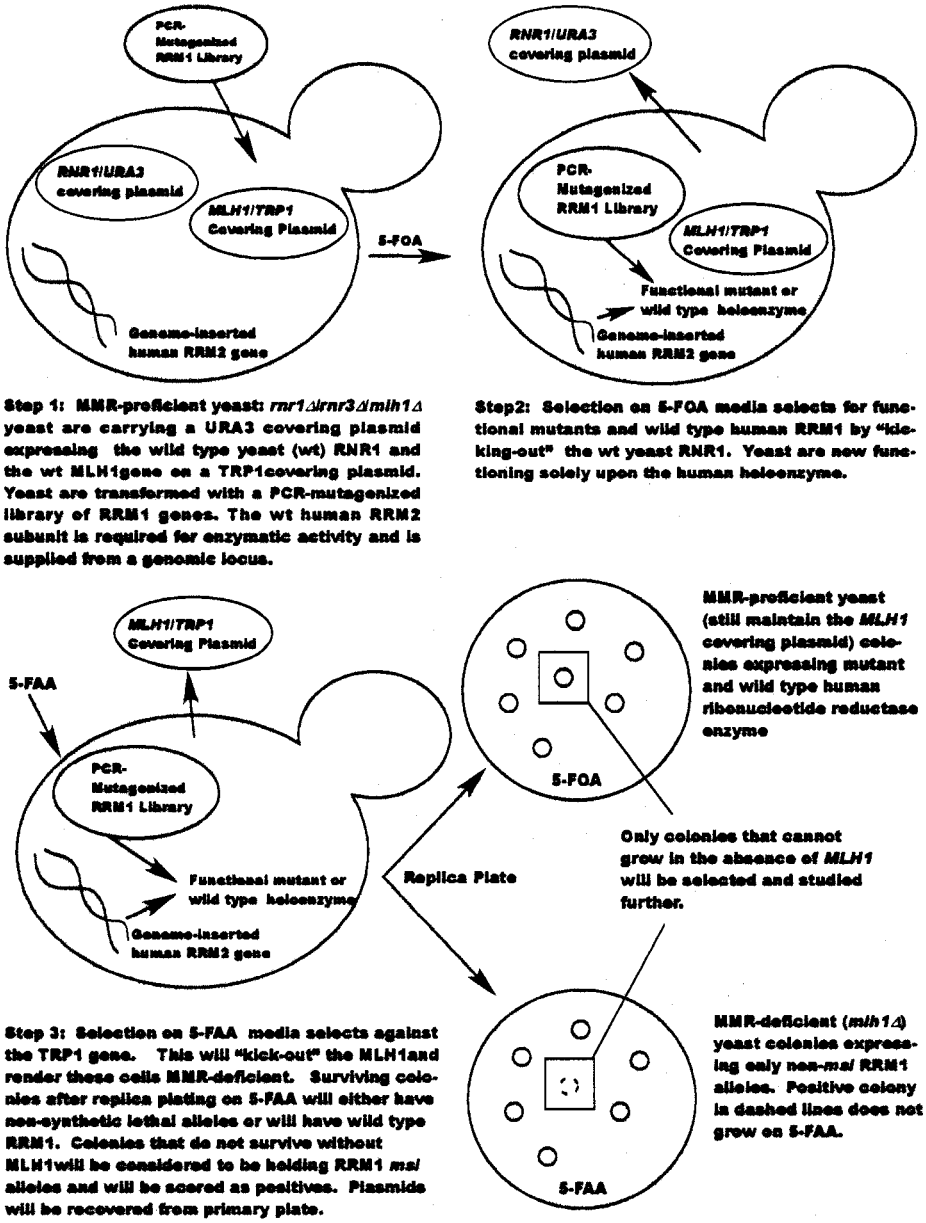

Figure 22. Screen for *msl* RRM1 alleles in *S. cerevisiae*. Steps of the screen and strain genotypes are indicated in the internal text.

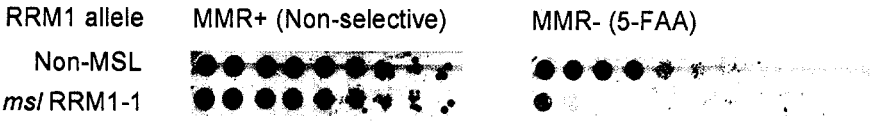

Figure 23. Spot assay of *msl* RRM1-1 double mutant K180R and D327N. Cells were normalized, diluted 1:5 in series and plated to the indicated medium. Limited growth under conditions counterselective for *TRP1*+- *MLH1* (5-FAA) indicate synthetic lethality with MMR defects.

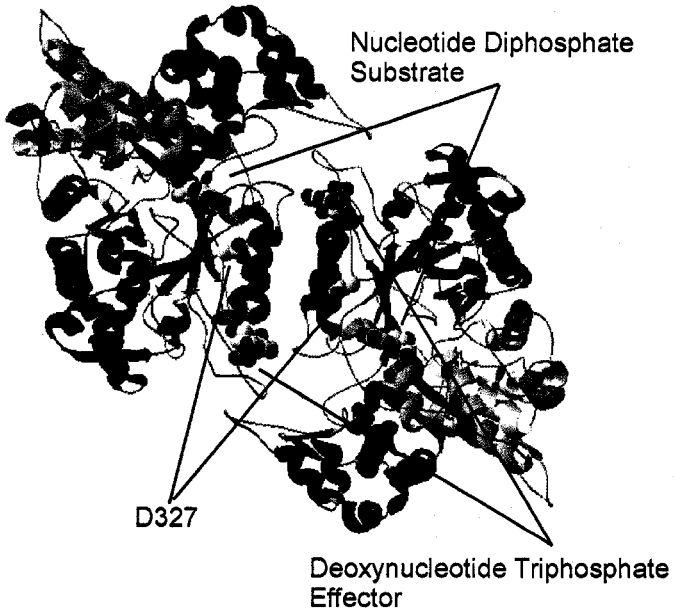

Figure 24. Structure of the *S. cerevisiae* Rnr1p. Rnr1p monomers were docked manually to illustrate the relative positions of the active site where the nucleotide diphosphates are bound and the specificity site where the deoxynucleotide triphosphates are bound. D327 is shown to be proximal to the dimer interface and between the active site of one monomer and the specificity site of the other monomer. Structure was adapted from (174).

expressing mutagenized M1 library. We plated cells on URA-/TRP- media to select for M1 transformants. Based upon a transformation with the linearized plasmid alone, we estimated an approximately 10-fold recombinant/vector recircularization ratio. Colonies were then replica plated directly to both TRP- media containing 5-FOA or TRP- media containing no counterselective agent as a plating control. Plates were then compared to identify any colonies with growth on TRP- media and no growth on plates containing 5-FOA (MMR-deficient cells). Approximately 300,000 colonies were inspected and potential positives were isolated and re-tested in a spot assay. None of the isolated cells showed distinctive growth defects after re-testing. We considered the possibility that the lack of recovered positives was due to a low mutagenesis efficiency of our RRM1 library. Therefore we subjected a sampling of 22 colonies to plasmid retrieval and sequencing, 11 of which contained mutations. Table 1 shows the varied mutations obtained. Based upon this data, we estimated approximately 1 nucleotide mutation per 911 basepairs which is about two or three mutations per M1 coding sequence. We were satisfied that our PCR efficiency was sufficient to accept the possibility that our screen failed for other reasons.

Understanding that dominant RNR mutants may not be obtainable with the methods we followed, or possibly not allowed by the restraints of nature, we

decided to pursue a third and final approach. We attempted to reduce wild type endogenous RRM1 activity in the HCT116 matched pair cell line through the use of RNA interference while expressing HA-tagged RRM1 recessive mutant in the background. These recessive mutants could be selectively expressed by introducing additional silent mutations engineered into the sequence targeted by the RNAi construct. In this case, expression of the mutant RRM1was expected to persist unaltered by the siRNA silencing apparatus while the wild type RRM1 is silenced. Importantly, the N-terminal

Clone #	Seq File	DNA Mutat	AA Mutation
1	sJJG459	C215A	P72H
		A671G	K224R
		A851C	SILENT
		A854G	T285C
11	sJJG468	A118G	T40A
		A202C	T68P
		A268G	T90A
		G363C	L121F
14	sJJG469	T764C	I255T
23	sJJG476	A292G	M98V
27	sJJG480	T230C	L77P
		A631G	N211D
29	sJJG482	T246C	SILENT
		T724A	S242T
31	sJJG484	A483G	SILENT
		G556C	A186P
32	sJJG485	T606C	S202P
33	sJJG486	A321T	SILENT
		A406G	I136V
35	sJJG488	A275G	K92R

Table 4. Mutation efficiency of a PCR mutagenized library used for the dominant *msl* M1 screen.

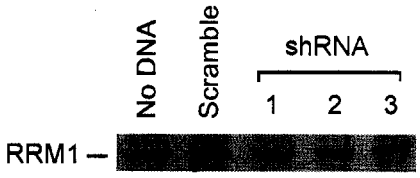

Figure 25. shRNA constructs have no effect on RRM1 protein levels. Western blot of RRM1in HCT116 cells expressing either a scrambled shRNA as a negative control, or one of three shRNA constructs targeting RRM1 mRNA. A mock transfection (No DNA) was conducted as an additional control.

HA-tagged RRM1 is functional in yeast so the tag was not expected to interfere (data not shown). We fist attempted to knock-down the endogenous RRM1 using a short hairpin RNA (shRNA) expressed in a retroviral vector. A GFP reporter gene was included to monitor transfection efficiency and FACS was used to measure GFP expression. Despite repeated attempts, we were unable to reduce RRM1 protein levels in these cells. Figure 25 shows a western blot of HCT116 cells virally transduced with shRNA constructs targeting RRM1. We see no reduction in RRM1 protein abundance across treatments. We attempted again to express four newly designed shRNA constructs utilizing a different viral vector pLNCX with the same results (data not shown).

Discussion

A genetic screen in DNA mismatch repair-deficient yeast revealed mutations in allosteric regulation of Rnr1p were synthetically lethal with MMR defects. This study suggested that the human RNR may be a possible target for human tumors lacking mismatch repair. We attempted to validate the human

RNR catalytic subunit RRM1 as a target in tumors lacking hMLH1 activity using three major approaches: 1) by transferring mutations identified in the yeast *RNR1* to the highly similar human gene and expressing these mutants in cancer cells lacking MMR function; 2) by screening for mutants of the human RRM1 synthetically lethal with MMR defects in yeast; and 3) by attempting to observe phenotypes from recessive RRM1 alleles through knocking-down endogenous wild type RNR using RNAi and replacing it with mutant enzyme.

We found that none of these approaches were successful in validating the human RNR as a target for MMR-deficient tumors. We attribute these failures mainly to the inability to obtain dominant *msl* RRM1 mutations showing the desired phenotype in a diploid system. The RNR enzyme is evolutionarily tuned to provide a balanced pool of nucleotides for DNA

replication and repair. Any RNR mutants that may upset the balance of nucleotides by over or under-producing one deoxynucleotide will be recessive to the wild type enzyme which is able to correct for this imbalance. Considering this constraint we question whether attaining dominant mutations is possible at all. Despite these apparent constraints, we did attempt to identify these mutants using a yeast strain where the yeast RNR genes were replaced by the genes for the human RNR holoenzyme- a seemingly perfect tool for identifying human *msl* RRM1 alleles. This attempt was unsuccessful and this further supported the possibility that validating the human RNR as a drug target using genetic tools was not possible.

Our attempts were also constrained by the fact that RNR activity is essential. Simply inhibiting overall RNR activity has not been successful in treating MMR-deficient cancers. We show that the *msl* mutations in the yeast *RNR1* alter RNR activity specifically such that nucleotide pools are not depleted, but skewed. We assert that these mutations are possibly very rare and this combined with the need for dominant alleles has prevented us from further discovery. The essentiality of RNR is also likely to be the reason for our failed attempts at knocking-down endogenous RRM1 using shRNA. It stands to reason that successful RRM1 knock-down would be strongly selected against in a system where cells are rapidly dividing. With this in mind, we

hoped to observe reductions in RRM1 within 24 hours after transduction with the shRNA constructs before any loss of viability is predicted to occur (Figure 25). However, reduction in RRM1 protein abundance was not observed.

Materials and Methods

Cell Culture, Viral Transduction and Western Blotting

HCT116 and subcloned cell lines were cultured in high glucose DMEM containing 10% fetal calf serum (Invitrogen. Carlsbad, CA) in a 37°C incubator at 5% CO_2. All proteins were expressed via viral transduction with pBabe containing the eGFP fluorescent marker. Viral particles were produced in HEK293T Phoenix Ampho cells as in Welcker, et al. (2003) (184). Transduction efficiency was judged by FACS analysis. All yeast manipulations were conducted according to established protocols (185). Western blotting was performed using standard methodologies. RRM1 was detected using mouse monoclonal antibodies (Millipore. Billerica, MA cat# MAB3033).

Strain Construction, Plasmids and Mutation Generation

RNR1Δ/RNR3Δ yeast strain was created as in Pincus, et al (2007)- in process). Human RRM1 and M2 expression constructs were created by cloning the native yeast promoter and terminator sequences for the corresponding genes in *S. cerevisiae* S288C and placing them 5' and 3' of the human sequences in Cen/ARS plasmids kindly provided by M. Funk (186). Gal1 promoter-driven expression of RRM1 WT and mutants was achieved by placing the RRM1 cDNA in the MCS of pRS415 Gal1. Site-directed mutagenesis was achieved using Quickchange kit (Stratagene. La Jolla, CA). All point mutations were verified by sequencing of the entire orf. Mutagenic PCR libraries were constructed using a copy of the Gal1 promoter-driven RRM1 in a pSKII cloning vector (no yeast replication elements) as a template. Error-prone Taq polymerase (Invitrogen) was used to amplify the gene. PCR products were added directly to transformation reactions along with linearized vector backbones (indicated in results section).

RNAi constructs: The following sequences were cloned into a modified pBABE viral expression construct carrying the eGFP reporter gene (184).
1) 5' GATCTaagacgctagagcggtcttatttTTCAAGAGAaaataagaccgctctagcgtctt

TTTTTG-3', 2) 5'-

GATCTaaggtcgtgtccgcaaagttgtaTTCAAGAGAtacaactttgcg

gacacgaccttTTTTTG-3', 3) 5'-GATCTgatcttaccgagcggggcctatgTTCAAGAGA

cataggccccgctcggtaagatcTTTTTG-3 4) Scrambled control: 5'-AAGCGCGCT

TTGTAGGATTCGttcaagagtCGAATCCTACAAAGCGCGCTTtttttt-3'

References:

1. Wegele, H., Muschler, P., Bunck, M., Reinstein, J., and Buchner, J. (2003) *J Biol Chem* **278**, 39303-39310

2. Hawle, P., Siepmann, M., Harst, A., Siderius, M., Reusch, H. P., and Obermann, W. M. (2006) *Mol Cell Biol* **26**, 8385-8395

3. Meyer, P., Prodromou, C., Hu, B., Vaughan, C., Roe, S. M., Panaretou, B., Piper, P. W., and Pearl, L. H. (2003) *Mol Cell* **11**, 647-658

4. Ban, C., and Yang, W. (1998) *Cell* **95**, 541-552

5. Wigley, D. B., Davies, G. J., Dodson, E. J., Maxwell, A., and Dodson, G. (1991) *Nature* **351**, 624-629

6. Dutta, R., and Inouye, M. (2000) *Trends Biochem Sci* **25**, 24-28

7. Jakob, U., Scheibel, T., Bose, S., Reinstein, J., and Buchner, J. (1996) *J Biol Chem* **271**, 10035-10041

8. Ali, M. M., Roe, S. M., Vaughan, C. K., Meyer, P., Panaretou, B., Piper, P. W., Prodromou, C., and Pearl, L. H. (2006) *Nature* **440**, 1013-1017

9. Stebbins, C. E., Russo, A. A., Schneider, C., Rosen, N., Hartl, F. U., and Pavletich, N. P. (1997) *Cell* **89**, 239-250

10. Prodromou, C., Roe, S. M., O'Brien, R., Ladbury, J. E., Piper, P. W., and Pearl, L. H. (1997) *Cell* **90**, 65-75

11. Weikl, T., Muschler, P., Richter, K., Veit, T., Reinstein, J., and Buchner, J. (2000) *J Mol Biol* **303**, 583-592

12. McLaughlin, S. H., Ventouras, L. A., Lobbezoo, B., and Jackson, S. E. (2004) *J Mol Biol* **344**, 813-826

13. Millson, S. H., Truman, A. W., King, V., Prodromou, C., Pearl, L. H., and Piper, P. W. (2005) *Eukaryot Cell* **4**, 849-860

14. Obermann, W. M., Sondermann, H., Russo, A. A., Pavletich, N. P., and Hartl, F. U. (1998) *J Cell Biol* **143**, 901-910

15. Panaretou, B., Prodromou, C., Roe, S. M., O'Brien, R., Ladbury, J. E., Piper, P. W., and Pearl, L. H. (1998) *Embo J* **17**, 4829-4836

16. Johnson, J. L., Halas, A., and Flom, G. (2007) *Mol Cell Biol* **27**, 768-776

17. Young, J. C., and Hartl, F. U. (2000) *Embo J* **19**, 5930-5940

18. Grenert, J. P., Johnson, B. D., and Toft, D. O. (1999) *J Biol Chem* **274**, 17525-17533

19. Jackson, A. P., and Maxwell, A. (1993) *Proc Natl Acad Sci U S A* **90**, 11232-11236

20. Grenert, J. P., Sullivan, W. P., Fadden, P., Haystead, T. A., Clark, J., Mimnaugh, E., Krutzsch, H., Ochel, H. J., Schulte, T. W., Sausville, E., Neckers, L. M., and Toft, D. O. (1997) *J Biol Chem* **272**, 23843-23850

21. Sullivan, W., Stensgard, B., Caucutt, G., Bartha, B., McMahon, N., Alnemri, E. S., Litwack, G., and Toft, D. (1997) *J Biol Chem* **272**, 8007-8012

22. Prodromou, C., Roe, S. M., Piper, P. W., and Pearl, L. H. (1997) *Nat Struct Biol* **4**, 477-482

23. Prodromou, C., Panaretou, B., Chohan, S., Siligardi, G., O'Brien, R., Ladbury, J. E., Roe, S. M., Piper, P. W., and Pearl, L. H. (2000) *Embo J* **19**, 4383-4392

24. Chadli, A., Bouhouche, I., Sullivan, W., Stensgard, B., McMahon, N., Catelli, M. G., and Toft, D. O. (2000) *Proc Natl Acad Sci U S A* **97**, 12524-12529

25. Shiau, A. K., Harris, S. F., Southworth, D. R., and Agard, D. A. (2006) *Cell* **127**, 329-340

26. Maruya, M., Sameshima, M., Nemoto, T., and Yahara, I. (1999) *J Mol Biol* **285**, 903-907

27. Richter, K., Muschler, P., Hainzl, O., and Buchner, J. (2001) *J Biol Chem* **276**, 33689-33696

28. Richter, K., Reinstein, J., and Buchner, J. (2002) *J Biol Chem* **277**, 44905-44910

29. Peng, X., Guo, X., Borkan, S. C., Bharti, A., Kuramochi, Y., Calderwood, S., and Sawyer, D. B. (2005) *J Biol Chem* **280**, 13148-13152

30. Sullivan, W. P., Owen, B. A., and Toft, D. O. (2002) *J Biol Chem* **277**, 45942-45948

31. Johnson, J. L., and Toft, D. O. (1995) *Mol Endocrinol* **9**, 670-678

32. Picard, D. (2007) *Webpage*

33. Xu, W., Yuan, X., Xiang, Z., Mimnaugh, E., Marcu, M., and Neckers, L. (2005) *Nat Struct Mol Biol* **12**, 120-126

34. Sato, S., Fujita, N., and Tsuruo, T. (2000) *Proc Natl Acad Sci U S A* **97**, 10832-10837

35. Fontana, J., Fulton, D., Chen, Y., Fairchild, T. A., McCabe, T. J., Fujita, N., Tsuruo, T., and Sessa, W. C. (2002) *Circ Res* **90**, 866-873

36. Citri, A., Harari, D., Shohat, G., Ramakrishnan, P., Gan, J., Lavi, S., Eisenstein, M., Kimchi, A., Wallach, D., Pietrokovski, S., and Yarden, Y. (2006) *J Biol Chem* **281**, 14361-14369

37. Hadden, M. K., Lubbers, D. J., and Blagg, B. S. (2006) *Curr Top Med Chem* **6**, 1173-1182

38. da Rocha Dias, S., Friedlos, F., Light, Y., Springer, C., Workman, P., and Marais, R. (2005) *Cancer Res* **65**, 10686-10691

39. Muller, P., Ceskova, P., and Vojtesek, B. (2005) *J Biol Chem* **280**, 6682-6691

40. Sollars, V., Lu, X., Xiao, L., Wang, X., Garfinkel, M. D., and Ruden, D. M. (2003) *Nat Genet* **33**, 70-74

41. Sasaki, K., Yasuda, H., and Onodera, K. (1979) *J Antibiot (Tokyo)* **32**, 849-851

42. Uehara, Y., Hori, M., Takeuchi, T., and Umezawa, H. (1985) *Jpn J Cancer Res* **76**, 672-675

43. Whitesell, L., Mimnaugh, E. G., De Costa, B., Myers, C. E., and Neckers, L. M. (1994) *Proc Natl Acad Sci U S A* **91**, 8324-8328

44. Kamal, A., Thao, L., Sensintaffar, J., Zhang, L., Boehm, M. F., Fritz, L. C., and Burrows, F. J. (2003) *Nature* **425**, 407-410

45. Hutchison, K. A., Stancato, L. F., Owens-Grillo, J. K., Johnson, J. L., Krishna, P., Toft, D. O., and Pratt, W. B. (1995) *J Biol Chem* **270**, 18841-18847

46. Pratt, W. B., and Toft, D. O. (2003) *Exp Biol Med (Maywood)* **228**, 111-133

47. Dittmar, K. D., and Pratt, W. B. (1997) *J Biol Chem* **272**, 13047-13054

48. Kosano, H., Stensgard, B., Charlesworth, M. C., McMahon, N., and Toft, D. (1998) *J Biol Chem* **273**, 32973-32979

49. McLaughlin, S. H., Sobott, F., Yao, Z. P., Zhang, W., Nielsen, P. R., Grossmann, J. G., Laue, E. D., Robinson, C. V., and Jackson, S. E. (2006) *J Mol Biol* **356**, 746-758

50. Siligardi, G., Hu, B., Panaretou, B., Piper, P. W., Pearl, L. H., and Prodromou, C. (2004) *J Biol Chem* **279**, 51989-51998

51. Garcia-Ranea, J. A., Mirey, G., Camonis, J., and Valencia, A. (2002) *FEBS Lett* **529**, 162-167

52. Lee, Y. T., Jacob, J., Michowski, W., Nowotny, M., Kuznicki, J., and Chazin, W. J. (2004) *J Biol Chem* **279**, 16511-16517

53. http://www.sanger.ac.uk/Software/Pfam/, S. I. (2007), Sanger Institute

54. Catlett, M. G., and Kaplan, K. B. (2006) *J Biol Chem* **281**, 33739-33748

55. Lingelbach, L. B., and Kaplan, K. B. (2004) *Mol Cell Biol* **24**, 8938-8950

56. Bansal, P. K., Abdulle, R., and Kitagawa, K. (2004) *Mol Cell Biol* **24**, 8069-8079

57. Mayor, A., Martinon, F., De Smedt, T., Petrilli, V., and Tschopp, J. (2007) *Nat Immunol* **8**, 497-503

58. Liu, Y., Burch-Smith, T., Schiff, M., Feng, S., and Dinesh-Kumar, S. P. (2004) *J Biol Chem* **279**, 2101-2108

59. da Silva Correia, J., Miranda, Y., Leonard, N., and Ulevitch, R. (2007) *Proc Natl Acad Sci U S A* **104**, 6764-6769

60. De Acetis, M., Notte, A., Accornero, F., Selvetella, G., Brancaccio, M., Vecchione, C., Sbroggio, M., Collino, F., Pacchioni, B., Lanfranchi, G., Aretini, A., Ferretti, R., Maffei, A., Altruda, F., Silengo, L., Tarone, G., and Lembo, G. (2005) *Circ Res* **96**, 1087-1094

61. Brancaccio, M., Fratta, L., Notte, A., Hirsch, E., Poulet, R., Guazzone, S., De Acetis, M., Vecchione, C., Marino, G., Altruda, F., Silengo, L., Tarone, G., and Lembo, G. (2003) *Nat Med* **9**, 68-75

62. Xie, J., Zhu, H., Larade, K., Ladoux, A., Seguritan, A., Chu, M., Ito, S., Bronson, R. T., Leiter, E. H., Zhang, C. Y., Rosen, E. D., and Bunn, H. F. (2004) *Proc Natl Acad Sci U S A* **101**, 10750-10755

63. Zhou, T., Zimmerman, W., Liu, X., and Erikson, R. L. (2006) *Proc Natl Acad Sci U S A* **103**, 9039-9044

64. Wu, J., Luo, S., Jiang, H., and Li, H. (2005) *FEBS Lett* **579**, 421-426

65. Brugge, J. S., Erikson, E., and Erikson, R. L. (1981) *Cell* **25**, 363-372

66. Siligardi, G., Panaretou, B., Meyer, P., Singh, S., Woolfson, D. N., Piper, P. W., Pearl, L. H., and Prodromou, C. (2002) *J Biol Chem* **277**, 20151-20159

67. Roe, S. M., Ali, M. M., Meyer, P., Vaughan, C. K., Panaretou, B., Piper, P. W., Prodromou, C., and Pearl, L. H. (2004) *Cell* **116**, 87-98

68. Stepanova, L., Leng, X., Parker, S. B., and Harper, J. W. (1996) *Genes Dev* **10**, 1491-1502

69. Zhang, W., Hirshberg, M., McLaughlin, S. H., Lazar, G. A., Grossmann, J. G., Nielsen, P. R., Sobott, F., Robinson, C. V., Jackson, S. E., and Laue, E. D. (2004) *J Mol Biol* **340**, 891-907

70. Shao, J., Grammatikakis, N., Scroggins, B. T., Uma, S., Huang, W., Chen, J. J., Hartson, S. D., and Matts, R. L. (2001) *J Biol Chem* **276**, 206-214

71. Wang, X., Venable, J., LaPointe, P., Hutt, D. M., Koulov, A. V., Coppinger, J., Gurkan, C., Kellner, W., Matteson, J., Plutner, H., Riordan, J. R., Kelly, J. W., Yates, J. R., 3rd, and Balch, W. E. (2006) *Cell* **127**, 803-815

72. Meyer, P., Prodromou, C., Liao, C., Hu, B., Mark Roe, S., Vaughan, C. K., Vlasic, I., Panaretou, B., Piper, P. W., and Pearl, L. H. (2004) *Embo J* **23**, 511-519

73. Lotz, G. P., Lin, H., Harst, A., and Obermann, W. M. (2003) *J Biol Chem* **278**, 17228-17235

74. Panaretou, B., Siligardi, G., Meyer, P., Maloney, A., Sullivan, J. K., Singh, S., Millson, S. H., Clarke, P. A., Naaby-Hansen, S., Stein, R., Cramer, R., Mollapour, M., Workman, P., Piper, P. W., Pearl, L. H., and Prodromou, C. (2002) *Mol Cell* **10**, 1307-1318

75. Harst, A., Lin, H., and Obermann, W. M. (2005) *Biochem J* **387**, 789-796

76. Chadli, A., Graham, J. D., Abel, M. G., Jackson, T. A., Gordon, D. F., Wood, W. M., Felts, S. J., Horwitz, K. B., and Toft, D. (2006) *Mol Cell Biol* **26**, 1722-1730

77. Barral, J. M., Hutagalung, A. H., Brinker, A., Hartl, F. U., and Epstein, H. F. (2002) *Science* **295**, 669-671

78. Cheung-Flynn, J., Roberts, P. J., Riggs, D. L., and Smith, D. F. (2003) *J Biol Chem* **278**, 17388-17394

79. Chen, S., Prapapanich, V., Rimerman, R. A., Honore, B., and Smith, D. F. (1996) *Mol Endocrinol* **10**, 682-693

80. Morishima, Y., Kanelakis, K. C., Silverstein, A. M., Dittmar, K. D., Estrada, L., and Pratt, W. B. (2000) *J Biol Chem* **275**, 6894-6900

81. Wegele, H., Wandinger, S. K., Schmid, A. B., Reinstein, J., and Buchner, J. (2006) *J Mol Biol* **356**, 802-811

82. Prodromou, C., Siligardi, G., O'Brien, R., Woolfson, D. N., Regan, L., Panaretou, B., Ladbury, J. E., Piper, P. W., and Pearl, L. H. (1999) *Embo J* **18**, 754-762

83. Richter, K., Muschler, P., Hainzl, O., Reinstein, J., and Buchner, J. (2003) *J Biol Chem* **278**, 10328-10333

84. Flom, G., Behal, R. H., Rosen, L., Cole, D. G., and Johnson, J. L. (2007) *Biochem J* **404**, 159-167

85. Johnson, B. D., Schumacher, R. J., Ross, E. D., and Toft, D. O. (1998) *J Biol Chem* **273**, 3679-3686

86. Murata, S., Minami, Y., Minami, M., Chiba, T., and Tanaka, K. (2001) *EMBO Rep* **2**, 1133-1138

87. Connell, P., Ballinger, C. A., Jiang, J., Wu, Y., Thompson, L. J., Hohfeld, J., and Patterson, C. (2001) *Nat Cell Biol* **3**, 93-96

88. Xu, W., Marcu, M., Yuan, X., Mimnaugh, E., Patterson, C., and Neckers, L. (2002) *Proc Natl Acad Sci U S A* **99**, 12847-12852

89. Zhao, R., Davey, M., Hsu, Y. C., Kaplanek, P., Tong, A., Parsons, A. B., Krogan, N., Cagney, G., Mai, D., Greenblatt, J., Boone, C., Emili, A., and Houry, W. A. (2005) *Cell* **120**, 715-727

90. Geller, R., Vignuzzi, M., Andino, R., and Frydman, J. (2007) *Genes Dev* **21**, 195-205

91. Fares, M. A., and Travers, S. A. (2006) *Genetics* **173**, 9-23

92. Falsone, S. F., Gesslbauer, B., Tirk, F., Piccinini, A. M., and Kungl, A. J. (2005) *FEBS Lett* **579**, 6350-6354

93. Te, J., Jia, L., Rogers, J., Miller, A., and Hartson, S. D. (2007) *J Proteome Res* **6**, 1963-1973

94. Falsone, S. F., Gesslbauer, B., Rek, A., and Kungl, A. J. (2007) *Proteomics* **7**, 2375-2383

95. Schumacher, J. A., Crockett, D. K., Elenitoba-Johnson, K. S., and Lim, M. S. (2007) *Proteomics* **7**, 2603-2616

96. Old, W. M., Meyer-Arendt, K., Aveline-Wolf, L., Pierce, K. G., Mendoza, A., Sevinsky, J. R., Resing, K. A., and Ahn, N. G. (2005) *Mol Cell Proteomics* **4**, 1487-1502

97. Zybailov, B., Coleman, M. K., Florens, L., and Washburn, M. P. (2005) *Anal Chem* **77**, 6218-6224

98. Kerner, M. J., Naylor, D. J., Ishihama, Y., Maier, T., Chang, H. C., Stines, A. P., Georgopoulos, C., Frishman, D., Hayer-Hartl, M., Mann, M., and Hartl, F. U. (2005) *Cell* **122**, 209-220

99. Elias, J. E., and Gygi, S. P. (2007) *Nat Methods* **4**, 207-214

100. Xia, Q., Hendrickson, E. L., Wang, T., Lamont, R. J., Leigh, J. A., and Hackett, M. (2007) *Proteomics* **7**, 2904-2919

101. Paoletti, A. C., Parmely, T. J., Tomomori-Sato, C., Sato, S., Zhu, D., Conaway, R. C., Conaway, J. W., Florens, L., and Washburn, M. P. (2006) *Proc Natl Acad Sci U S A* **103**, 18928-18933

102. Florens, L., Carozza, M. J., Swanson, S. K., Fournier, M., Coleman, M. K., Workman, J. L., and Washburn, M. P. (2006) *Methods* **40**, 303-311

103. Al-Shahrour, F., Diaz-Uriarte, R., and Dopazo, J. (2004) *Bioinformatics* **20**, 578-580

104. Sreedhar, A. S., Kalmar, E., Csermely, P., and Shen, Y. F. (2004) *FEBS Lett* **562**, 11-15

105. Somji, S., Ann Sens, M., Garrett, S. H., Gurel, V., Todd, J. H., and Sens, D. A. (2002) *Toxicol Lett* **133**, 241-254

106. Nimmanapalli, R., O'Bryan, E., and Bhalla, K. (2001) *Cancer Res* **61**, 1799-1804

107. An, W. G., Schulte, T. W., and Neckers, L. M. (2000) *Cell Growth Differ* **11**, 355-360

108. Yun, B. G., Huang, W., Leach, N., Hartson, S. D., and Matts, R. L. (2004) *Biochemistry* **43**, 8217-8229

109. Whitesell, L., and Cook, P. (1996) *Mol Endocrinol* **10**, 705-712

110. Parusel, C. T., Kritikou, E. A., Hengartner, M. O., Krek, W., and Gotta, M. (2006) *Development* **133**, 621-629

111. Gstaiger, M., Luke, B., Hess, D., Oakeley, E. J., Wirbelauer, C., Blondel, M., Vigneron, M., Peter, M., and Krek, W. (2003) *Science* **302**, 1208-1212

112. Jeronimo, C., Forget, D., Bouchard, A., Li, Q., Chua, G., Poitras, C., Therien, C., Bergeron, D., Bourassa, S., Greenblatt, J., Chabot, B., Poirier, G. G., Hughes, T. R., Blanchette, M., Price, D. H., and Coulombe, B. (2007) *Mol Cell* **27**, 262-274

113. Prieto, C., and De Las Rivas, J. (2006) *Nucleic Acids Res* **34**, W298-302

114. Alfarano, C., Andrade, C. E., Anthony, K., Bahroos, N., Bajec, M., Bantoft, K., Betel, D., Bobechko, B., Boutilier, K., Burgess, E., Buzadzija, K., Cavero, R., D'Abreo, C., Donaldson, I., Dorairajoo, D., Dumontier, M. J., Dumontier, M. R., Earles, V., Farrall, R., Feldman, H., Garderman, E., Gong, Y., Gonzaga, R., Grytsan, V., Gryz, E., Gu, V., Haldorsen, E., Halupa, A., Haw, R., Hrvojic, A., Hurrell, L., Isserlin, R., Jack, F., Juma, F., Khan, A., Kon, T., Konopinsky, S., Le, V., Lee, E., Ling, S., Magidin, M., Moniakis, J., Montojo, J., Moore, S., Muskat, B., Ng, I., Paraiso, J. P., Parker, B., Pintilie, G., Pirone, R., Salama, J. J., Sgro, S., Shan, T., Shu, Y., Siew, J., Skinner, D., Snyder, K., Stasiuk, R., Strumpf, D., Tuekam, B., Tao, S., Wang, Z., White, M., Willis, R., Wolting, C., Wong, S., Wrong, A., Xin, C., Yao, R., Yates, B., Zhang, S., Zheng, K., Pawson, T., Ouellette, B. F., and Hogue, C. W. (2005) *Nucleic Acids Res* **33**, D418-424

115. Salwinski, L., Miller, C. S., Smith, A. J., Pettit, F. K., Bowie, J. U., and Eisenberg, D. (2004) *Nucleic Acids Res* **32**, D449-451

116. Peri, S., Navarro, J. D., Amanchy, R., Kristiansen, T. Z., Jonnalagadda, C. K., Surendranath, V., Niranjan, V., Muthusamy, B., Gandhi, T. K., Gronborg, M., Ibarrola, N., Deshpande, N., Shanker, K., Shivashankar, H. N., Rashmi, B. P., Ramya, M. A., Zhao, Z., Chandrika, K. N., Padma, N., Harsha, H. C., Yatish, A. J., Kavitha, M. P., Menezes, M., Choudhury, D. R., Suresh, S., Ghosh, N., Saravana, R., Chandran, S., Krishna, S., Joy, M., Anand, S. K., Madavan, V., Joseph, A., Wong, G. W., Schiemann, W. P., Constantinescu, S. N., Huang, L., Khosravi-Far, R., Steen, H., Tewari, M., Ghaffari, S., Blobe, G. C., Dang, C. V., Garcia, J. G., Pevsner, J., Jensen, O. N., Roepstorff, P., Deshpande, K. S., Chinnaiyan, A. M., Hamosh, A., Chakravarti, A., and Pandey, A. (2003) *Genome Res* **13**, 2363-2371

117. Kerrien, S., Alam-Faruque, Y., Aranda, B., Bancarz, I., Bridge, A., Derow, C., Dimmer, E., Feuermann, M., Friedrichsen, A., Huntley, R., Kohler, C., Khadake, J., Leroy, C., Liban, A., Lieftink, C., Montecchi-Palazzi, L., Orchard, S., Risse, J., Robbe, K., Roechert, B., Thorneycroft, D., Zhang, Y., Apweiler, R., and Hermjakob, H. (2007) *Nucleic Acids Res* **35**, D561-565

118. Hermjakob, H., Montecchi-Palazzi, L., Lewington, C., Mudali, S., Kerrien, S., Orchard, S., Vingron, M., Roechert, B., Roepstorff, P., Valencia, A., Margalit, H., Armstrong, J., Bairoch, A., Cesareni, G., Sherman, D., and Apweiler, R. (2004) *Nucleic Acids Res* **32**, D452-455

119. Chatr-aryamontri, A., Ceol, A., Palazzi, L. M., Nardelli, G., Schneider, M. V., Castagnoli, L., and Cesareni, G. (2007) *Nucleic Acids Res* **35**, D572-574

120. Zanzoni, A., Montecchi-Palazzi, L., Quondam, M., Ausiello, G., Helmer-Citterich, M., and Cesareni, G. (2002) *FEBS Lett* **513**, 135-140

121. Shannon, P., Markiel, A., Ozier, O., Baliga, N. S., Wang, J. T., Ramage, D., Amin, N., Schwikowski, B., and Ideker, T. (2003) *Genome Res* **13**, 2498-2504

122. Niikura, Y., Ohta, S., Vandenbeldt, K. J., Abdulle, R., McEwen, B. F., and Kitagawa, K. (2006) *Oncogene* **25**, 4133-4146

123. Brancaccio, M., Menini, N., Bongioanni, D., Ferretti, R., De Acetis, M., Silengo, L., and Tarone, G. (2003) *FEBS Lett* **551**, 47-52

124. Hahn, J. S. (2005) *FEBS Lett* **579**, 4513-4519

125. Inohara, N., Ogura, Y., Chen, F. F., Muto, A., and Nunez, G. (2001) *J Biol Chem* **276**, 2551-2554

126. Chen, S., Sullivan, W. P., Toft, D. O., and Smith, D. F. (1998) *Cell Stress Chaperones* **3**, 118-129

127. Maloney, A., Clarke, P. A., Naaby-Hansen, S., Stein, R., Koopman, J. O., Akpan, A., Yang, A., Zvelebil, M., Cramer, R., Stimson, L., Aherne, W., Banerji, U., Judson, I., Sharp, S., Powers, M., deBilly, E., Salmons, J., Walton, M., Burlingame, A., Waterfield, M., and Workman, P. (2007) *Cancer Res* **67**, 3239-3253

128. Muskett, P. R., Kahn, K., Austin, M. J., Moisan, L. J., Sadanandom, A., Shirasu, K., Jones, J. D., and Parker, J. E. (2002) *Plant Cell* **14**, 979-992

129. Takahashi, A., Casais, C., Ichimura, K., and Shirasu, K. (2003) *Proc Natl Acad Sci U S A* **100**, 11777-11782

130. Michos, A., Gryllos, I., Hakansson, A., Srivastava, A., Kokkotou, E., and Wessels, M. R. (2006) *J Biol Chem* **281**, 8216-8223

131. Levy, R. J. (2007) *Shock* **28**, 24-28

132. Koterski, J. F., Nahvi, M., Venkatesan, M. M., and Haimovich, B. (2005) *Infect Immun* **73**, 504-513

133. Kempf, V. A., Lebiedziejewski, M., Alitalo, K., Walzlein, J. H., Ehehalt, U., Fiebig, J., Huber, S., Schutt, B., Sander, C. A., Muller, S., Grassl, G., Yazdi, A. S., Brehm, B., and Autenrieth, I. B. (2005) *Circulation* **111**, 1054-1062

134. Angers, S., Thorpe, C. J., Biechele, T. L., Goldenberg, S. J., Zheng, N., MacCoss, M. J., and Moon, R. T. (2006) *Nat Cell Biol* **8**, 348-357

135. Hutchison, K. A., Czar, M. J., Scherrer, L. C., and Pratt, W. B. (1992) *J Biol Chem* **267**, 14047-14053

136. Motojima, F., and Yoshida, M. (2003) *J Biol Chem* **278**, 26648-26654

137. Chen, G. I., and Gingras, A. C. (2007) *Methods* **42**, 298-305

138. Craig, R., and Beavis, R. C. (2004) *Bioinformatics* **20**, 1466-1467

139. Rauch, A., Bellew, M., Eng, J., Fitzgibbon, M., Holzman, T., Hussey, P., Igra, M., Maclean, B., Lin, C. W., Detter, A., Fang, R., Faca, V., Gafken, P., Zhang, H., Whiteaker, J., States, D., Hanash, S., Paulovich, A., and McIntosh, M. W. (2006) *J Proteome Res* **5**, 112-121

140. MacLean, B., Eng, J. K., Beavis, R. C., and McIntosh, M. (2006) *Bioinformatics* **22**, 2830-2832

141. Powell, D. W., Weaver, C. M., Jennings, J. L., McAfee, K. J., He, Y., Weil, P. A., and Link, A. J. (2004) *Mol Cell Biol* **24**, 7249-7259

142. Marti, T. M., Kunz, C., and Fleck, O. (2002) *J Cell Physiol* **191**, 28-41.

143. Modrich, P. (1997) *J Biol Chem* **272**, 24727-24730.

144. Fishel, R., Ewel, A., and Lescoe, M. K. (1994) *Cancer Res* **54**, 5539-5542.

145. Fishel, R., Ewel, A., Lee, S., Lescoe, M. K., and Griffith, J. (1994) *Science* **266**, 1403-1405.

146. Alani, E., Chi, N. W., and Kolodner, R. (1995) *Genes Dev* **9**, 234-247.

147. Johnson, R. E., Kovvali, G. K., Prakash, L., and Prakash, S. (1996) *J Biol Chem* **271**, 7285-7288.

148. Marsischky, G. T., Filosi, N., Kane, M. F., and Kolodner, R. (1996) *Genes Dev* **10**, 407-420.

149. Hughes, M. J., and Jiricny, J. (1992) *J Biol Chem* **267**, 23876-23882.

150. Palombo, F., Gallinari, P., Iaccarino, I., Lettieri, T., Hughes, M., D'Arrigo, A., Truong, O., Hsuan, J. J., and Jiricny, J. (1995) *Science* **268**, 1912-1914.

151. Palombo, F., Iaccarino, I., Nakajima, E., Ikejima, M., Shimada, T., and Jiricny, J. (1996) *Curr Biol* **6**, 1181-1184.

152. Habraken, Y., Sung, P., Prakash, L., and Prakash, S. (1996) *Curr Biol* **6**, 1185-1187.

153. Marsischky, G. T., and Kolodner, R. D. (1999) *J Biol Chem* **274**, 26668-26682.

154. Allen, D. J., Makhov, A., Grilley, M., Taylor, J., Thresher, R., Modrich, P., and Griffith, J. D. (1997) *Embo J* **16**, 4467-4476.

155. Gradia, S., Subramanian, D., Wilson, T., Acharya, S., Makhov, A., Griffith, J., and Fishel, R. (1999) *Mol Cell* **3**, 255-261.

156. Genschel, J., Littman, S. J., Drummond, J. T., and Modrich, P. (1998) *J Biol Chem* **273**, 19895-19901.

157. Drummond, J. T., Li, G. M., Longley, M. J., and Modrich, P. (1995) *Science* **268**, 1909-1912.

158. Reenan, R. A., and Kolodner, R. D. (1992) *Genetics* **132**, 963-973.

159. Li, G. M., and Modrich, P. (1995) *Proc Natl Acad Sci U S A* **92**, 1950-1954.

160. Prolla, T. A., Pang, Q., Alani, E., Kolodner, R. D., and Liskay, R. M. (1994) *Science* **265**, 1091-1093.

161. Peltomaki, P. (2003) *J Clin Oncol* **21**, 1174-1179.

162. Samowitz, W. S., Curtin, K., Lin, H. H., Robertson, M. A., Schaffer, D., Nichols, M., Gruenthal, K., Leppert, M. F., and Slattery, M. L. (2001) *Gastroenterology* **121**, 830-838

163. Aaltonen, L. A., Salovaara, R., Kristo, P., Canzian, F., Hemminki, A., Peltomaki, P., Chadwick, R. B., Kaariainen, H., Eskelinen, M., Jarvinen, H., Mecklin, J. P., and de la Chapelle, A. (1998) *N Engl J Med* **338**, 1481-1487

164. Herman, J. G., Umar, A., Polyak, K., Graff, J. R., Ahuja, N., Issa, J. P., Markowitz, S., Willson, J. K., Hamilton, S. R., Kinzler, K. W., Kane, M. F., Kolodner, R. D., Vogelstein, B., Kunkel, T. A., and Baylin, S. B. (1998) *Proc Natl Acad Sci U S A* **95**, 6870-6875

165. Duval, A., Iacopetta, B., Ranzani, G. N., Lothe, R. A., Thomas, G., and Hamelin, R. (1999) *Oncogene* **18**, 6806-6809

166. Duval, A., Reperant, M., and Hamelin, R. (2002) *Oncogene* **21**, 8062-8066.

167. Lawes, D. A., SenGupta, S., and Boulos, P. B. (2003) *Eur J Surg Oncol* **29**, 201-212

168. Drake, A. C., Campbell, H., Porteous, M. E., and Dunlop, M. G. (2003) *Int J Gynecol Cancer* **13**, 262-277

169. Sia, E. A., Kokoska, R. J., Dominska, M., Greenwell, P., and Petes, T. D. (1997) *Mol Cell Biol* **17**, 2851-2858

170. Strand, M., Prolla, T. A., Liskay, R. M., and Petes, T. D. (1993) *Nature* **365**, 274-276.

171. Scott, C. P., Kashlan, O. B., Lear, J. D., and Cooperman, B. S. (2001) *Biochemistry* **40**, 1651-1661

172. Kashlan, O. B., Scott, C. P., Lear, J. D., and Cooperman, B. S. (2002) *Biochemistry* **41**, 462-474

173. Eriksson, M., Uhlin, U., Ramaswamy, S., Ekberg, M., Regnstrom, K., Sjoberg, B. M., and Eklund, H. (1997) *Structure* **5**, 1077-1092

174. Xu, H., Faber, C., Uchiki, T., Fairman, J. W., Racca, J., and Dealwis, C. (2006) *Proc Natl Acad Sci U S A* **103**, 4022-4027

175. Xu, H., Faber, C., Uchiki, T., Racca, J., and Dealwis, C. (2006) *Proc Natl Acad Sci U S A* **103**, 4028-4033

176. Nocentini, G. (1996) *Crit Rev Oncol Hematol* **22**, 89-126

177. Kunz, B. A., Kohalmi, S. E., Kunkel, T. A., Mathews, C. K., McIntosh, E. M., and Reidy, J. A. (1994) *Mutat Res* **318**, 1-64

178. Caras, I. W., and Martin, D. W., Jr. (1988) *Mol Cell Biol* **8**, 2698-2704.

179. Amin, N. S., Nguyen, M. N., Oh, S., and Kolodner, R. D. (2001) *Mol Cell Biol* **21**, 5142-5155

180. Koi, M., Umar, A., Chauhan, D. P., Cherian, S. P., Carethers, J. M., Kunkel, T. A., and Boland, C. R. (1994) *Cancer Res* **54**, 4308-4312

181. Domkin, V., Thelander, L., and Chabes, A. (2002) *J Biol Chem* **277**, 18574-18578

182. Toyn, J. H., Gunyuzlu, P. L., White, W. H., Thompson, L. A., and Hollis, G. F. (2000) *Yeast* **16**, 553-560

183. Ullman, B., Gudas, L. J., Caras, I. W., Eriksson, S., Weinberg, G. L., Wormsted, M. A., and Martin, D. W., Jr. (1981) *J Biol Chem* **256**, 10189-10192

184. Welcker, M., Singer, J., Loeb, K. R., Grim, J., Bloecher, A., Gurien-West, M., Clurman, B. E., and Roberts, J. M. (2003) *Mol Cell* **12**, 381-392

185. Ausubel, F. M., Brent, R., Kingston, R. E., Moore, D. D., Seidman, J. G., Smith,, and J. A., a. S., K. (1998) *John Wiley &Sons, New York*

186. Mumberg, D., Muller, R., and Funk, M. (1995) *Gene* **156**, 119-122

Vita

Jacob Gano was born and raised in Washington where he has enjoyed being in the outdoors fishing, hiking and hunting. He earned his B.A. and BS in 1999 at The Evergreen State College in Olympia, Washington and his Doctor of Philosophy in Molecular and Cellular Biology from the University of Washington in 2007.